INVESTIGATING THE ROLES OF HSP40s AND AN E3 UBIQUITIN LIGASE IN THE BIOGENESIS OF APOLIPOPROTEIN B

by

Deepa Kumari

Integrated B.S./M.S. in Life Sciences, National Institute of Science Education and Research, India, 2014

Submitted to the Graduate Faculty of

The Kenneth P. Dietrich School of Arts and Sciences in partial fulfillment

of the requirements for the degree of

Doctor of Philosophy

University of Pittsburgh

2021

UNIVERSITY OF PITTSBURGH

DIETRICH SCHOOL OF ARTS AND SCIENCES

This dissertation was presented

by

Deepa Kumari

It was defended on

June 7, 2021

and approved by

Dr. Karen M. Arndt, PhD., Professor, Department of Biological Sciences

Dr. Andrea J. Berman, PhD., Associate Professor, Department of Biological Sciences

Dr. Gerald R.V. Hammond, PhD., Assistant Professor, Department of Cell Biology

Dr. Kirill I. Kiselyov, PhD., Associate Professor, Department of Biological Sciences

Thesis Advisor: Dr. Jeffrey L. Brodsky, PhD., Professor, Department of Biological Sciences

INVESTIGATING THE ROLES OF HSP40s AND AN E3 UBIQUITIN LIGASE IN THE BIOGENESIS OF APOLIPOPROTEIN B

Deepa Kumari, PhD

University of Pittsburgh, 2021

Apolipoprotein B (ApoB) is the primary component of atherogenic lipoproteins and is responsible for the transport of dietary and endogenous fats and cholesterol in the blood stream. Elevated levels of ApoB-containing particles lead to the development of Coronary Artery Disease, which kills millions of people every year. As it is synthesized, ApoB is co-translationally translocated into the endoplasmic reticulum (ER) through the Sec61 translocon and is lipidated, leading to the formation of a lipoprotein particle that is eventually secreted into the plasma. However, in the absence of lipidation, ApoB is retrotranslocated to the cytosol and destroyed via ER Associated Degradation (ERAD), a regulated pathway that maintains proteostasis by normally degrading misfolded proteins in the early secretory pathway. In this thesis, I investigated the contributions of select cytosolic Hsp40s on ApoB biogenesis. To this end, I used a rodent cell line that endogenously synthesizes and secretes ApoB. By performing siRNA mediated knockdown and metabolic pulse chase experiments, I discovered that a class A Hsp40, DNAJA1, associates with and facilitates ApoB degradation. Consistent with these data, Ydj1 (the yeast homolog of DNAJA1) also facilitates ApoB degradation in a heterologous yeast expression system. The ablation of DNAJA1 also leads to the accumulation of ubiquitinated ApoB, suggesting that DNAJA1 functions prior to degradation. In stark contrast to DNAJA1, DNAJB1, a class B member, stabilizes ApoB. Because knockdown decreases the levels of ubiquitinated ApoB,

DNAJB1 might act prior to DNAJA1 as ApoB enters the ER. Finally, because ERAD substrates must be ubiquitinated after chaperone-dependent selection, I examined the contributions of E3 ubiquitin ligases on ApoB stability and discovered that Hrd1 targets ApoB for degradation in the rodent cell line. Together, my findings highlight the unexpected functional diversity of Hsp40s during the biogenesis of ApoB.

TABLE OF CONTENTS

LIST OF TABLES

LIST OF FIGURES

LIST OF ABBREVIATIONS

ApoB	Apolipoprotein B
Apobec1	ApolipoproteinB mRNA Editing Enzyme Catalytic Subunit 1
BAP31	B cell Receptor Associated Protein 31
CAD	Coronary Artery Disease
CE	Cholesterol Ester
COPII	Coat Complex II
ddH_2O	Double Distilled Water
DMEM	Dulbecco's Modified Eagle Medium
DMSO	Dimethyl Sulfoxide
DPBS	Dulbecco's Phosphate Buffered Saline
E3	Ubiquitin Ligase
EDTA	Ethylenediaminetetraacetic Acid
ERAD	Endoplasmic Reticulum Associated Degradation
FDA	Food and Drug Administration
FBS	Fetal Bovine Serum
gp78/AMFR	Glycoprotein of 78 kDa/Autocrine Motility Factor Receptor
HDL	High Density Lipoprotein
HEK293	Human Embryonic Kidney 293
HRP	Horseradish Peroxidase
HSP	Heat Shock Protein
Hsc70	70 kDa Heat Shock Cognate Protein
Hsp40	40 kDa Heat Shock Protein (DNAJ/J-protein)
Hsp70	70 kDa Heat Shock Protein
Hsp90	90 kDa Heat Shock Protein
IP	Immunoprecipitation
JDP	J-Domain Protein (Hsp40)

KD	Knockdown
KLHL12	Kelch-Like Protein 2
KO	Knockout
LDL	Low Density Lipoprotein
LDLR	Low Density Lipoprotein Receptor
McA	Rh7777 McArdle cells
MG132	Proteasome Inhibitor Carbobenzoxy-Leu-Leu-Leucinal
MTP	Microsomal Triglyceride Transfer Protein
NEM	N-Ethylmaleimide
OA	Oleic Acid
OD_{600}	Optical Density at 600 nm
p97/VCP	Valosin Containing Protein
PBS	Phosphate Buffered Saline
PCSK9	Preprotein convertase subtilisin/kexin type 9
PDI	Protein Disulfide Isomerase
PERPP	Post ER Presecretory Proteolysis
PIs	Protease Inhibitors
PIC	Roche cOmplete™ EDTA-Free Protease Inhibitor Cocktail
PLs	Phospholipids
PMSF	Phenylmethylsulfonyl Fluoride
PMT	Photomultiplier Tube
PQC	Protein Quality Control
RING	Really Interesting New Gene
RIPA	Radioimmunoprecipitation assay buffer
S35	Radioactively labeled cysteine and methionine
SDS	Sodium Dodecyl Sulfate
SDS-PAGE	Sodium Dodecyl Sulfate Polyacrylamide Gel Electrophoresis
Sec61	Secretory Protein 61
siRNA	Small Interfering Ribonucleic Acid

SRP	Signal Recognition Particle
TAG	Triacylglycerol
TBST	Tris Buffered Saline + 0.2% Tween 20
Tris	2-Amino-2-(Hydroxymethyl) Propane-1,3-Diol
Ub	Ubiquitin
UPS	Ubiquitin Proteasome System
VLDL	Very Low Density Lipoprotein

PREFACE

I have been immensely blessed and fortunate to be surrounded by people who have guided and helped me navigate through this adventurous journey. First my sincerest and heartfelt gratitude to my thesis advisor Dr. Jeff Brodsky who has been an excellent mentor to me for the past several years. It has been an absolute honor and privilege to be under Jeff's tutelage. Jeff's mentorship has provided me a very nurturing atmosphere where I have continued growing as a scientist and a human being. I am thankful to him for helping me build my scientific acumen, encouraging me to think independently and critically, and providing me opportunities to develop my communication skills. Jeff's enthusiasm, passion and love for science and his perfect work ethic have always inspired me. I also really appreciate Jeff's eagerness to help his students in any and all the ways he can. His support, understanding and patience particularly in the past year since the pandemic began, have been a major driving force for my journey forward. Thank you very much Jeff, for giving me the opportunity to be a member of the Brodsky lab family.

Many thanks to the lovely, supportive, fun and science loving Brodsky lab members, who I call my second family. Being part of the Brodsky lab family has been one of the best chapters of my life. My heartfelt gratitude to Jen Goeckeler-Fried, our lab manager for the smooth running of our lab; research professors - Dr. Teresa Buck, Dr. Chris Guerriero, Dr. Patrick Needham, and Dr. Sara Sannino; medical fellows - Dr. Brighid O'Donnell and Dr. Aiden Porter; post-doctoral fellows - Dr. Annette Chiang, and Dr. Miguel Betegon; graduate students - Dr. Mike Preston, Dr. Lynley Doonan, Dr. Tim Mackie, Dr. Zhihao Sun, Dr. Sam Estabrooks, Grant Daskivich, Katie Nguyen, and Morgan Webb. Many thanks to all the undergraduates who I have had the privilege to overlap with for being such a fun company and all you help, particularly Arjun Mittal, who I have had the

privilege to train. You have each helped me grow as a scientist and a person and given me indelible beautiful memories I will cherish my entire life.

I would want to thank my dissertation committee- Dr. Karen Arndt, Dr. Andrea Berman, Dr. Kirill Kiselyov and Dr. Gerald Hammond for their continued support, valuable feedback and suggestions to steer my project forward. I also am very grateful to all my friends- thank you for your friendship and support. I am also very thankful to all the members of our department for their support. Special thanks to Cathy Barr who has always been very helpful and encouraging.

Finally, words can't express how grateful I am towards my parents Kamini Jha and Bijay Chandra Jha for their infinite love, unwavering support, and faith in me. Thank you so much for always being there for me and helping me follow my dreams. Being your daughter has been the biggest blessing and honor of my life. To my elder brothers Vikash and Vivek, I am very lucky to have you both as my brothers; thank you for your love, care and support. I am also very grateful to my grandparents for their blessings, love, and faith in me that will always keep my heart warm and strong.

1.0 INTRODUCTION

Cardiovascular diseases kill ~18 million people world-wide every year and cause one in every four deaths in the United States (Benjamin et al., 2019; Heron, 2017). Elevated levels of apolipoprotein B (ApoB) are a major risk factor for Coronary Artery Disease (CAD). Current CAD treatments include statins and a drug that directly targets ApoB, but side effects and/or the cost limit their efficacy and availability. A better understanding of the mechanism of ApoB regulation is imperative to identify new therapeutics to help combat CAD.

ApoB is the primary component of atherogenic lipoprotein particles and is regulated by Endoplasmic Reticulum Associated Degradation (ERAD), a major protein surveillance mechanism that targets misfolded proteins for degradation. Interestingly, ApoB is an atypical ERAD substrate since it is metabolically regulated by ERAD. In this chapter, I will discuss the role of ApoB in lipid metabolism, the regulation of ApoB by ERAD, diseases caused due to abnormal levels of ApoB, current treatment options for those with CAD, and a discussion of other natively folded cellular substrates whose activities are regulated by ERAD.

1.1 Apolipoprotein B

1.1.1 Lipid transport

Lipid and cholesterol can be acquired through dietary intake or synthesized endogenously. Triacylglycerols (TAGs), lipids, phospholipids (PLs), cholesterol, and cholesterol esters (CEs) are

transported in lipoprotein particles, which are categorized based on their densities (Hamilton, 1972; Havel, 1975; Havel et al., 1955; Kwiterovich, 2000). Ranging from the lightest to the densest, these particles are chylomicrons, very low-density lipoproteins (VLDL), low density lipoproteins (LDL), and high-density lipoproteins (HDL) (Table 1). These lipoprotein particles contain neutral lipids, such as TAGs and CEs in their core, surrounded by a monolayer of amphipathic PLs. The major protein component of chylomicrons, VLDLs, and LDLs is a single molecule of a protein called Apolipoprotein B (ApoB) that aids the assembly of these supramolecular spheres, thereby providing structural rigidity (Boren et al., 1994; Bostrom et al., 1986; Olofsson et al., 1987) (Figure 1). These lipoprotein particles carry both dietary and endogenous lipids from the liver and small intestine to the peripheral tissues through the aqueous bloodstream where they are used for several essential metabolic processes, including energy generation and the synthesis of biological membranes, hormones, bile salts, and vitamins.

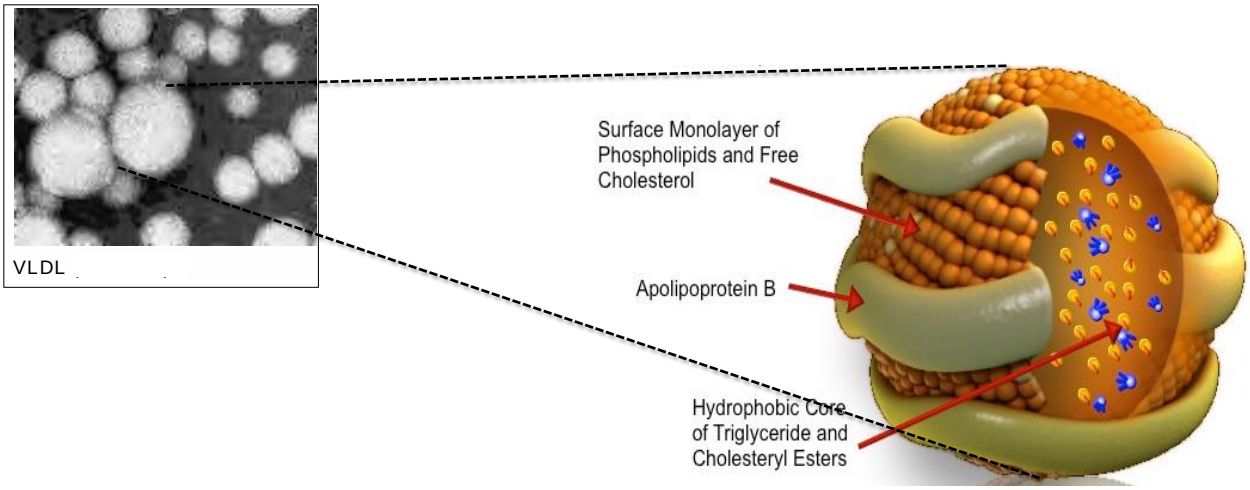

Figure 1. Artistic representation of a VLDL particle

VLDL particle consists of a core of neutral lipids and cholesterol. Phospholipids and free cholesterol form a surface monolayer. A single molecule of ApolipoproteinB 100 is responsible for the assembly of the VLDL particle and

provides structural rigidity to the spherical aggregate. Reprinted from (Feingold & Grunfeld 2000) and Lehninger Principles of Biochemistry.

Table 1. Lipoprotein particles in human plasma and some of their characteristics

	Chylomicron	VLDL	LDL	HDL
Diameter (nm)	>75	30-80	18-25	5-12
Density (g/mL)	<1.006	0.95-1.006	1.006-1.063	1.063-1.210
Site of Expression	Small Intestine	Liver	Liver	Liver, Small Intestine
Apolipoproteins	A1, A4, B48, E	B100, C1, C2, C3, E	B100, C3, E	A1, A2, C1, C2, C3, D, E
Composition (wt %)				
Protein	2	10	23	55
Phospholipids	9	18	20	24
Free Cholesterol	1	7	8	2
Cholesteryl Esters	3	12	37	15
Triacylglycerols	85	50	10	4

Dietary cholesterol, TAGS, CEs are assembled in chylomicrons in the small intestine and are secreted into the lymphatic system as well as into the bloodstream (Hamilton, 1972; Havel, 1975; Havel et al., 1955; Kwiterovich, 2000) (Figure 2). Chylomicrons are then hydrolyzed into fatty acids and glycerol by lipoprotein lipase (whose activity is activated by a chylomicron resident co-factor, ApoC-II) in endothelial cells and primarily in muscle and adipose tissue (Havel, 1975; Kwiterovich, 2000). The resulting metabolites are then utilized for subsequent biological processes, such as energy generation, or they are converted into triglycerides for storage. The chylomicron remnant is then endocytosed by the liver where the remaining cholesterol and lipids are recycled into denser VLDL and LDL particles for secretion to peripheral tissues. The main protein component of VLDLs and LDLs is ApoB100, the full-length isoform that is expressed in

the liver and ApoB48, which is the N-terminal 48% of ApoB100 that is expressed in the small intestine and is the protein component of chylomicrons (see below). As TAGs are metabolized and lipids are depleted, the C-terminal region of ApoB100 becomes exposed, which then serves as a ligand for the LDL receptor on the

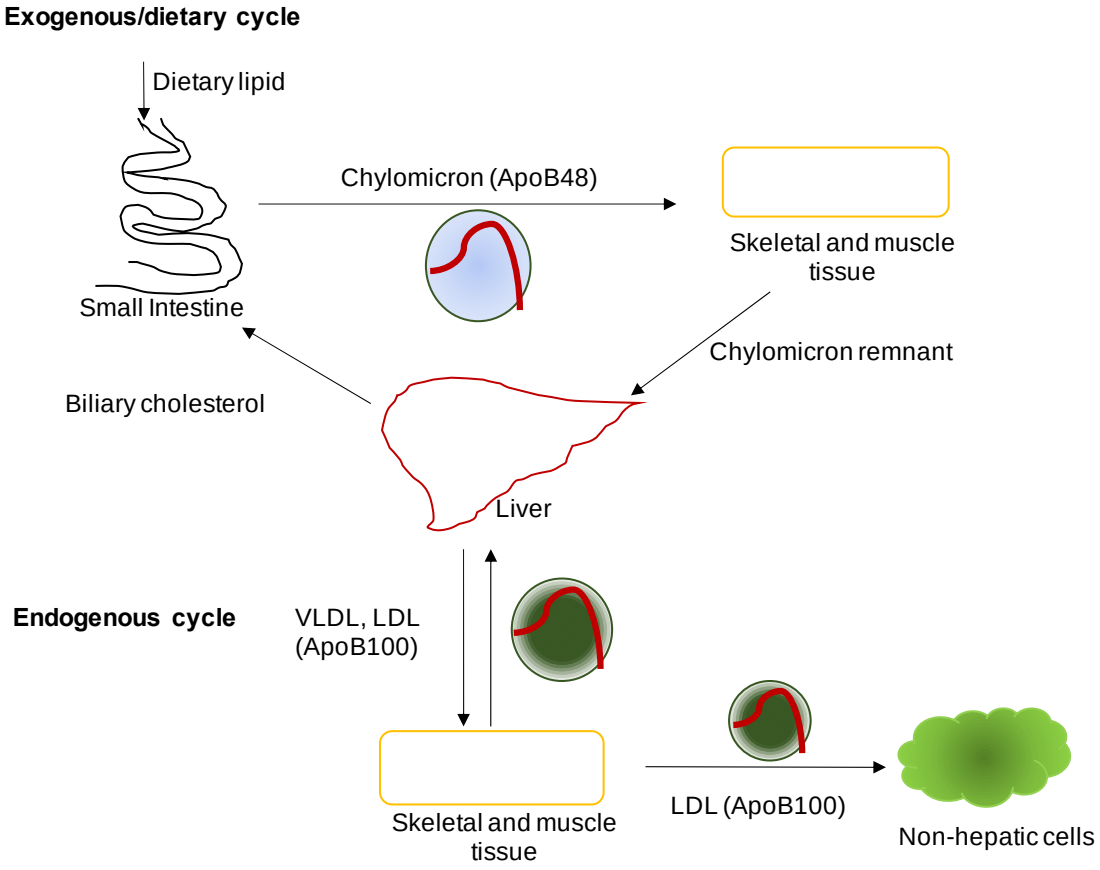

Figure 2. Role of ApoB in lipid metabolism.

Dietary/exogenous lipids and cholesterol are absorbed in the small intestine and packaged with ApoB48 in chylomicrons, which deliver fatty acids to the peripheral tissues. Chylomicron remnants are endocytosed into the liver via ApoE receptors and dietary cholesterol is repackaged with endogenous fatty acids and ApoB100 into VLDL particles through the exogenous cycle. These VLDL particles deliver fatty acids to peripheral tissues. VLDL remnants (or "IDLs") are formed and returned to the liver prior to synthesis of LDL in the liver. These fat depleted particles are now denser and also expose the C-terminal end of ApoB, which mediates LDL uptake in non-hepatic cells through receptor mediated endocytosis. VLDL=very low density lipoprotein, LDL=low density lipoprotein

1.1.2 ApoB isoforms and structural features

Human plasma harbors more than 10 different apolipoproteins, which serve as carrier proteins for water-insoluble cholesterol as well as CEs, TAGs, and PLs (Table 2). ApoB contains 4,536 amino acids and has a mass of ~550 kDa (Chen et al., 1988; Chen et al., 1987; Chen et al., 1986; Hussain et al., 2005; Hussain et al., 1996; Powell et al., 1987). As noted above, the protein exists in two isoforms: ApoB100 is the full-length protein and is synthesized in the liver. It is the major structural component of VLDLs and LDLs. In contrast, ApoB48, which is synthesized only in higher mammals, is the N-terminal 48% of ApoB100. ApoB48 is synthesized in the small intestine and is the major structural component of chylomicrons (Figure 3A). ApoB48 is produced by the Apob mRNA editing enzyme catalytic subunit 1 (Apobec1)-dependent deamidation of a cytidine in a CAA codon, which converts glutamine into a stop codon (UAA), thus producing the ApoB48 mRNA (Chen et al., 1988; Chen et al., 1987; Chen et al., 1986; Hussain et al., 2005; Hussain et al., 1996; Powell et al., 1987) (Figure 3B). As a result, ApoB48 lacks the LDL receptor binding domain and thereby chylomicrons do not undergo LDL receptor mediated endocytosis (Chen et al., 1988; Chen et al., 1987; Chen et al., 1986; Hussain et al., 2005; Hussain et al., 1996; Powell et al., 1987). Immediately after a meal, this enables chylomicrons to rapidly deliver lipids and cholesterol to peripheral capillaries, muscles, and adipocytes where the triglycerides are hydrolyzed and then used or stored. The depleted chylomicron remnants are endocytosed in an ApoE-dependent manner in the liver.

Table 2. Apolipoproteins found in human plasma

Apolipoprotein	Major site of expression	Molecular Weight (kD)	Lipoprotein	Function
ApoA-I	Liver, small intestine	~28	HDL	Activates Lecithin cholesterol Acyltransferase (LCAT)
ApoA-II	Liver, small Intestine	~17	HDL	Inhibits LCAT
ApoA-IV	Liver, small intestine	~44	Chylomicrons, HDL	Activates LCAT; transport and clearance of cholesterol
ApoB48	Small Intestine	~248	Chylomicrons	Cholesterol and lipid transport and clearance
ApoB100	Liver	~550	VLDL, LDL	Cholesterol and lipid transport, uptake
ApoC-I	Liver, small intestine	~7	VLDL, HDL	Inhibition of cholesterol ester transfer protein (CETP)
ApoC-II	Liver, small intestine	~9	Chylomicrons, VLDL, HDL	Activates Lipoprotein Lipase
ApoC-III	Liver, small intestine	~9	Chylomicrons, VLDL, HDL	Inhibits Lipoprotein Lipase
ApoD	Liver, intestine, pancreas, kidney	~32	HDL	Not well known, Transport of small hydrophobic molecules, aging
ApoE	Liver, Brain	~34	Chylomicrons, VLDL, HDL	Clearance of VLDL and chylomicron remnants, lipid transport in CNS
ApoF	Liver	~35kD	LDL, VLDL	Inhibits CETP
ApoH	Liver	~50	VLDL, binds to cardiolipin	Coagulation, apoptosis, inflammation, lipid metabolism
ApoJ	Liver	~70	HDL, LDL	Binds to Lipoprotein Receptor Protein 2 in skeletal muscles

Although a high resolution tertiary structure of ApoB has not been solved, the secondary structure of both the ApoB isoforms consists of amphipathic alpha helices and ß-sheets, which facilitate interaction with the hydrophobic lipids while easing movement through the blood stream (Cladaras et al., 1986; Knott et al., 1985; Segrest et al., 1999; Segrest et al., 1992; Segrest et al., 2001). Computational analyses have suggested a pentapartite model for the secondary structure of ApoB100 that consists of consecutive alternating domains organized in a NH_2-$\beta\alpha_1$-β_1-α_2-β_2-α_3-COOH manner (Segrest et al., 1994; Yang et al., 1989a; Yang et al., 1989b) (Figure 3A). The amino acids corresponding to these domains are as follows: $\beta\alpha_1$ (N terminal region 1-827), β_1 (827-2001), α_2 (2045-2587), β_2 (2571-4032), and α_3 (4017-4515) (Segrest et al., 1994; Yang et al., 1989a; Yang et al., 1989b). Results from trypsin digestion revealed that residues 1-827 of $\beta\alpha_1$ are solvent exposed and thereby are not bound to lipids (Yang et al., 1989a; Yang et al., 1989b). This domain also contains 16 cysteine residues (of the 25 found in ApoB100) that form disulfide bonds, indicating that this domain is tightly folded. This domain is also highly similar to lipovitellin, whose structure has been solved (Anderson et al., 1998; Mann et al., 1999). In contrast, residues 1701-3101 and 4101-4536 represent the lipid associating domains (Segrest et al., 2001; Yang et al., 1989a; Yang et al., 1989b). An intervening 37 amino acid sequence (from 3345-3381) acts as the LDL receptor ligand (Boren et al., 1998; De Loof et al., 1987; Krul et al., 1992; Law and Scott, 1990; Milne et al., 1989; Weisgraber et al., 1985; Welty et al., 1995a; Welty et al., 1995b; Yang et al., 1989b). A low-resolution structure of solubilized human ApoB 100 suggested that the N- and C-termini interact, most likely providing structural rigidity to the lipoprotein particle (Johs et al., 2006). ApoB100 also has 19 glycosylation sites which are added as it enters the ER (see below), and 10 of these are between amino acids 2752 and 4210 (Harazono et al., 2005) (Figure 3A). Overall, ApoB100 is both solvent exposed and penetrates the phospholipid monolayer and resides

in the hydrophobic core, thereby functioning as a detergent/surfactant to aid in the delivery of hydrophobic metabolites.

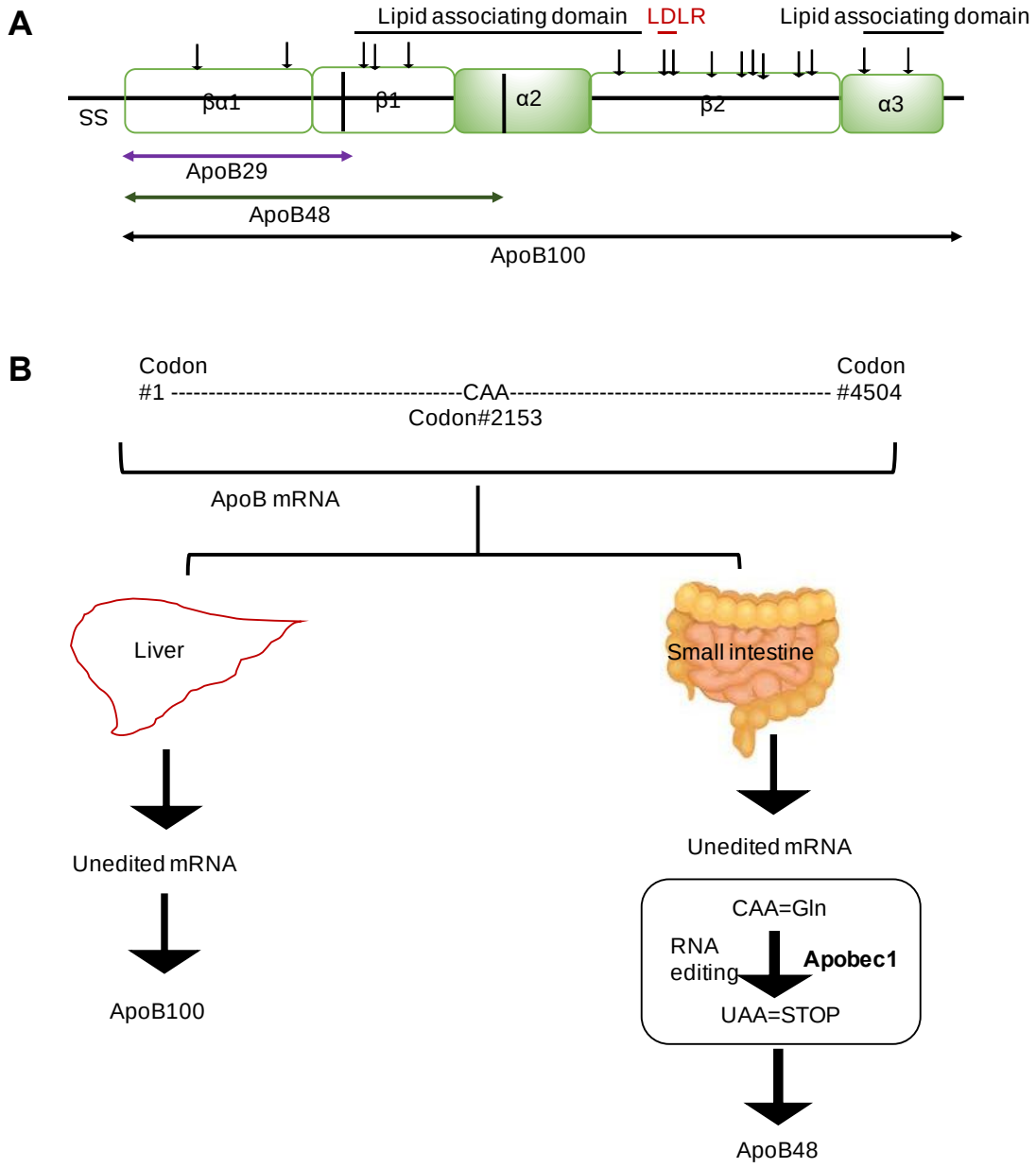

Figure 3. Secondary structure and isoforms of ApoB.

A. Secondary structure of ApoB100 is organized in a $\beta\alpha_1$ (N terminal region 1-827) -β_1 (827-2001)-α_2 (2045-2587)-β_2 (2571-4032) -α_3 (4017-4515) –COOH fashion. All the three isoforms, ApoB29, ApoB48, and ApoB100, are depicted in this figure. The downward arrows represent the 16 glycosylated asparagine residues (158, 956, 1341, 1350, 1496, 2752, 2955, 3074, 3197, 3309, 3331, 3384, 3438, 3868, 4210, 4404). Residues from 1701-3101 and 4101-4536 are

the lipid-associating domains. A 37 amino acid sequence from 3345-3381 binds the LDL receptor for delivery into recipient cells via endocytosis. B. ApoB48 is the product of an mRNA editing event catalyzed by Apobec1 in the small intestine in humans (see text for additional details).

1.1.3 ApoB levels are metabolically regulated by degradation

Almost one-third of all nascent polypeptides in eukaryotes, including ApoB, enter the ER to undergo folding, post-translational modifications, and/or membrane insertion (Ghaemmaghami et al., 2003; Kanapin et al., 2003). However, if a protein is misfolded or damaged, it is targeted for degradation by ER Associated Degradation (ERAD) (McCracken and Brodsky, 1996; Werner et al., 1996). This protein quality control pathway clears the secretory pathway of potentially toxic proteins and consists of four main events (Brodsky, 2007). The aberrant protein is first recognized by chaperones which include Hsps, it is then retrotranslocated into the cytosol and ubiquitinated by an E3 ubiquitin ligase, and the ERAD substrate is finally transported to and degraded by the proteasome.

Because a delicate balance in the level of ApoB is imperative to maintain human health, ApoB undergoes tight metabolic regulation. Surprisingly, ERAD is one of several mechanisms that regulate ApoB levels (Benoist and Grand-Perret, 1997; Liao et al., 1998; Mitchell et al., 1998) (also see below). However, ApoB is an unconventional ERAD substrate since it is typically degraded not due to any aberration within the protein itself, but rather due to the lipid status in the cell/ER. As it is being synthesized, ApoB is co-translationally translocated into the ER through the Sec61 translocon, guided by its signal peptide (Figure 4A) (Mitchell et al., 1998; Robson and Collinson, 2006). As it undergoes translocation into the ER lumen, the nascent ApoB polypeptide is lipidated to form a primordial lipoprotein particle. Lipidation of ApoB is catalyzed by the

Microsomal Transfer Protein (MTP) complex, which consists of the "M" subunit and a molecule of Protein Disulfide Isomerase (PDI) that also exhibits chaperone-like activity (Hussain et al., 1997; Hussain et al., 2003a; Hussain et al., 2003b; Jamil et al., 1996; Leung et al., 2000; Liao et al., 2003). MTP directly transfers lipids since ApoB co-immunoprecipitates with MTP (Bradbury et al., 1999; Patel and Grundy, 1996; Wu et al., 1996), and the PDI portion of the complex forms disulfide bonds as ApoB translocates into the ER (Wetterau et al., 1990). Lipidation and disulfide bond formation help support uni-directional translocation as the nascent ApoB polypeptide moves into the ER lumen. However, the presence of β sheets and pause transfer sequences slow the translocation of ApoB (Chuck and Lingappa, 1992; Chuck et al., 1990; Yamaguchi et al., 2006). This translocational pause favors ApoB lipidation. Ultimately, in the presence of enough

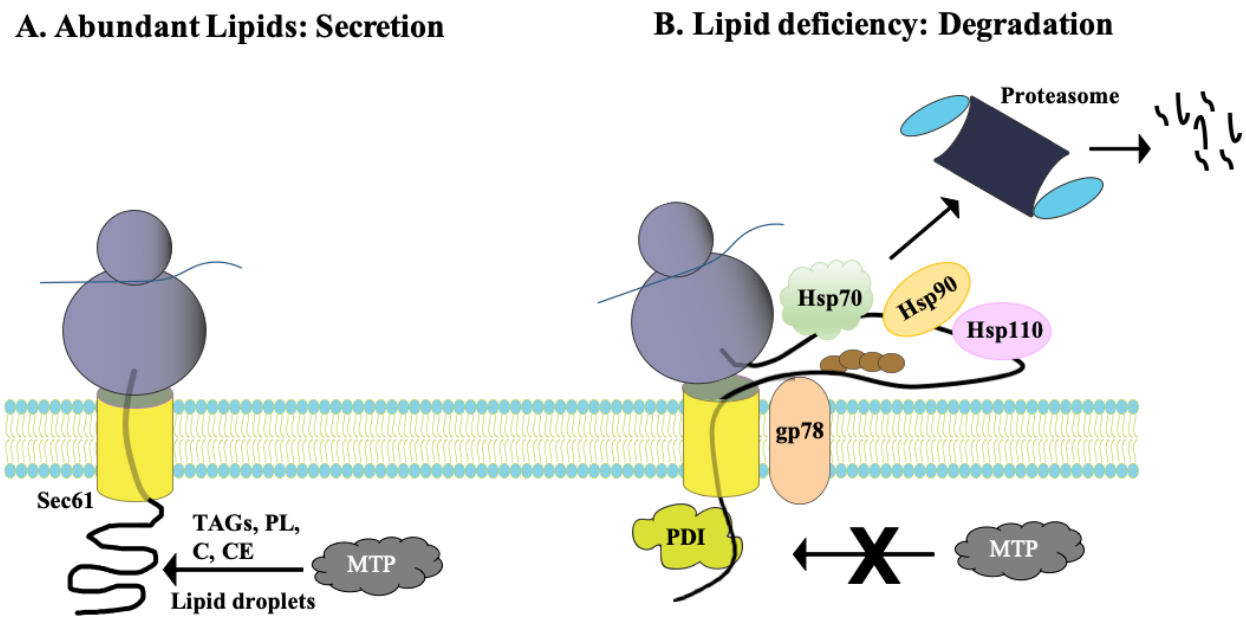

Figure 4. Levels of lipid and cholesterol determine the fate of ApoB.

A. Upon lipidation, ApoB is secreted as a primordial lipoprotein particle. ApoB undergoes co-translational translocation into the ER driven by its signal sequence through the Sec61 translocon (1). In the presence of sufficient lipids and MTP complex, ApoB is cotranslationally folded with triacylglycerol and cholesterol ester molecules (2). A precursor VLDL particle is formed which is subsequently secreted into the secretory pathway (3) B. In the absence of

lipidation, ApoB undergoes ERAD. After co-translational translocation (1), and due to insufficient lipidation, translocation of ApoB is slowed down. Continued translation leads to the exposure of hydrophobic loops into the cytosol (2), which are recognized by chaperones (see below) which recruit gp78 that ubiquitinate the loops (yellow circles, 3). ApoB is finally degraded by the proteasome (4).

phospholipids, fatty acids, and cholesterol, a primordial particle is formed. After disulfide bond formation (Wetterau et al., 1992; Wetterau et al., 1990) and glycosylation (Harazono et al., 2005), the primordial particle exits the ER in coat complex II (COPII) vesicle (Gusarova et al., 2003; Siddiqi et al., 2003) and enters the Golgi apparatus where it undergoes further lipidation and is finally secreted from cells (Figure 4A) (Brodsky et al., 2004; Butkinaree et al., 2014; Fisher and Ginsberg, 2002; Fryer et al., 2014; Gusarova et al., 2003; Gusarova et al., 2007).

When a cell lacks adequate lipids (low dietary intake) or in the absence of the MTP complex—as occurs in a rare human genetic disorder known as abetalipoproteinemia (Benayoun et al., 2007; Di Leo et al., 2005; Leiper et al., 1994; Pons et al., 2011; Walsh et al., 2015; Welty, 2020; Wetterau et al., 1992)—translocation is slowed (Figure 4B). Low levels of lipids and cholesterol impede LDL assembly, eliminating the driving force needed to pull the polypeptide into the ER lumen. Continued translation subsequently exposes hydrophobic loops into the cytosol. These aggregation-prone cytoplasmic loops are recognized by Heat shock proteins (Hsps). This family of proteins play key roles during ERAD as well as other quality control systems by facilitating protein translocation into the ER, helping proteins fold, preventing their aggregation, and targeting misfolded proteins to the proteasome (Brodsky, 2007, 2012; Nishikawa et al., 2005; Rosenzweig et al., 2019; Saibil, 2013; Vembar and Brodsky, 2008). Hsps act as foldases, holdases, or disaggregase. In some cases, Hsps facilitate the interaction of ERAD substrates with E3 ubiquitin ligases (Nakatsukasa et al., 2008). To date, an ER membrane-localized E3 ubiquitin ligase, gp78, is the only ligase reported to ubiquitinate ApoB (Fisher et al., 2011; Liang et al., 2003). After ubiquitination, ApoB is

is “retrotranslocated” back through the Sec61 translocon and is degraded by the cytosolic 26S proteasome (Fisher et al., 1997; Pariyarath et al., 2001; Yokota et al., 2000).

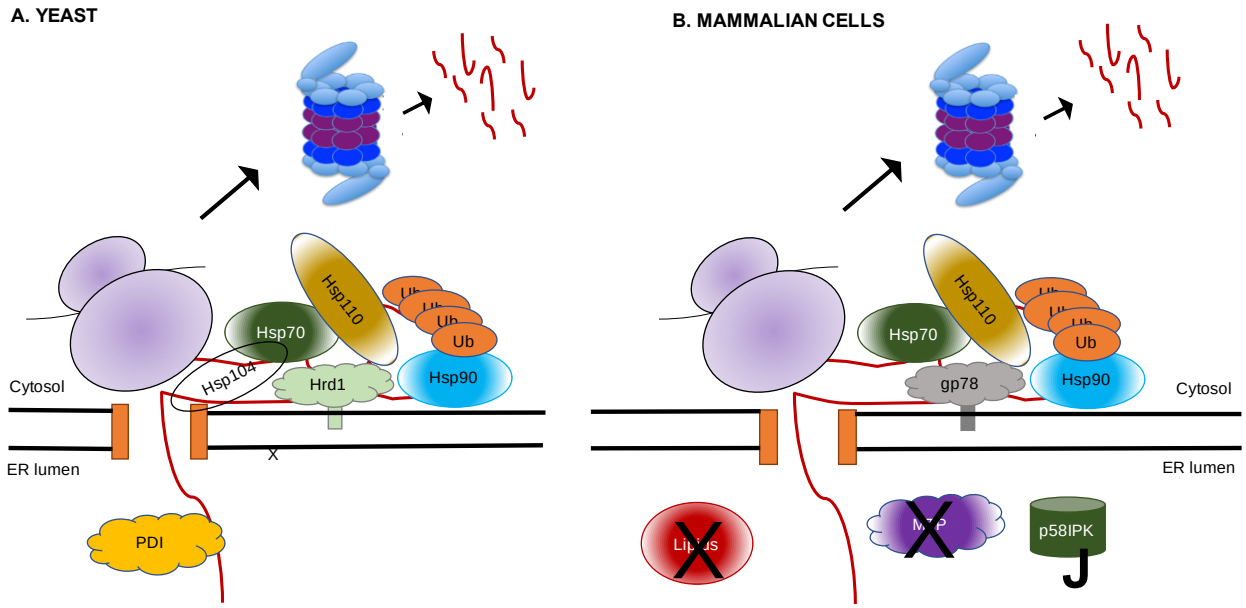

Figure 5. Schematic showing factors involved in ApoB ERAD.

A. Since yeast lack the MTP complex, ApoB is always destined for ERAD. In yeast, Hsp70, Hsp90, Hsp104, PDI, and the Hrd1 ubiquitin ligase, which is related to gp78, have been shown to facilitate ApoB degradation, whereas Hsp110 stabilizes ApoB. **B.** In mammalian hepatoma cells, Hsp70, Hsp90, Hsp110, p58IPK, and gp78 have been shown to facilitate degradation of ApoB.

To date, studies conducted in yeast (Figure 5A) and mammalian cell models (Figure 5B) have identified and characterized several classes of Hsps, including Hsp110, Hsp90, Hsp70, BiP, p58IPK (DNAJC3), calnexin, calreticulin, and PDI, which play critical roles during the ERAD of ApoB (Chen et al., 1998; Doonan et al., 2019; Fisher et al., 1997; Ginsberg, 1997; Gusarova et al., 2001; Hrizo et al., 2007; Rutledge et al., 2013; Tatu and Helenius, 1999; Zhou et al., 1995). Although not shown directly, these chaperones most likely help ubiquitinate and target the exposed ApoB loops to the proteasome and prevent the aggregation of this large, hydrophobic protein in

the cytosol until it is degraded. However, the full panel of factors that regulate ApoB degradation along with the chaperones that deliver ApoB to the ubiquitin machinery remain unknown.

1.1.4 ApoB is also degraded by post ER presecretory proteolysis (PERPP)

Although the lipid status of the cell regulates ApoB levels by the ERAD pathway, how does the Protein Quality Control (PQC) machinery respond if ApoB is damaged and potentially becomes toxic? Under these conditions, a PQC mechanism called post ER presecretory proteolysis (PERPP) targets ApoB for degradation (Brodsky and Fisher, 2008; Fisher et al., 2001; Fisher and Williams, 2008; Olofsson and Boren, 2012; Pan et al., 2004; Pan et al., 2008). PERPP is independent of the lipid status of the cell, is characterized by a specialized form of autophagy, and in some cases upwards of 90% of newly translated ApoB can be degraded by this pathway. There are two major factors that can direct ApoB to PERPP. First, PERPP can be triggered by oxidative damage caused by poly unsaturated fatty acids (PUFAs), including N-3 fatty acids like eicosapentaenoic and docosahexaenoic acid, which are abundant in fish oils (Fisher et al., 2001; Olofsson and Boren, 2012; Pan et al., 2004; Pan et al., 2008). Interestingly, a high intake of N-3 fatty acids is correlated with lower circulating triglyceride levels in humans, likely by stimulating the PERPP of ApoB (Djousse et al., 2003; Harris, 1989). Second, after an acute increase in insulin, the phosphatidylinositol 3-kinase (PI_3K) pathway is activated, which in turn inhibits the lipidation of ApoB and subsequent LDL formation (Au et al., 2004; Chirieac et al., 2006; Phung et al., 1997; Sparks and Sparks, 1990). This process has also been termed as Insulin Dependent ApoB Degradation (IDAD) (Sparks et al., 2013). Interestingly, patients with insulin resistance or type II diabetes mellitus have higher levels of circulating ApoB and VLDL (Khavandi et al., 2017).

1.1.5 Diseases caused due to abnormal ApoB levels

As noted above, cardiovascular diseases are one of the leading causes of death worldwide. In the U.S., cardiovascular diseases cause one-in-four deaths (Benjamin et al., 2019; Heron, 2017). As per a CDC report on mortality in 2019, cardiovascular diseases caused 659,041 deaths, followed by cancer (599,601) and chronic lower respiratory disease (159,979). One person dies of cardiovascular disease every 36 seconds, and cardiovascular diseases incur a cost of over $200 billion every year in health care services, treatment, and lost productivity.

Coronary artery disease (CAD), caused due to the gradual deposition of cholesterol and fat forming plaques in the arteries, is the most common form of cardiovascular disease. CAD kills approximately 400,000 people annually, and it is estimated that ~6.7% of adults (~18.2 million individuals) suffer from CAD (Benjamin et al., 2019; Heron, 2017). CAD occurs when arteries carrying blood to the heart become narrowed due to the deposition of cholesterol and fat molecules, which in turn become oxidized and aggregate, thereby forming arterial plaques.

Elevated levels of LDLs/VLDLs circulating in the bloodstream lead to the build-up of plaques, resulting in the constriction of arteries and restricting blood flow (Libby et al., 2019). Endothelial cells retain these lipoproteins, which get oxidized and aggregate over time. This then leads to increased expression of selective monocyte adhesion molecules. The recruited monocytes differentiate into macrophages and engulf the ApoB-containing lipoprotein particles. Over time, foam cells form, and inflammatory signals and the continued oxidization of lipids eventually lead to plaque formation. If these fail to regress (Bittencourt and Cerci, 2015; Daida et al., 2019), the plaque can grow and can completely cut off blood supply to the heart, leading to fatal heart injuries. Plaques can also become dislodged and circulate through the bloodstream to other parts of the body, including heart or brain (Insull, 2009; Stefanadis et al., 2017).

In most cases, diseases linked to high levels of circulating cholesterol and other lipids arise from high-fat diets, lifestyle choices, and environmental factors. There are also likely to be many unknown genetic causes of these diseases (Butler, 2010; Kupper et al., 2006; Surendran et al., 2016). However, one known disease is Familial Hypercholesterolemia (FH) (Sharifi et al., 2017). FH is an inherited disease symptomized by high cholesterol levels in bloodstream and arises most commonly from loss-of-function mutations in the gene encoding the LDL receptor (LDLR) (Hobbs et al., 1992). Mutations in the LDLR binding region in ApoB100 also lead to FH (Fernandez-Higuero et al., 2015; Thomas et al., 2013). In this case, LDL particles can no longer be endocytosed into peripheral cells, resulting in higher levels of circulating atherogenic LDL in the bloodstream. FH affects about 1.3 million people in the US but only 10% are aware of it, which puts these individuals at an increased risk of developing atherosclerosis (thefhfoundation.org). Overall, homozygous FH can cause fatal heart injuries if untreated in early adulthood (Abul-Husn et al., 2016; Wiegman et al., 2015).

In contrast to FH, low circulating levels of ApoB-containing particles can cause familial hypobetalipoproteinemia (FHB; also see above), which is symptomized by neuromuscular degeneration, vitamin deficiency, ataxia, and sensory disorders (Collins et al., 1988). FHB most commonly arises from mutations in ApoB, but rare mutations in MTP can cause abetalipoproteinemia (Krul et al., 1992; Leung et al., 2000; Linton et al., 1993; Musialik et al., 2020; Pons et al., 2011; Schonfeld et al., 2005; Talmud et al., 1992; Welty, 2020; Whitfield et al., 2003; Young et al., 1990). Patients suffering with FHB or abetalipoproteinemia are required to take fat-soluble vitamin supplements, particularly vitamins A, K and E.

1.1.6 Treatments for CAD

Current treatments for CAD include drugs that target various aspects of lipid metabolism, including the synthesis, transport, and endocytosis of lipids and/or cholesterol (Adhyaru and Jacobson, 2018; Goldstein and Brown, 2015; Larsen et al., 2019; Libby and Everett, 2019). For example, statins, which have been in use for >35 years, inhibit a reaction catalyzed by one of the rate-limiting steps of cholesterol synthesis (HMG-CoA reductase). Statins not only inhibit cholesterol synthesis but also increase levels of LDL receptors through upregulation of Sterol Regulatory Element-Binding Proteins (SREBPs), which are transcription factors that regulate expression of genes involved in lipid metabolism. Statins lower cholesterol levels which upregulate SREBPs that upregulate LDLR causing increased uptake of LDLs from the bloodstream (Shimano, 2009). However, not all patients respond equally to statins. The decrease in levels of LDL can vary from 5-70% in an individual (Reiner et al., 2013; Reiner and Tedeschi-Reiner, 2013), and this variation is attributed to polymorphisms in genes linked to statin metabolism (pharmacodynamics and pharmacokinetics) (Dadu and Ballantyne, 2014; Reiner, 2014; Sikka et al., 2011; Ward et al., 2019). Additionally, statins elicit multiple side-effects including statin-associated muscle symptoms (SAMSs), including muscle weakness, leg cramps, and myopathy, forcing some patients to discontinue medication or lower the dose.

To circumvent these issues, other targets are being considered to reduce the risk of cardiovascular disease. Two recently approved drugs include Mipomersen and Evolucumab. Mipomersen is an antisense oligonucleotide that depletes ApoB and lowers lipid and cholesterol levels (Crooke et al., 2005; Doonan et al., 2018; Linton et al., 2000; McGowan et al., 2012; Merki et al., 2008; Raal et al., 2010; Wong and Goldberg, 2014; Zimmermann et al., 2006). In contrast, evolucumab is an inhibitor of PCSK9, an enzyme that facilitates LDL receptor degradation, so

more receptors reside at the surface and LDL is endocytosed more effectively (Narasimhan, 2017; Sabatine et al., 2017; Schulz and Schluter, 2017; Zhang et al., 2015b). Mipomersen and Evolucumab are prescribed to patients with FH (see section 1.1.5). Nevertheless, each of the currently used drugs can elicit side effects, are costly, and/or have not been approved for all patients due to these limitations. Overall, despite the progress made towards combating CAD, we still lack an effective and affordable treatment. The identification of factors that regulate circulating cholesterol levels in the bloodstream will provide new potential therapeutic targets to treat CAD.

1.2 Select examples of natively folded proteins that are targeted for ERAD

(Following section has been modified and published as a review article in *Biomolecules.* Kumari, D.; Brodsky, J.L. The Targeting of Native Proteins to the Endoplasmic Reticulum Associated Degradation (ERAD) Pathway: An Expanding Repertoire of Regulated Substrates. Biomolecules 2021, 11, 1185. https://doi.org/ 10.3390/ biom11081185)

1.2.1 Introduction

Proteins play myriad roles in a cell, and the acquisition of their final folded state and structural integrity are imperative for function. Misfolded or non-native proteins structures can lead to a plethora of diseases (Guerriero and Brodsky, 2012; Morimoto, 2008; Wentink et al., 2019). To destroy these misfolded and potentially toxic proteins, eukaryotic cells survey protein integrity at multiple checkpoints as a protein matures. The factors that survey nascent proteins,

attempt to repair misfolded species, facilitate maturation, and target misfolded substrates for degradation collectively maintain protein quality control (PQC).

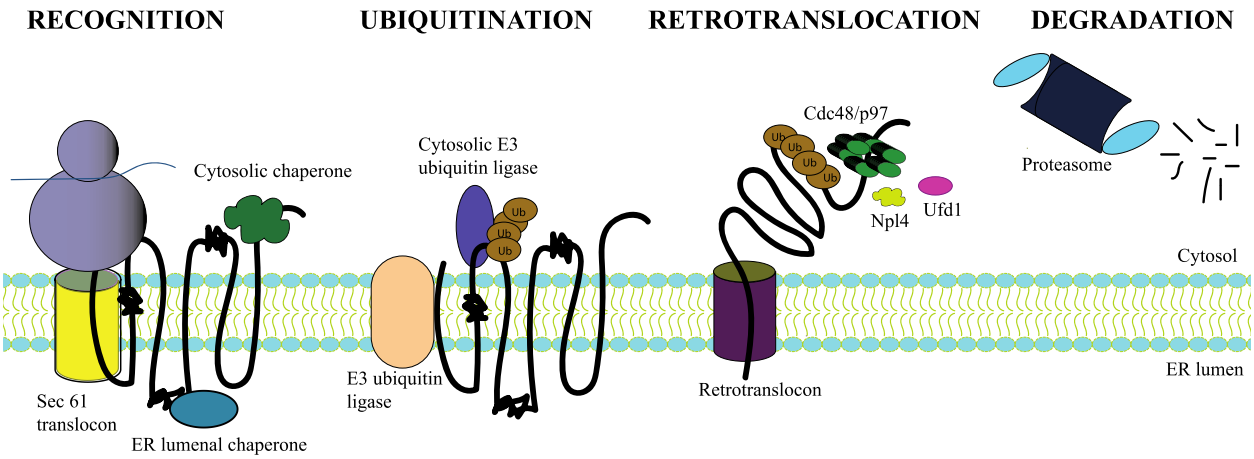

Figure 6. Four major steps in Endoplasmic Reticulum Associated Degradation (ERAD).

1. Recognition: A misfold region (condensed) in the nascent polypeptide's luminal, transmembrane or cytosolic domain is recognized by cytosolic or luminal chaperones. 2. Ubiquitination: Chaperones then recruit the ubiquitination machinery, and a E3 ubiquitin ligase tags the misfolded protein with ubiquitin. 3. Retrotranslocation: Ubiquitinated protein is then retrotranslocated through the retrotranslocon, which is mediated by the ATP-hydrolyzing Cdc48 complex (not shown). 4. Degradation: The misfolded protein is finally degraded by the 26S proteasome into short peptides.

Between a quarter and one-third of all nascent proteins enter the endoplasmic reticulum (ER) during or soon after synthesis to fold, become post-translationally modified, and/or insert into the membrane (Braakman and Bulleid, 2011; Ghaemmaghami et al., 2003; Kanapin et al., 2003). As a protein undergoes these processes, it is also subject to surveillance by several ER quality control pathways. As noted above, one of these pathways is ERAD (McCracken and Brodsky, 1996; Werner et al., 1996), which constitutes a complex array of factors to eliminate

aberrant proteins that pose a threat to ER and consequently cellular homeostasis (Christianson and Ye, 2014; Meusser et al., 2005; Stevenson et al., 2016; Vembar and Brodsky, 2008). This PQC pathway clears the secretory pathway of potentially toxic proteins and consists of four main events (Brodsky, 2007). The aberrant protein is first recognized by chaperones, it is then retrotranslocated into the cytosol and next ubiquitinated by an E3 ubiquitin ligase, and the ERAD substrate is finally transported to and degraded by the proteasome (Figure 6).

Although ERAD was first discovered and was initially thought to primarily target misfolded proteins (Needham and Brodsky, 2013), ERAD also regulates the levels and thus the activities of several natively folded proteins (Table 3). In retrospect, this is not surprising since there are >7000 proteins that interact with the ER at some point during biogenesis (Venter et al., 2001). These factors support myriad processes, many of which are regulated. In effect, the rapid degradation of these proteins represents the best and most complete way to downregulate function. But besides maintaining the levels of these natively folded proteins, the ERAD pathway can also regulate the stoichiometry of multimeric protein complexes. Overall, ERAD maintains cellular protein quantity as well as protein quality control.

In this section, I provide a brief overview on the classes of natively folded proteins that are regulated by ERAD. In general, these fall into two classes, those that are linked to lipid metabolism and those that are linked to metabolite and solute transport. To better focus on these active enzymes and transporters that are regulated by ERAD, I will be excluding ERAD substrates that are misfolded, represent unassembled units, or are regulated by pathogens but please see (van de Weijer et al., 2015).

1.2.2 Lipid metabolism

The ER serves a major hub of lipid metabolism. A variety of lipids, including fatty acids, triacylglycerol, phospholipids, and cholesterol, are synthesized in the ER. The lipids synthesized in the ER can be used by the cell or can be assembled into lipoprotein particles in the ER lumen, which are then transported to the circulatory system (Funato et al., 2020; Goldstein and Brown, 2015). Consequently, extensive mechanisms to regulate these processes are used since an imbalance can disrupt cellular homeostasis and cause several diseases, including dyslipidemia, insulin resistance, fatty liver, and cardiovascular diseases (Jacquemyn et al., 2017). These regulatory processes can occur at the level of transcription, translation, altered enzyme kinetics, or degradation. Indeed, some of the earliest and best described ERAD substrates are linked to lipid metabolism (van den Boomen et al., 2020; Wangeline et al., 2017). The following section outlines the activity and regulation of some of these enzymes via ERAD.

1.2.3 Ergosterol synthesis in yeast

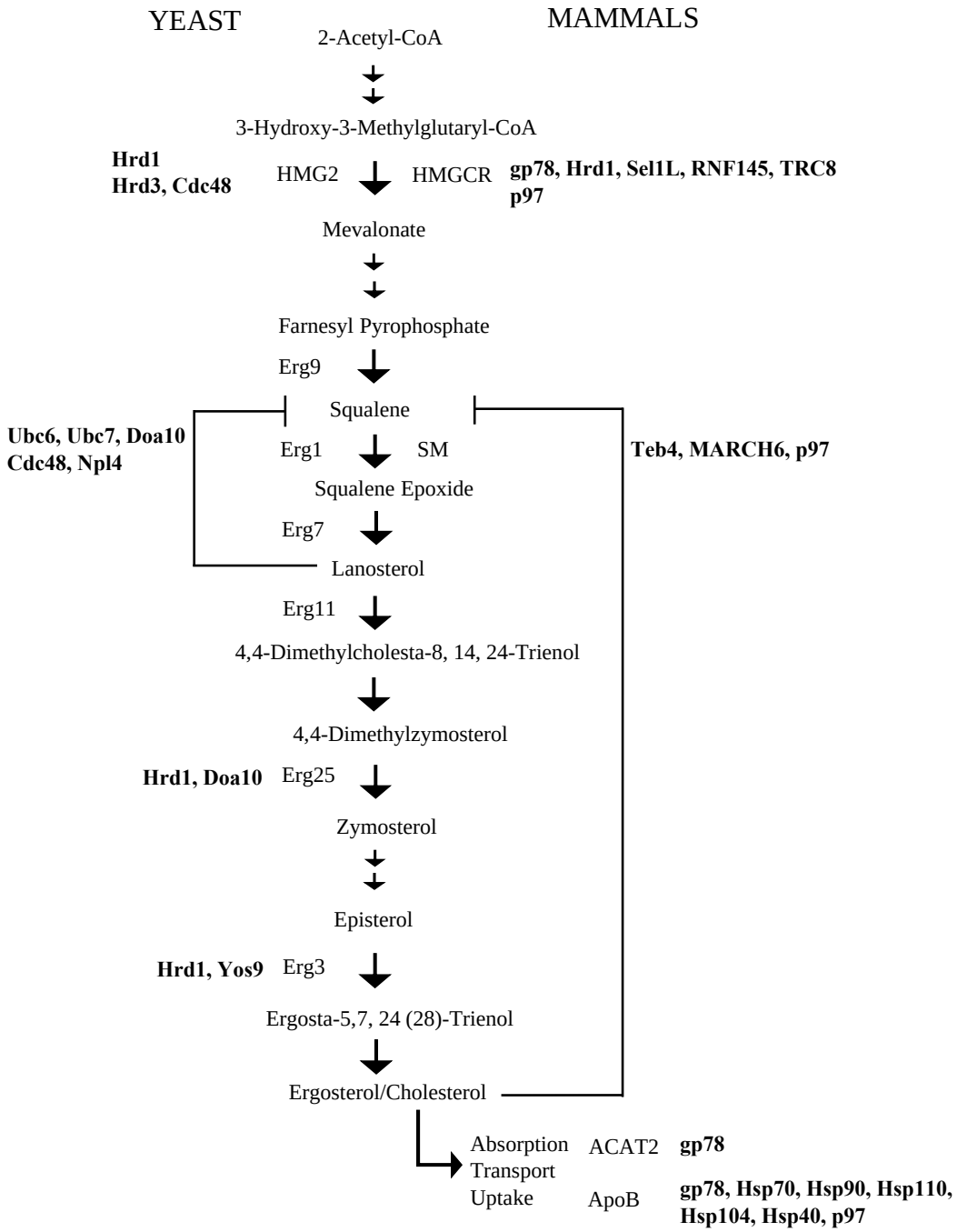

Figure 7. Ergosterol/Cholesterol biosynthetic pathway.

A cascade of enzymes catalyzes the ergosterol (yeast/fungi) and cholesterol (mammals) biosynthetic pathways. Key enzymes regulated by ERAD are shown in yeast (blue) and mammals (orange). ERAD effectors are shown in bold.

1.2.3.1 Erg1

Erg1, or squalene monooxygenase, catalyzes the epoxidation of squalene to 2,3 oxidosqualene (squalene epoxide) (Figure 7). A SILAC (Stable Isotope labeling by amino acids in cell culture) based screen for substrates in a yeast strain deleted for Doa10, an ER membrane E3 ubiquitin ligase, identified Erg1 as an ERAD substrate (Foresti et al., 2013; Hitchcock et al., 2003). Treatment with inhibitors of ergosterol synthesis pathway indicated that Doa10 dependent proteasomal degradation of Erg1 was caused when levels of lanosterol rose in the cells. Several lysine residues in the C-terminal region of Erg1 were shown to be ubiquitinated (Foresti et al., 2013; Hitchcock et al., 2003). For example, a lysine residue at position 311 was essential for Doa10 dependent proteasomal degradation. Moreover, deletion of Ubc6 or Ubc7, which serve as ubiquitin conjugating enzymes for Doa10 (Carvalho et al., 2006), also stabilized Erg1. Notably, this pathway appears to be conserved since squalene monooxygenase in mammals is ubiquitinated by the E3 ubiquitin ligase Teb4, the mammalian homolog of Doa10 (Foresti et al., 2013).

1.2.3.2 Erg3

Erg3 is a C-5 sterol desaturase that introduces a C-5(6) double bond into episterol, an intermediate during ergosterol biosynthesis (Figure 7). A SILAC based screen in yeast cells lacking another ER membrane E3 ubiquitin ligase, Hrd1 revealed Erg3 as an endogenous ERAD substrate (Jaenicke et al., 2011). Erg3 also co-immunoprecipitated with Hrd1, and this interaction was further stabilized when Ubc7 was deleted. Unlike Erg1, Erg3 is neither ubiquitinated by Doa10 nor dependent on the levels of sterol.

1.2.3.3 Erg25

Erg25, or methylsterol monooxygenase, converts dimethylzymosterol to zymosterol (Figure 7). Although previous hints that the enzyme was targeted for ERAD were provided by mass spec experiments in which Hrd1 deletion in yeast increased Erg25 half-life (Buck et al., 2020; Christiano et al., 2014), Erg25 was also isolated by a substrate capture experiment in yeast expressing an epitope tagged proteasome subunit (Buck et al., 2020; Christiano et al., 2014). Addition of proteasome inhibitor detected Erg25 as a proteasome substrate. Interestingly, Erg25 degradation was enhanced in the presence of an anti-fungal, and in contrast to Erg1 and Erg3, degradation required both Hrd1 and Doa10. Since these enzymes recognize distinct domains in ERAD substrates (ER lumen and membrane versus cytosolic region, respectively) (Carvalho et al., 2010), these data suggest that the "decision" leading to Erg25 degradation requires lipid-mediated destabilization of domains throughout the Erg25 protein.

1.2.3.4 3-Hydroxy-3-methylglutaryl-coenzyme A reductase (HMGCR)

Like ergosterol, cholesterol is synthesized from isoprene units via the mevalonate pathway and requires ~20 steps/reactions. Most of the enzymes catalyzing these steps are situated in the ER. In contrast to yeast, cholesterol can be acquired from the diet or is manufactured in cells. The ER localized enzyme, HMGCR, catalyzes the production of HMG-CoA from acetoacetyl-CoA, which is a rate-limiting step in both the production of ergosterol and cholesterol as well as thousands of isoprene derivatives, including sterols, terpenes, bile salts, dolichol, heme-A, and ubiquinone. Thus, HMGCR is subject to multiple levels of regulation, including transcription, translation, post-translational modifications, and degradation (Goldstein and Brown, 1990; Jo and Debose-Boyd, 2010). When levels of circulating cholesterol are low, the transcription of HMGCR increases and upregulates endogenous cholesterol synthesis. Based on the long-term focus on

HMGCR, which is the target of statins (Adhyaru and Jacobson, 2018; Goldstein and Brown, 2015; Larsen et al., 2019; Libby and Everett, 2019), and based on the development of a powerful yeast genetic screen in which its biogenesis can be examined (Wangeline et al., 2017), HMGCR is one of the most widely studied ERAD substrates that is metabolically regulated by ERAD.

Early work established that the degradation of HMGCR is entirely via the proteasome and that vacuole or lysosomal inhibition in yeast or mammalian cells, respectively, do not affect HMGCR levels (Hampton and Rine, 1994; Inoue et al., 1991; Lecureux and Wattenberg, 1994). Work in mammalian cells also indicated that one or potentially several E3 ubiquitin ligases, e.g., gp78, Hrd1 and TRC8, regulate HMGCR levels (DeBose-Boyd, 2008; Kikkert et al., 2004; Song et al., 2005) (Jo et al., 2011a). Role of gp78 has however been inconsistent in the several model systems (mice models, mouse fibroblasts, cell lines) used, potentially due to genetic variability, experimental factors, or off-target effects. HMGCR is then recognized by p97, retrotranslocated and finally degraded by the proteasome (Ikeda et al., 2009) (Jo and Debose-Boyd, 2010; Jo et al., 2011a; Jo et al., 2011b; Song et al., 2005).

1.2.3.5 Squalene monooxygenase (SM)

Squalene monooxygenase (SM) catalyzes the conversion of squalene to 2,3 monooxidosqualene, which is the second rate-limiting step in cholesterol synthesis. Unlike HMGCR (see section 1.2.3.4 above), the degradation of SM is directly driven by cholesterol (Chua et al., 2020; Chua et al., 2019a; Chua et al., 2019b). The N-terminal 100 amino acids of SM act as a cholesterol responsive regulatory domain. Like HMGCR, it is likely that the binding of cholesterol alters the conformation, thereby triggering recognition by the membrane-associated E3 ubiquitin ligase RING finger 6 (MARCH6) or Teb4. In yeast, the degradation of the enzyme (Erg1) is driven by Doa10 (Foresti et al., 2013; Hitchcock et al., 2003).

1.2.3.6 Acetyl-coA acetyltransferase 2 (ACAT2)

ACAT2, expressed in the liver and small intestine, converts cholesterol and fatty acid to cholesterol esters and aids cholesterol absorption and lipoprotein assembly. Higher levels of ACAT2 have been linked to atherosclerosis (Parini et al., 2009; Rudel et al., 2001). When lipids are deficient, ACAT2 is surprisingly ubiquitinated at Cys-277 (C277), an event that is mediated by gp78 (Wang et al., 2017). Although ubiquitin is usually conjugated onto Lys resides, non-canonical ubiquitination of cysteine residues has been observed for several other proteins, including Pex5p and Pex20p, that play roles in protein translocation (Carvalho et al., 2007; Leon and Subramani, 2007; McDowell and Philpott, 2013). In contrast, high concentrations of cholesterol, sterol intermediates (lanosterol), or saturated fatty acids generate reactive oxygen species that oxidize C277 to a sulfenic acid (-SOH), stabilizing ACAT2 and thereby increasing the levels of cholesterol esters.

1.2.4 Metabolite and solute transporters

1.2.4.1 Apolipoprotein B

ApoB is an unconventionally regulated ERAD substrate as it is cotranslationally degraded (Benoist and Grand-Perret, 1997; Mitchell et al., 1998). As ApoB undergoes translocation through Sec61 (Mitchell et al., 1998; Robson and Collinson, 2006), the MTP complex transfers TAGs, PLs, cholesterol and CEs to ApoB through lipid associating domains (Hussain et al, 1997; Hussain et al, 2003), and a primordial lipoprotein particle is formed. Lipid loading is facilitated by pause transfer sequences (Chuck & Lingappa, 1992; Kivlen et al, 1997; Yamaguchi et al, 2006), which slow translocation, and the lipids are thought to become bound to

a β-sheet-rich domain in ApoB (see above). Once lipidated, the primordial particle enters the Golgi complex for further lipidation to become a mature very low density lipoprotein (VLDL) particle or a chylomicron, which are then secreted into the circulatory and lymphatic systems (Gusarova et al., 2003; Sane et al., 2017; Siddiqi et al., 2003).

However, when lipids are deficient, ApoB translocation slows (Dixon et al, 1991), and continued translation exposes large hydrophobic loops to the cytosol where molecular chaperones and the ubiquitination machinery target it for degradation (Fisher et al., 1997; Pariyarath et al., 2001) (also see Figure 4). As noted in Figure 5, the chaperones that associate with ApoB include the ER lumenal lectin, calnexin, as well as lumenal protein disulfide isomerase and cytosolic Hsp70, Hsp90, Hsp110, and in yeast, Hsp104. Whereas some of these proteins promote the degradation of ApoB (Hsp70, Hsp90, the PDIs, Hsp104), Hsp110 stabilizes the protein (Chen et al., 1998; Doonan et al., 2019; Fisher et al., 1997; Ginsberg, 1997; Gusarova et al., 2001; Hrizo et al., 2007; Rutledge et al., 2013; Tatu and Helenius, 1999; Zhou et al., 1995). The identification of these factors was made possible by utilizing yeast, hepatoma cell lines and in vitro experiments. After selection, ApoB is ubiquitinated by Hrd1 in yeast or gp78 in humans (Fang et al., 2001; Rubenstein et al., 2012; Rutledge et al., 2009) and degraded by 26S proteasome. It is stunning that this ~500 kDa protein is constitutively targeted for ERAD between meals, suggesting that the importance of regulated degradation outweighs the energetic cost of synthesizing this large, labile protein.

1.2.4.2 Inositol 1, 4, 5-triphosphate receptors (IP_3R)

IP_3 receptors are tetrameric ER transmembrane channels responsible for the release of stored calcium upon binding to the second messenger IP_3, which is generated in the plasma

membrane in response to various signal transduction pathways (Wojcikiewicz et al., 2009). IP_3 receptors are conserved among many species and expressed in all animal tissues. They play key roles in several processes dependent on calcium signaling, including cell division, apoptosis, fertilization, development, and memory (Hamada and Mikoshiba 2020; Mikoshiba 2015). Interestingly, elevated levels of IP_3 resulting from treatment with certain activators leads to receptor ubiquitination and subsequent proteasomal degradation (Khan and Joseph 2003; Pearce, et al. 2007). Because IP_3 receptor degradation is independent of treatment with Brefeldin A or inhibition of lysosomal proteases, early work suggested they are degraded in the ER, thereby positioning ERAD as a means to downregulate receptor activation (Alzayady et al., 2005; Lu et al., 2011; Webster et al., 2003; Wojcikiewicz et al., 1999; Wojcikiewicz et al., 1994; Wojcikiewicz and Nahorski, 1991). Consistent with this view, the ERAD-associated E2 ubiquitin conjugating enzyme Ubc7 mediates receptor ubiquitination, and degradation requires the VCP/p97 complex (Alzayady et al., 2005; Lu et al., 2011; Webster et al., 2003; Wojcikiewicz et al., 1999; Wojcikiewicz et al., 1994; Wojcikiewicz and Nahorski, 1991). Other factors required for degradation include two transmembrane proteins in the ER, SPFH1 and SPFH2. SPFH1/2 localize to cholesterol rich regions in the ER membrane are thought to recognize the lumenal regions of activated IP_3 receptors and then recruit Ubc7 as well as E3 ubiquitin ligases. To date, the ER membrane localized ubiquitin ligase RNF170 is the only E3 shown to ubiquitinate IP3 receptors (Alzayady et al., 2005; Lu et al., 2011; Webster et al., 2003; Wojcikiewicz et al., 1999; Wojcikiewicz et al., 1994; Wojcikiewicz and Nahorski, 1991).

1.2.4.3 Pca1

Pca1 is a P-type ATPase multi-transmembrane heavy metal (cadmium) transporter in the yeast *Saccharomyces cerevisiae* expressed at the plasma membrane (Kuhlbrandt, 2004; Rad et al.,

1994; Shiraishi et al., 2000). In the absence of cadmium in the growth media, Pca1 is degraded by the ERAD pathway as a result of the function of its N-terminal domain, which acts as a cadmium sensor (Adle and Lee, 2008). Moreover, cadmium binds to cysteine residues in the N-terminal domain, thereby masking the degradation signal. A genetic screen revealed that Pca1-GFP was stabilized when the gene encoding Cue1, which recruits the ubiquitin conjugating enzyme Ubc7 to the ER membrane (Biederer et al., 1997), was deleted. Pca1 was also stabilized in yeast lacking Doa10, which was further validated by observing decreased ubiquitination levels when Doa10 was absent. Moreover, chemical crosslinking revealed association between the N-terminal domain of Pca1 and Doa10 (Adle and Lee, 2008). Thus, this system allows yeast cells to respond rapidly and effectively to the presence of cadmium by regulating the levels of Pca1 by ERAD.

Table 3. Natively folded ERAD substrates

Organism	Substrate	Function	ERAD effectors	References
Yeast	Erg1	Ergosterol synthesis	Doa10/Teb4, Ubp3	(Foresti et al., 2013) (Hitchcock et al., 2003) (Lan et al., 2021)
Yeast	Erg3	Ergosterol synthesis	Hrd1, Yos9, Ubp3	(Jaenicke et al., 2011; Lan et al., 2021)
Yeast	Erg 25	Ergosterol synthesis	Hrd1, Doa10	(Buck et al., 2020; Christiano et al., 2014)
Yeast	Pca1	Cadmium transporter	Cue1, Ubc6, Doa10, Cdc48	(Adle et al., 2009; Smith et al., 2016)
Mammals	Acetyl-CoA Acetyltransferase 2	TAG synthesis cholesterol	gp78	(Wang et al., 2017)
Yeast, Mammals	ApoB	Lipoprotein assembly, transport, uptake	Hsp70, Hsp90, Hsp110, Hsp104, PDI, gp78	(Benoist and Grand-Perret, 1997; Doonan et al., 2019; Fisher et al., 1997; Grubb et al., 2012; Hrizo et al., 2007; Sakata et al., 1999; Yeung et al., 1996)
Yeast, Mammals	3-Hydroxy-3-Methylglutaryl-CoA Reductase (HMGCR)	Sterol synthesis	Hrd1, Hrd3, Cdc48/p97, gp78, Trc8	(Elsabrouty et al., 2013; Hampton et al., 1996; Inoue et al., 1991; Jansson, 1970; Jo et al., 2011b; Ravid et al., 2000; Sever et al., 2003; Tsai et al., 2012; Zelcer et al., 2014)
Mammals	Squalene Monooxygenase	Sterol synthesis	p97, MARCH6	(Chua et al., 2020; Chua et al., 2019a; Chua et al., 2019b; Foresti et al., 2013; Gill et al., 2011; Zelcer et al., 2014)
Mammals	IP3 receptor	Calcium signaling	Spfh1, p97, Gp78, and Ufd1	(Khan and Joseph, 2003; Pearce et al., 2007)

2.0 ROLES OF HSP40s AND HRD1 E3 UBIQUITIN LIGASE IN THE BIOGENESIS OF APOB

2.1 Introduction

Each year, cardiovascular diseases kill ~18 million people, and one-in-four deaths in the United States is due to cardiovascular disease (Benjamin et al., 2019; Heron, 2017). Coronary artery disease (CAD) is the most common form of cardiovascular disease and arises when arteries narrow due to the gradual deposition of cholesterol and fat forming plaques. This process, known as atherosclerosis, limits blood supply to the heart, leading to fatal heart injury. Current treatments for CAD include drugs that target various aspects of lipid metabolism, including the synthesis, transport, and endocytosis of lipids and/or cholesterol (Adhyaru and Jacobson, 2018; Goldstein and Brown, 2015; Larsen et al., 2019; Libby and Everett, 2019). Nevertheless, each of the currently used drugs can elicit side effects, are costly, or have not been approved for all patients due to these or other limitations. Therefore, it is imperative to identify new therapeutic targets to combat CAD.

Triacylglycerol, phospholipids, cholesterol, and cholesterol esters are transported in lipoprotein particles. The major structural component of these atherogenic very low-density lipoproteins (VLDLs), low-density lipoproteins (LDLs), and chylomicrons is Apolipoprotein B (ApoB), a ~550 kDa amphipathic protein (Boren et al., 1994; Bostrom et al., 1986; Olofsson et al., 1987). ApoB aids in the assembly, secretion, transport and cellular uptake of these particles. In mammals, ApoB is expressed in the liver and small intestine in two different isoforms, ApoB-100 and ApoB-48, which represents the N-terminal 48% of the full-length protein (Chen et al., 1988; Chen et al., 1987; Chen et al., 1986; Hussain et al., 2005; Hussain et al., 1996; Powell et al., 1987).

There is a direct correlation between these circulating ApoB isoforms and CAD: Higher levels cause CAD, while lower levels are either associated with normal homeostasis or, if severely limited, can lead to hypobetalipoproteinemia, which presents as delayed development, hepatomegaly, steatorrhea, and cytolysis (Jang et al., 2020; Welty, 2020). More recently, ApoB has also been targeted to treat CAD (Boekholdt et al., 2014; Nandakumar et al., 2018; Reyes-Soffer et al., 2016; Zimmermann et al., 2006). However, the ApoB-targeted drugs, which consist of antisense oligonucleotides, are expensive, exhibit side-effects, and has been approved for only a select group of patients. Nevertheless, these data position ApoB as a *bona fide* therapeutic target.

Unlike most metabolic processes, ApoB is regulated by Endoplasmic Reticulum Associated Degradation (ERAD), which in turn is determined by lipid levels in the ER (Benoist and Grand-Perret, 1997; Fisher et al., 1997; Liao et al., 1998; Sakata et al., 1999; Yeung et al., 1996). Notably, most lipid metabolism takes place in the ER, and perhaps not surprisingly several key proteins in the cholesterol biosynthetic pathway, such as 3-Hydroxy-3-Methylglutaryl-CoA Reductase (HMGCR), squalene monooxygenase, Insulin Induced Gene 1 (Insig1), and Acetyl-CoA Acetyltransferase 2 (ACAT2), are also regulated by ERAD (Jo et al., 2011a; Song et al., 2005; Stevenson et al., 2016; Tsai et al., 2012; Wang et al., 2017; Zelcer et al., 2014). In particular, as the nascent ApoB polypeptide chain is co-translationally translocated into the ER lumen through the Sec61 translocon, ApoB is lipidated by the lumenal microsomal triglyceride transfer protein (MTP) complex and a premature lipoprotein particle is formed (Fisher et al., 1997; Mitchell et al., 1998; Wu et al., 1996; Zhou et al., 1998). The premature VLDL particle then exits the ER via a non-classical pathway requiring enlarged COPII vesicles, enters the Golgi where it undergoes further lipidation, and is finally secreted (Gusarova et al., 2003; Sane et al., 2017; Siddiqi et al., 2003). In the serum, the C-terminus of ApoB acts as a ligand for the LDL receptor (Brown et al.,

1997). In contrast, when a cell lacks adequate lipids or in the absence of the MTP function, ER entry is slowed, so continued translation exposes hydrophobic loops of ApoB in the cytosol (Gordon et al., 1996). These potentially aggregation-prone loops are recognized by molecular chaperones, which help maintain solubility and facilitate ubiquitination by an ER resident E3 ubiquitin ligase (Fisher et al., 2011; Liang et al., 2003). ApoB is then degraded by the cytosolic 26S proteasome with the aid of the ER-associated AAA^{+}-ATPase, p97/VCP (Fisher et al., 2008; Fisher et al., 1997; Rutledge et al., 2009). Our group and others have identified and characterized several classes of molecular chaperones, including BiP, Hsp70, Hsp90, Hsp110, Hsp104, Protein Disulfide Isomerase (PDI), calnexin and calreticulin that play various roles in the ERAD of ApoB (Chen et al., 1998; Doonan et al., 2019; Fisher et al., 1997; Ginsberg, 1997; Gusarova et al., 2001; Hrizo et al., 2007; Rutledge et al., 2013; Tatu and Helenius, 1999; Zhou et al., 1995). It is likely that many of these chaperones function in a coordinated fashion to orchestrate ApoB biogenesis.

Although Hsp70 is one of many chaperones that regulate the ERAD of ApoB, the function of this chaperone normally requires an Hsp40 partner. Hsp40s, also known as J domain proteins (JDPs), are present in all cell types and assist Hsp70s by enhancing Hsp70 ATPase activity and facilitating substrate targeting and selectivity (Craig and Marszalek, 2017; Kampinga and Craig, 2010). Like Hsp70s, Hsp40s also play essential roles during protein folding, assembly, translocation, the prevention of aggregation, ubiquitination, and degradation (Kampinga et al., 2019). Hsp40s are one of the largest families of Hsps, and mammalian cells express more than 50 members. This network of Hsp70 co-factors has expanded during evolution to accommodate the concomitant expansion of potential substrates and roles required to maintain cellular protein homeostasis, or “proteostasis” (Rebeaud et al., 2021). To date, however, only one lumenal Hsp40

has been shown to facilitate ApoB degradation (Oyadomari et al., 2006; Rutkowski et al., 2007). In contrast, the roles of cytosolic Hsp40s in ApoB ERAD has never been explored.

Based on sequence similarity and domain architecture, cytosolic Hsp40s reside in one of three classes. Notably, class A and B Hsp40 chaperones function in tandem with Hsp70 and an Hsp70 nucleotide-exchange factor, Hsp110, to dissolve small aggregates (Kirstein et al., 2017; Nillegoda et al., 2015; Nillegoda et al., 2017). Based on the importance of preventing ApoB aggregation before proteasome delivery, it is possible that the class A and class B co-chaperones might also facilitate the metabolic control of ApoB ERAD. Therefore, in this study, we asked whether cytosolic Hsp40s target ApoB for ERAD. By using a yeast model as well as a rodent cell line that endogenously synthesizes and secretes ApoB, we observed that a Class A (DNAJA1) and Class B (DNAJB1) Hsp40 associate with ApoB. We also found that class A Hsp40 facilitates the degradation of ApoB. Surprisingly, the class B member instead stabilizes ApoB. In line with these data, the ablation of the class A Hsp40 led to the accumulation of ubiquitinated ApoB, whereas class B knockdown decreased the levels of ubiquitinated ApoB. We also found that the Hrd1 E3 ubiquitin ligase, an integral ER membrane protein, can modify and target ApoB-100 for degradation, most likely by acting downstream of the Hsp40s. These data highlight the requirements for molecular chaperones in the regulated degradation of ApoB and indicate for the first time that different Hsp40s can play opposing roles during ERAD.

2.2 Materials and methods

2.2.1 Yeast strains, plasmids, and growth conditions

Yeast strains were grown at 30°C using standard growth, media and transformation conditions (Adams A, 1997). All the strains used in this study are listed in Table 4.

To drive expression of ApoB, yeast were transformed with pSLW1-B29-HA (Doonan et al., 2019; Grubb et al., 2012; Hrizo et al., 2007), which contains a *URA3* selection marker and encodes ApoB29 with a triple HA tag at the C-terminus. The ApoB29 isoform causes hypobetalipoproteinemia in humans but is the shortest isoform that can successfully traffic through the secretory pathway and is regulated by lipids (Collins et al., 1988; Linton et al., 1993; McLeod et al., 1994). The expression of ApoB29 is under the control a galactose inducible promoter, but because galactose is a non-optimal carbon source and causes additional stress in yeast (Adams, 1972; Balch et al., 2008), we used a ß-estradiol inducible expression system driven by pACT1-GEV chimeric transcription factor. GEV is composed of a GAL4 DNA binding domain, an estrogen binding domain, and the VP16 transcription factor. Once ß-estradiol is added, the hormone binds to the estrogen receptor domain of GEV, releasing GEV from the Hsp90 complex. The released GEV enters the nucleus, binds to the upstream activating sequence of GAL promoters and thereby rapidly activates the transcription of genes under GAL promoter via its VP16 domain. In contrast to the use of galactose-inducible expression, this system is rapid, does not require a change in carbon source that slows yeast growth, and allows for the addition of the hormone to a yeast culture without further manipulations (McIsaac et al., 2011).

To make yeast strains ß-estradiol inducible, EcoRV (New England Biolabs) linearized pACT1-GEV plasmid was transformed into log phase yeast cells and integrated at the *leu2 Δ0* site

using standard lithium acetate protocol (Adams, 1972; Doonan et al., 2019; McIsaac et al., 2011; Veatch et al., 2009). Transformants were selected on Yeast Peptone Dextrose (YPD) plates containing 0.1mg/mL Nourseothricin (Werner Bioagents, Jena, Germany). To ensure selection of colonies with successful integration of the plasmid, positive colonies were restruck three times on YPD Nourseothricin plates.

Table 4. Yeast strains utilized in this study

Strain	**Genotype**	**Source**
W3031b GEV	*MAT α, ade2-1, can1-100, his3-11,15, leu2-3,112, trp1-1, ura3-1 ACT1-GEV-NatMX::leu2Δ0*	Our lab
pdr5Δ GEV	*MAT α, ade2-1, can1-100, his3-11,15, leu2-3,112, trp1-1, ura3-1, pdr5::KANMX4, ACT1-GEV-NatMX::leu2Δ0*	Our lab
ydj1-151 GEV	*MAT α, ade2-1, can1-100, his3-11,15, leu2-3,112, trp1-1, ura3-1 ydj1-2 ∷ HIS3, LEU2 ∷ydj1-151, ACT1-GEV-NatMX::leu2Δ0*	This study
BY4742 GEV	*MAT α, his3Δ1, leu2Δ0, ura3Δ0, lys2Δ0, ACT1-GEV- NatMX::leu2Δ0*	Our lab
Δhlj1 GEV	*MAT α, ade2-1, can1-100, his3-11,15, leu2-3,112, trp1-1, ura3-1* Δhlj1 ∷ HIS3 *ACT1-GEV- NatMX::leu2Δ0*	This study
Δhlj1 ydj1-151 GEV	*MAT a, leu2, ura3, his3, trp1, ade2, ydj1-2::HIS3, LEU2::ydj1-151, Δhlj1::TRP1 ACT1-GEV-NatMX::leu2Δ0*	This study
SSA1 GEV	*MATα, his3-11,15, leu2-3,112, ura3-52. trp1-Δ1, lys2, ssa2- 1(LEU2), ssa3-1(TRP1), ssa4-2(LYS2) ACT1-GEV- NatMX::leu2Δ0*	This study
ssa1-45 GEV	*MATα, his3-11,15, leu2-3,112, ura3-52. trp1-Δ1, lys2, ssa1-45, ssa2-1(LEU2), ssa3-1(TRP1), ssa4-2(LYS2) ACT1-GEV- NatMX::leu2Δ0*	This study

2.2.2 Yeast cycloheximide chase assays

Cycloheximide chase assays were conducted following published protocols (Doonan et al., 2019; Grubb et al., 2012; Hrizo et al., 2007). In brief, to examine the rate of degradation of ApoB, yeast transformed with pSLW1-B29-HA were grown overnight in synthetic media lacking uracil (SC-ura) supplemented with 2% glucose at 30°C and were then diluted with the same media and grown to logarithmic phase (OD_{600} = 0.4-0.6). Cells were harvested to obtain 1 OD_{600} equivalent of cells per time point and resuspended again in the same media but supplemented with 300 nM ß-estradiol to induce expression of ApoB. All temperature sensitive strains were pre-incubated at 37°C for 30 min, and then to inhibit protein translation, cycloheximide at a final concentration of 50ug/mL was added to cells and 1 OD_{600} of cells was harvested as the 0-minute time point. Equivalent amounts of cells were collected for the indicated subsequent time points. Total protein was precipitated using Trichloroacetic acid (TCA) following published protocols and resolved by SDS-PAGE and quantitative western blotting (Zhang et al., 2001). The triple HA tagged ApoB was detected using an anti HA-horseradish peroxidase conjugated antibody (Table 5). G6PD levels were examined as a loading control with an anti-G6PD antibody (Table 5).

2.2.3 Co-immunoprecipitation (Co-IP) assays in yeast

To probe for specific protein-protein interactions, published protocols for ApoB in yeast were utilized (Doonan et al., 2019; Grubb et al., 2012; Hrizo et al., 2007). I brief, yeast containing pSLW1-B29-HA were grown overnight at 30°C, the cells were diluted to 0.25 OD_{600}/mL, then grown to an OD_{600} of 0.5, and 300 nM ß-estradiol was added. Cell growth was continued for 2 hrs at 30°C. Once the OD_{600} reached 1.0, 100 OD_{600} of cells were harvested, which were then

resuspended in 1 mL Roche Lysis buffer (150mM NaCl, 50mM Tris-HCl pH 7.5, 0.1% NP-40, 20mM sodium molybdate, 1mM PMSF, 1ug/mL Leupep, 0.5ug/mL pepstatin and cOmplete EDTA-free protease inhibitor cocktail tablet (Millipore Sigma), hereafter referred to PIs + PIC for protease inhibitors and protease inhibitor cocktail).

Next, the cells were lysed using acid-washed mini glass beads by vigorous agitation on a Vortex mixer 3 times for 2 min each with 2 min intervals on ice after each agitation. The lysate was collected and centrifuged for 2 min in a microcentrifuge at 5000 rpm, 4°C, and the supernatant was then carefully transferred to a new microfuge tube and centrifugation was repeated. The cleared lysates were then transferred to new tubes, and 30 µL of a 1:1 slurry of Protein A Fast Flow Sepharose beads (GE Healthcare) was added to each lysate and tubes were placed on an end-to-end rotator for 1 hr at 4°C. The tubes were centrifuged at 5000 rpm for 5 min at 4°C, the lysate was carefully transferred to fresh tubes, and 5% (50 µL) of the initial volume was saved as input and processed by TCA precipitation as described earlier. The remaining lysate was diluted to 1.5 mL with Roche Lysis buffer + PIs + PIC, and 50 µL of HA (anti HA affinity matrix, Roche) or Sepharose 6B beads (negative control) was added to the lysate and the samples were placed on an end-to-end rotator at 4°C overnight. To isolate the bead-bound proteins, the lysates were centrifuged at 5000 rpm for 2 min at 4°C in a refrigerated microcentrifuge, and the supernatant (unbound fraction) was saved and stored at -80°C. The beads were then washed with 1 mL of cold Roche lysis buffer + PIs+ PIC and again spun at 5000 rpm for 2 min at 4°C. This step was repeated twice, and two additional washes were conducted with the Roche lysis buffer containing PIs+ PIC but supplemented with 300 mM NaCl. After the final wash, any residual supernatant was removed, the beads were resuspended in 50 µL TCA sample buffer, and the solution was incubated at 37°C for 20 min and finally processed by SDS PAGE and western blotting. Proteins were detected using

anti-HA, anti-ApoB, anti-Ydj1, anti-Ssa1, anti-PDI, anti-rpL5, and anti-G6PD antibody (see Table 5).

Table 5. Antibodies used in this study

Antibody	Company and Catalog Number	Dilution
Horseradish peroxidase (HRP) conjugated rabbit anti-HA	Roche Applied Science, 3F10	1:6000
Ydj1	Our lab	1:4000
Ssa1	Our lab	1:4000
rpL5	Woolford Lab, Carnegie Mellon University	1:2000
PDI	Dr. Vlad Denic, Harvard University	1:2000
Rabbit glucose 6 phosphate dehydrogenase (G6PD)	Sigma-Aldrich #A952	1:6000
Mouse ApoB	Santa Cruz Biotechnology #393636	1:1000 (WB), 1:200 (IF)
ApoB HRP	Santa Cruz #sc-393636 HRP	1:1000
Anti ApoB goat polyclonal antibody	Calbiochem #178467	3-5 µL per IP
Rabbit anti sheep secondary antibody HRP	ThermoFisher #61-8620	1:5000
Mouse Apobec1	Santa Cruz Biotechnology #sc-166508	1:2000
Mouse HSP70	Cell signaling #4872S	1:2000
Mouse HDJ2	Thermo Fisher MA5-12748	1:3000
Rabbit SYVN1	Proteintech 13473-1-AP	1:2000
Mouse gp78	Santa Cruz Biotechnology sc-166358	1:2000
Mouse CHIP (G-2)	Santa Cruz Biotechnology sc-133066)	1:1000
Rabbit AMFR	Proteintech 16675-1-AP	1:2000
Mouse Beta actin	Proteintech 66009-1-1g	1:4000
Rabbit DNAJC19	Proteintech #12096-1-AP	1:3000
Rabbit DNAJB1	Proteintech #50-172-8542	1:3000
Rabbit HMGCR	Biorbyt orb340767	1:2000 (WB), 1:200 (IF)
BAP31 (B-10)	Santa Cruz Biotechnology sc-365347	1:2000
Mouse Anti-Bovine HSP70 Monoclonal IgG1	StressMarq Biosciences	1:2000

Rabbit Hsp70	Cell Signalling Technologies 4872S	1:2000
Rabbit Beta Actin antibody	Cell Signalling technology 4967L	1:2000
Rabbit CFTR	Cell Signalling technology 78335S	1:2000

2.2.4 Yeast metabolic pulse chase assays

Pulse Chase assays were performed following published protocols (Morrow and Brodsky, 2001; Vembar et al., 2010) using cultures that were grown overnight at 30°C in SC-ura to an OD_{600} of 1.0. After the cells were concentrated to 3 OD_{600}/mL, they were labelled with EasyTag Express 35-S (Perkin Elmer) to a final concentration of 100 µCi/sample for 15 min at 26°C in O-ring tubes. The cells were then centrifuged at 4500g for 3 min in a table-top clinical centrifuge, washed with SC-ura and resuspended in SC-ura containing non-radioactive 13 mM methionine, 40 mM cysteine, and 200 µg/mL cycloheximide. For each time point, 1.2 OD_{600} of cells were collected at 0, 15, 30, and 60 min and mixed with 400 µl of quench buffer (80 mM Cys, 80 mM Met, and 100 mM NaN_3) and placed on ice. Harvested cells were washed in Buffer 88 (20 mM HEPES, pH 6.8, 150 mM KOAc, 250 mM sorbitol 5 mM MgOAc) and resuspended in Extract buffer (50 mM Tris-HCl, pH 7.4, 1 mM EDTA, 1% SDS + PI (3X) + PIC (3X)). Acid-washed mini glass beads were then added to half of the cell volume, and the cells were vigorously agitated 3 times for 2 min each followed by a 2 min incubation on ice. Next, the lysates were centrifuged in a refrigerated microcentrifuge at 5000 rpm at 4°C for 2 min. The supernatant was collected, and centrifugation was repeated as above before 350 µL of IP buffer (50mM Tris-HCl pH 7.4, 150mM NaCl, 5mM EDTA, 1% Triton X-100, and 0.2% SDS) was added to each sample. To preclear the lysate, 30 µL of a 1:1 slurry of Protein-A Sepharose beads (GE Healthcare) was added, and tubes were placed

on an end-to-end rotator for 3 hrs at 4°C. The tubes were then centrifuged at 5000 rpm for 5 min at 4°C in a refrigerated centrifuge before 35 µL of 1:1 slurry of Protein A Sepharose beads and 3 µL of anti-ApoB antibody (Calbiochem) were added to each precleared lysate and incubated overnight. Next, the beads were collected by centrifugation at 5000 rpm at 2 min at 4°C in a refrigerated microcentrifuge and then washed twice with IP buffer and then IP wash buffer supplemented with 2 M urea and then once with 1X TAE buffer (50 mM Tris-HCl, pH 7.4, 150 mM NaCl, and 5 mM EDTA). Residual wash buffer was aspirated, and the beads were resuspended in 50 µL of TCA sample buffer. Proteins were resolved by SDS PAGE, the gels were dried, and then exposed to a phosphorimager screen. Radiographs were developed at 50µM resolution using PMT voltage of 1000V on a Typhoon FLA 7000 or Amersham Typhoon phosphorimager (GE Healthcare). The final signal was quantified using ImageJ (NIH).

2.2.5 Yeast *in vivo* crosslinking assays

In vivo crosslinking using DSP was performed following a published protocol (Gardner et al., 2000) with yeast containing pSLW1-B29-HA that were grown in selective media overnight at 30°C. The cells were then diluted to 0.25 OD_{600}/mL and grown to an OD_{600} of 0.5. Next, ApoB was induced with 300nM ß-estradiol for ~2 hrs. Once the OD_{600} reached 1, 5 OD_{600} of cells were harvested and resuspended in XL buffer (1.2 M sorbitol, 5mM EDTA, 0.1M KH_2PO_4/K_2HPO_4, pH 7.5), 50 µg/mL Zymolase, and DSP (at a final concentration of 200 µg/mL). Cultures were incubated at 30°C for 40 min, collected by centrifugation and lysis in 300 µl SUME buffer (0.5% deoxycholate, 1% Triton X-100, 1% SDS). The crosslinking reaction was quenched with 1M Tris-Cl, pH 7.5, ApoB was immunoprecipitated with anti-ApoB antibody, and the samples were processed as described above.

2.2.6 Cell culture

McArdle RH-7777 cells (McA) (ATCC CRL-1601) were purchased from American Type Culture Collection (ATCC) and grown at 37°C in a 5% CO_2 incubator in DMEM High glucose pyruvate (Thermo Scientific, Gibco) supplemented with 10% fetal bovine serum (FBS) (VWR), 10% horse serum (HS) (Sigma-Aldrich) and 0.1mg/mL penicillin/streptomycin (P/S) (Thermo Fisher Scientific), on collagen-coated 10 mL dishes (Cellcoat Collagen Type I coated petridishes Greiner). Cells were detached with 3 mL TrypLE Express Enzyme (No phenol Red Gibco) for 3 min at 37°C. To quantify cell numbers, 40 µL of resuspended cells were mixed with 40 µL of Trypan Blue Stain (Life Technologies) and an aliquot was analyzed on a hemocytometer. Cell culture experiments were performed in a 1300 Series A2 biosafety hood (Thermo Fisher Scientific).

For some experiments, humanized McA cells that lack the enzyme Apobec1 and HepG2 cells, which are a human hepatoma cell line, were obtained from the Fisher lab (NYU School of Medicine) and grown and maintained as described above.

Plasmids used in experiments with McA cells included HA-tagged ubiquitin (Kamitani et al., 1997), pcDNA3.1-CFTR (Han et al., 2018), and pcDNA3.1-HRD1 and pcDNA3.1- Hrd1C1A (Liang et al., 2003). For transfection, 2×10^5 cells were seeded/well in 6 well collagen-coated plates (Greiner Bio-One), grown overnight, and treated with Lipofectamine 2000 following the manufacturer's instructions using Opti-MEM I Reduced Serum Medium (Thermo Scientific Gibco) with 10 µL Lipofectamine 2000 and Opti-MEM I Reduced Serum Medium (Thermo Scientific Gibco) with 4 µg plasmid DNA. The solutions were then mixed and incubated for 20 min, and 500 µL of the mix was added to each well, followed by the addition of 2 mL of complete

media. For transfection using 10 cm dishes, reagents were scaled up by 6-fold. Cells were harvested or lysed after 20 hrs of transfection.

For knockdown studies, siRNAs in Table 6 were purchased from Dharmacon/Horizon discovery. Initially, a set of four individual siRNAs (ON-TARGET plus Set of 4 Upgrade siRNA) was used to optimize knockdown conditions/siRNA, followed by experiments using the most efficient siRNA. Lyophilized siRNAs were resuspended in nuclease free water to a final concentration of 20 µM.

Table 6. siRNAs used in this study

Gene	**Catalog number of a set**	**Catalog number of the siRNA used**	**Sequence**
DNAJA1	LQ-098641-02-0002	J-098641-09-0010	GGGGCGAGCAGGCGAUUAA
DNAJB1	LU-093306-02-0002	J-093306-09-0010	GCGAGAUUUUCGACCGCUA
DNAJC19	LU-107234-02-0002	J-107234-07-0010	CAGUGGUAGCAGUCGGAUU
AMFR (gp78)	LU-092779-02-0002	J-092779-09-0002	
SYNVIOLIN (Hrd1)	LU-084977-02-0002	J-084977-09-0010	GCUUAAAUUUGUCUUUCGA

For transfection, McA cells (1×10^5) were seeded in 6 well collagen-coated plates (see above) in 2 mL media (Greiner Bio-One) and grown overnight. Cells were transfected when 30-40% confluent with Lipofectamine RNAi MAX transfection reagent (Invitrogen) as per the manufacturer's instructions. In brief, 4 µL RNAiMAX and 246 µL Opti-MEM I Reduced Serum Medium (Thermo Scientific Gibco) per well were mixed in a total volume of 250 µL with the siRNA along with Opti-MEM per well. After incubation for 20 min, the mixture was added to the

cells along with 1 mL of complete media. After 6 hrs, fresh complete fresh media was added, and the cells were harvested after 48 or 72 hrs. Knockdown efficiency was measured after cell lysis, SDS-PAGE, and western blotting. For all knockdown experiments, the levels of actin were also examined as a control, and equal concentrations of fluorescent scrambled siRNA (BlockIt Alexa Fluor Red Fluorescent Control Oligo Invitrogen) were used. Transfection efficiency was calculated by counting the percentage of cells that took up the scrambled siRNA in a random field of observation under a fluorescence microscope.

2.2.7 Pulse chase assays and measurements of ApoB ubiquitination

Pulse chase assays were performed after modifications of published protocols (Borchardt and Davis, 1987; Boren et al., 1992; Boren et al., 1994; Bostrom et al., 1986; Fisher et al., 1997; Grubb et al., 2012; Gusarova et al., 2001). McA cells (1×10^5) were seeded in 6-well collagen coated plates (see above) in 2 mL complete media and grown overnight. The cells were starved for 1 hr in media lacking cysteine and methionine (Dulbecco's modified eagle medium) but containing L-glutamine for 1 hr at 37°C, washed with 1X DPBS (Dulbecco Phosphate Buffered Saline), and then starvation media containing 100 µCi of S-35 (EasyTag Express 35-S Protein labelling mix Perkin Elmer) supplemented with 2% L-glutamine was added. After15 min, the cells were washed with 1X DPBS twice and 1 mL of chase media (Starvation media/2% glutamine/5% FBS/5% HS/100 µM non-radioactive cysteine and 40 µM methionine) was added to each well. Cells and media were collected at 15, 60 and 90 min into the chase. The media was collected into tubes with 25 µl of 1 mM PMSF. The cells were washed once with DPBS and lysed with 700 µL Radioimmunoprecipitation Assay buffer (RIPA) buffer (50mM Tris-Cl, pH 7.4, 150mM NaCl, 1% NP-40, 0.5% deoxycholate, 0.1% SDS and PIs + PC) for 20-30 min on ice. The lysates were then

centrifuged at 1600g for 20 min in a microcentrifuge at 4°C, and the supernatant was collected. Radioactive counts were determined for each lysate and media sample in a scintillation counter, and immunoprecipitation reactions were set-up (for each cellular lysate/well) with 680 µL 1X DPBS, 120 µl 5X NET buffer (150 mM NaC1, 5 mM EDTA, and 50 mM Tris, pH 7.4, 0.5% Triton X-100, and 0.1% SDS), 5 µL of anti-ApoB antibody, 50 µL of a 1:1 Protein G bead slurry, 600 µL of lysate, and PIs + PIC. For each media sample, each immunoprecipitation contained 360 µL double distilled water, 240 µL 5X NET buffer, 5 µL of anti-ApoB antibody, 50 µL of a 1:1 Protein G bead slurry, 800 µL sample, and PIs + PIC. After an overnight incubation at 4°C, the tubes were centrifuged at ~1600g for 1 min at 4°C in a microcentrifuge, the beads were washed three times with 1X NET buffer with PIs + PIC, the residual IP wash buffer was aspirated, and the beads were suspended in 75 µL urea sample buffer (8M urea, 1% SDS, 10mM EDTA, 150mM Tris-Cl, pH 6.8). Proteins were resolved on 5% polyacrylamide SDS gels, and after the gels were dried and exposed to a phosphorimager screen, the radiograph was developed using a Typhoon FLA 7000 or Amersham Typhoon phosphorimager (GE Healthcare). Phosphorimages were collected at 50 µM resolution using a PMT voltage of 1000V, and signals were quantified using ImageJ.

To measure the extent of protein ubiquitination, McA cells were transfected with an siRNA targeting the gene of interest as described earlier, and on the next day cells were transfected with the HA-tagged ubiquitin expression plasmid. After an overnight incubation, the media was aspirated, and fresh complete media with either the vehicle control (DMSO) or 25 µM of MG-132 (Selleck Chemicals #S2619) was added and the cells were incubated at 37°C for 1 hr. Next, the media was aspirated and 500 µL of TrypLE was added. Following a 5 min incubation, the cells were harvested, and the cell pellets were lysed with 1mL RIPA buffer + PIC supplemented with 25 µM MG-132 and 10 mM NEM for 20-30 min on ice. After centrifugation at ~1600g for 20 min

at 4°, the supernatant was collected and precleared with 30 µl of a 1:1 slurry of Protein G Sepharose (GE Healthcare 17061801) beads for 1 hr at 4°C. The cleared lysate was collected after a ~1000g spin for 5 min at 4°C, and protein levels were normalized using BCA assay (ThermoScientific) following the manufacturer's instructions. A fraction (20%) of the total lysate was saved for each reaction as the input, and equal amounts of protein plus 120 µL 1X NET buffer and 100 µl DPBS (Life Technologies) including PIC, 25 µM MG-132, and 50 µL of a 1:1 slurry of Protein G Sepharose (GE Healthcare) and 3 µl anti-ApoB antibody (Calbiochem) were added to each immunoprecipitation. The tubes were incubated at 4°C overnight, centrifuged at ~1600g for 1 min at 4°C, washed three times with 1X NET including PIs + PIC, and the beads were suspended in urea sample buffer. Proteins were resolved on 5% polyacrylamide SDS gels, and ubiquitinated ApoB was detected with HA-HRP conjugated antibody. Another set of blots was probed with anti-ApoB antibody.

2.2.8 Other biochemical methods

To perform chemical crosslinking in McA cells, 1 x 10^6 cells were seeded in a 10 cm dishes in 10 mL complete media and grown overnight. The cells were washed twice with DPBS, and 2 mM Dithiobis succinimidylpropionate (DSP) (ThermoFisher) was added at room temperature for 30 min. Next, stop solution (20 mM Tris-Cl, pH 7.5) was added and the cells were incubated for another 15 min before the cells were trypsinized and isolated as above. The cells were lysed in RIPA buffer, and IP reactions were set up as described for the pulse chase protocol. To cleave DSP, 75 µL of urea sample buffer with 50 mM DTT was added to samples, which were then incubated at 37°C for 30 min.

Sucrose gradient analysis of ApoB-containing lipoproteins was conducted following published protocols (Boren et al., 1992; Boren et al., 1994), using cells that had been were seeded at 6×10^5 cells/petridish and grown overnight in complete medium. The next day, siRNA transfections were performed, as above, and after 48 hrs a pulse chase was conducted as described earlier, but media was collected only at the 90-min time point. Next, a gradient was set-up with 2 mL 50% and 25% (w/v) sucrose, onto which the isolated media containing identical amounts of radioactivity diluted to 12.5% (w/v) sucrose concentration in a total volume of 5 mL was loaded. Each solution also contained 50 mM Na_3PO_4, pH 7.4, 150 mM NaCl, 5 mM EDTA, and PIs + PIC. Finally, 3 mL of media was layered on top. After centrifugation in a SW Ti41 rotor in a Beckman LM centrifuge at 150,000g for 65 hrs at 4°C, twelve 1 mL fractions were carefully collected from the top and radioactivity and the refractive index of each fraction was calculated using a scintillation counter and an Abbe refractometer, respectively. Next, an overnight IP with anti-ApoB antibody and protein G beads as performed, as outlined above. Samples were subjected to SDS-PAGE (5%), the gels were dried, and then exposed to a phosphorimager screen, which was developed using a Typhoon FLA 7000 or Amersham Typhoon phosphorimager (GE Healthcare). Phosphorimages were collected at 50 µM resolution using PMT voltage of 1000V, and the signal was quantified using ImageJ.

To assay ApoB solubility in various detergents, cells were grown overnight and siRNA mediated JA1 knockdown was conducted as described above. Scrambled control and JA1 depleted cells were incubated with multiple 0.1%, 1%, or 5% dodecyl D-maltoside (DDM) (Sigma Aldrich) in 0.3 M sucrose, 0.1 M KCl, 2.5 mM $MgCl_2$,1 mM sodium-free EDTA, 10 mM PIPES, pH 6.8, and PIs + PIC on ice for 20 min. After centrifugation at 100,000g at 4°C for 1 hr, the soluble (supernatant) and insoluble (pellet) fractions were processed for SDS-PAGE and developed by

western blot analysis with anti-ApoB antibody. The levels of JA1 were also examined with JA1 antibody, and ribophorin, an ER membrane protein (Crimaudo et al., 1987), was assessed as a control.

Alternatively, the detergent solubility of nascent ApoB was assessed following a published protocol sequentially treating cells with 25 μg/mL digitonin, 1% NP40, and 0.5% sodium deoxycholate and 0.1% SDS in 150 mM NaCl, 50 mM HEPES, pH 7.4 (Holden and Horton, 2009). All the buffer solutions were supplemented with PIs and PIC. ApoB was isolated from the 60 min after a pulse chase using cells treated with a scrambled siRNA or the JA1-targeted siRNA. After each detergent treatment, the supernatant was collected, and an overnight immunoprecipitation was set up as described earlier. Samples were washed and processed for SDS-PAGE and phosphorimage analysis.

To perform sequential immunoprecipitations for ubiquitinated ApoB, McA cells were transfected with the indicated siRNAs followed by the HA tagged ubiquitin plasmid as described above. The next day, a pulse chase was conducted as explained above, and cells were collected after a 60 min chase. After lysis with RIPA buffer and immunoprecipitation with anti-HA antibody conjugated beads and washing, the bound proteins were eluted by heating the beads in 2% SDS for 4 min at 95°C following a published protocol (Liang et al., 2003). The SDS concentration was then adjusted to 0.1% and 10% was this was saved as the input. A second overnight immunoprecipitation was then set up with anti-ApoB antibody, and the bound protein was liberated and examined as above.

Oleic Acid BSA conjugates were made following a protocol from our collaborators at the Fisher lab at New York School of Medicine. A total of 1.2 mL of oleic acid (OA) was dissolved in 2.5mL of 99.9% ethanol by sonication, and 2.8 g of BSA was dissolved in 13.8 ml of 0.9M

NaCl solution. A total f 135 µl of this OA solution was added to the BSA-saline solution and agitated at 50°C until it was completely mixed. The pH was adjusted to 7.8 with 1M NaOH, and 14 mM aliquots of OA-BSA were made and stored at -20C.

2.2.9 Indirect immunofluorescence (IF)

McA cells were grown on fibronectin coated coverslips and fixed in paraformaldehyde solution before they were incubated with primary antibodies (ApoB, HMGCR) at 4°C overnight. Slides containing bound primary antibodies were then washed with a BSA solution and incubated with Alexa dye conjugated secondary antibodies for 1 hr in the dark. Mounting solution containing DAPI was used to label the nucleus. Images were taken on a Nikon A1R confocal microscope with 60X objective and analyzed with Fuji software (NIH).

2.2.10 Quantification and statistical analysis

For quantitative western blots, proteins were visualized using SuperSignal West Pico or the Femto Chemiluminescent kit (ThermoFisher) along with the respective Pro-Signal Pico or Femto developer solutions (Prometheus) using a BioRAD universal Hood II Imager. Image J software (NIH) were used to obtain and quantify images. Sample size comprised of the stated number of independent biological replicates that individually also included 3-4 technical replicates. Statistical significance was calculated by unpaired t-tests using the GraphPad statistical software.

For pulse chase experiments, samples were normalized based on radioactive counts and the signal was quantified using ImageJ (NIH). Radiographs were saved as TIFF files (8/16 bit), and

quantification was performed using Image J (NIH) to collect raw integrated densities and Microsoft Excel. Student's unpaired two-tailed t tests were performed on graph pad, average and standard errors were calculated and significance was calculated. Where indicated, ApoB100 and ApoB48 were individually quantified. Independent experiments were biological replicates which included the average of 2-3 technical replicates. For ubiquitination assay, data were normalized to the corresponding ApoB100 levels. Statistical significance was determined by conducting unpaired t-tests via the GraphPad statistical software.

Table 7. Primers used in this study

Primer	**Sequence**
KLHL12Fw1	CAGCAGTCTCCCATTGATGT
KLHL12Rev1	GAGGCCACATAACGTCTCTTAC
KLHL12Fw2	GGGTATTAGGAGTGTGGGAATG
KLHL12Rev2	CAACTCAGGGAAAGAGGGAAA
Hrd1seq_Fw1	CTGAGGACCGTGTGGACTTT
Hrd1seq_Fw2	GGCCATGAGACAGTTCAAGA
Hrd1seq_Rev1	GAGAAAGGGCTGCACTGGT

Table 8. Catalog numbers of reagents

Reagent	**Company and Catalog Number**
Anti ApoB goat antibody	Calbiochem 178467
Dulbecco's modified eagle medium HIG	Gibco D0422-11
EasyTag Express 35-S Protein labelling mix	Perkin Elmer NEG772007MC
Oleic acid-BSA	Sigma Aldrich O1008-5G
Rabbit anti sheep secondary HRP antibody	ThermoFisher 61-8620
Collagen coated 6 well plates	Greiner Bio-One 82050-924
Protein G Sepharose 4 fast flow	GE Healthcare 17061801
Lift away	Medline 114000
Horse Serum Sigma-Aldrich	H1138-500mL
DMEM High glucose pyruvate	Gibco 11995-065
Lipofectamine 2000 Transfection reagent	Thermofisher 11668030
Bovine serum Albumin lyophilized powder	Sigma Aldrich A6003-10G
Lipofectamine RNAiMAX Transfection Reagent	Invitrogen 13778150
HDJ2 monoclonal antibody (KA2A5.6)	Thermo Fisher MA5-12748

HSP70 antibody	Cell signaling 4872S
Apobec1 (E-2) enzyme	Santa Cruz Biotechnology sc-166508
Cellcoat Collagen Type I coated petridishes	Greiner Bio-One 82050-924
Anti-SYVN1 Rabbit Polyclonal Antibody	Proteintech 13473-1-AP
ApoB (A-6) (mouse monoclonal), non-conjugated	Santa Cruz Biotechnology 393636
gp78 antibody (rat, mouse and human)	Santa Cruz Biotechnology sc-166358
CHIP (G-2) (mouse, rat, human)	Santa Cruz Biotechnology sc-133066
Thermo Scientific Pierce DSP	ThermoFisher PI-22585
MGC Rat Dnaja1 cDNA	Dharmacon MRN1768-202786872
Z-VAD-FMK	Selleck Chemicals S7023
DPBS, no calcium, no magnesium	Life Technologies 14190144
Anti-AMFR Rabbit Polyclonal Antibody	Proteintech 16675-1-AP
VWR Life Sciences Seradigm Premium Grade Fetal Bovine Serum (FBS), Premium	VWR 97068-085
DNAJB1/Hdj1 antibody	Thermofisher Scientific PA5-17382
Thermo Scientific PageRuler plus Prestained 10 250kDa Protein ladder	Thermo Fisher Scientifc 26620
Anti-ActB Mouse monoclonal antibody [clone 2D4H5]	Proteintech 66009-1-1g
Sodium Dodecyl Sulfate (SDS), micropellets,	Fisher BioReagents Fisher Scientific BP8200100
Anti DNAJC19 Rabbit polyclonal antibody	Proteintech 12096-1-AP
Rat AMFR/gp78 siRNA	Dharmacon LU-092779-02-0002
DNAJC19 siRNA	Dharmacon LU-107234-02-0002
siRNA DNAJB1 10nM	Dharmacon J-093306-09-0010
ProSignal Femto ECL Reagent	Prometheus 20-302B
ProSignal Pico ECL Reagent	Prometheus 20-300B
Pageruler plus prestained protein standard	thermo Fisher Scientific 26619
DNAJB1 antibody	Proteintech 50-172-8542
Opti-MEM I Reduced Serum Medium	Gibco 31985070
Hrd1 siRNA	Dhamacon J-084977-09-0010

Block it Alexa Fluor Red Fluorescent Control Oligo	Invitrogen 4750100
HMGCR antibody	Biorbyt orb340767
BAP31 (B-10)	Santa Cruz Biotechnology sc-365347
RNase-free DNase set	Qiagen 79254
qScript cDNA SuperMix 1X	Quantabio 95048-100
Penicillin Streptomycin (10,000U/mL)	Thermo Fisher Scientific 15-140-122
ZymoPURE II plasmid Maxiprep Kits Spin Column	Zymo Research D4203
TryLE Express Enzyme (1X) No phenol Red	Gibco 12-604-021
Pierce BCA Protein Assay Kits and Reagents,	Thermo Scientific Fisher 23225
Mouse Anti-Bovine HSP70 Monoclonal IgG1 [1.86]	StressMarq Biosciences
Hsp70 antibody	Cell Signalling Technologies 4872S
Universal Mycoplasma Detection Kit	ATCC 30-1012K
CellTiter-Glo Luminescent Cell Viability Assay	Promega G7572
Beta Actin antibody	Cell Signalling technology 4967L
RNeasy Mini Kit	Qiagen 74104
BiP (C50B12) Rabbit mAb	cell signaling technology 3177S
cOmplete, Mini EDTA-free protease inhibitor cocktail Protease inhibitor complete tablets EDTA-free	Roche 11 836 170 001
Sybr Green Master Mix BioSci	Stockroom FERK0222
NEEDLE DISP HYPO 25GX1	Fisher Scientifc 14-821-13D
Super signal west pico	thermoscientifc 34078
CFTR (D6W6L) Rabbit mAb	Cell Signalling technology 78335S
DNAJA1	Dharmacon (LQ-098641-02)
Dodecyl maltoside	Sigma Aldrich D4641

2.3 Results

2.3.1 Development of β-estradiol inducible strains to study the effects of Hsp40s/J Domain Protein (JDP) function on ApoB

Prior work established that the cytoplasmic Hsp70 chaperone system facilitates the degradation of ApoB (Fisher et al., 1997; Gusarova et al., 2001). These discoveries were made possible by an *in vitro* system using reagents prepared from yeast cells and in cell culture systems. Yet, the role of cytoplasmic Hsp40s in ApoB biogenesis had never before been examined. To investigate whether Hsp40s contribute to the biogenesis of ApoB—and to confirm that the yeast Hsp70 was also required for ApoB ERAD in this model organism—I utilized a β-estradiol inducible expression system in the yeast *Saccharomyces cerevisiae* (Doonan et al., 2019). In brief, the creation of a β-estradiol inducible system requires the transformation of recipient yeast with a linearized plasmid encoding a chimeric transcription factor, pACT1-GEV (McIsaac et al., 2011). Strains are then selected in which the construct has stably integrated. This chimeric transcription factor is composed of a GAL4 DNA binding domain, an estrogen binding domain, and the VP16 transcription factor. The GEV chimeric transcription factor is constitutively expressed under the control of an ACT1 promoter but remains inactive in the cytosol and bound to Hsp90. Once β-estradiol is added, the hormone binds to the estrogen receptor domain of GEV, releasing GEV from the Hsp90 complex. The released GEV enters the nucleus, binds to the upstream activating sequence of GAL promoters, and thereby rapidly activates the transcription of genes under the control of the GAL promoter via its VP16 domain. In contrast to the use of galactose-inducible expression, this system is rapid, does not require a change in the carbon source that slows yeast

growth, and allows for the simple addition of an inexpensive hormone to a yeast culture without any other manipulations.

To identify and characterize a potential role of Hsp40s in ApoB ERAD, I conducted a candidate-based study in yeast and explored the role of two Hsp40s with previously known roles in ERAD. Yeast express over 22 Hsp40 isoforms (Kampinga et al., 2019; Kampinga and Craig, 2010), but of the 13 Hsp40s present in the cytosol, only Hlj1 and Ydj1 are associated with the ER membrane. Whereas Hlj1, a class B Hsp40, is anchored to the membrane by its C-terminus, Ydj1, a class A Hsp40, is tethered to the ER membrane by a farnesyl moiety (Becker et al., 1996; Beilharz et al., 2003; Costanzo et al., 2001; Cyr et al., 1992; Hoe et al., 1998; Walsh et al., 2004). An earlier study from our lab found that Hlj1 and Ydj1 play a redundant role in the degradation of another ERAD substrate, the Cystic Fibrosis Transmembrane Conductance Regulator (CFTR), when heterologously expressed in yeast: While strains containing single mutations of each gene had little effect on CFTR degradation, the double mutant significantly stabilized CFTR (Youker et al., 2004). Based on these data, I asked whether Hlj1 and Ydj1 facilitate the ERAD of ApoB.

To this end, I used strains in which the gene encoding Hlj1 was deleted *(*Δ*hlj1*) and/or that contained a temperature-sensitive *YDJ1* allele (*ydj1-151*) since—in some backgrounds—the Ydj1 protein is essential (Caplan and Douglas, 1991; Cyr and Douglas, 1994). After yeast containing either mutant allele or both mutations were transformed with the GEV plasmid and colonies containing the stably integrated gene were isolated, I confirmed temperature sensitivity by isolating single colonies and incubating them at permissive (26ºC, 30ºC), semi-permissive (34ºC), and non-permissive (37ºC) temperatures. As expected, the *ydj1-151* and Δ*hlj1 ydj1-151* strains were temperature sensitive (Figure 8A). To calculate the doubling time of these strains, I next conducted a growth assay where I measured the OD_{600} of cells from 0-24 hrs at 30ºC. As

anticipated from established roles of Ydj1 in essential processes such as cell size determination, cell cycle, protein folding, and protein translocation (Becker et al., 1996; Brodsky et al., 1998; Caplan et al., 1992a; Caplan and Douglas, 1991), and consistent with a penetrant phenotype even at permissive temperatures, the *ydj1-151* strain grew somewhat slower than the other strains (Figure 8B). Surprisingly, however, the viability of the Δ*hlj1 ydj1-151* strain remained robust at non-permissive temperatures, which most likely indicated genetic suppression caused by the deletion of the gene encoding Hlj1 (Figure 8A). To then confirm that a known ERAD substrate was stabilized in these strains, I also transformed them with a plasmid engineered for the expression of Chimera A*, an ERAD substrate shown by our lab to be stabilized in *ydj1-151* yeast (Preston et al., 2018). Consistent with these previous findings, Chimera A* degradation was slowed in the *ydj1-151* and Δ*hlj1 ydj1-151* strains even when cells were incubated at 30°C (Figure

8C).

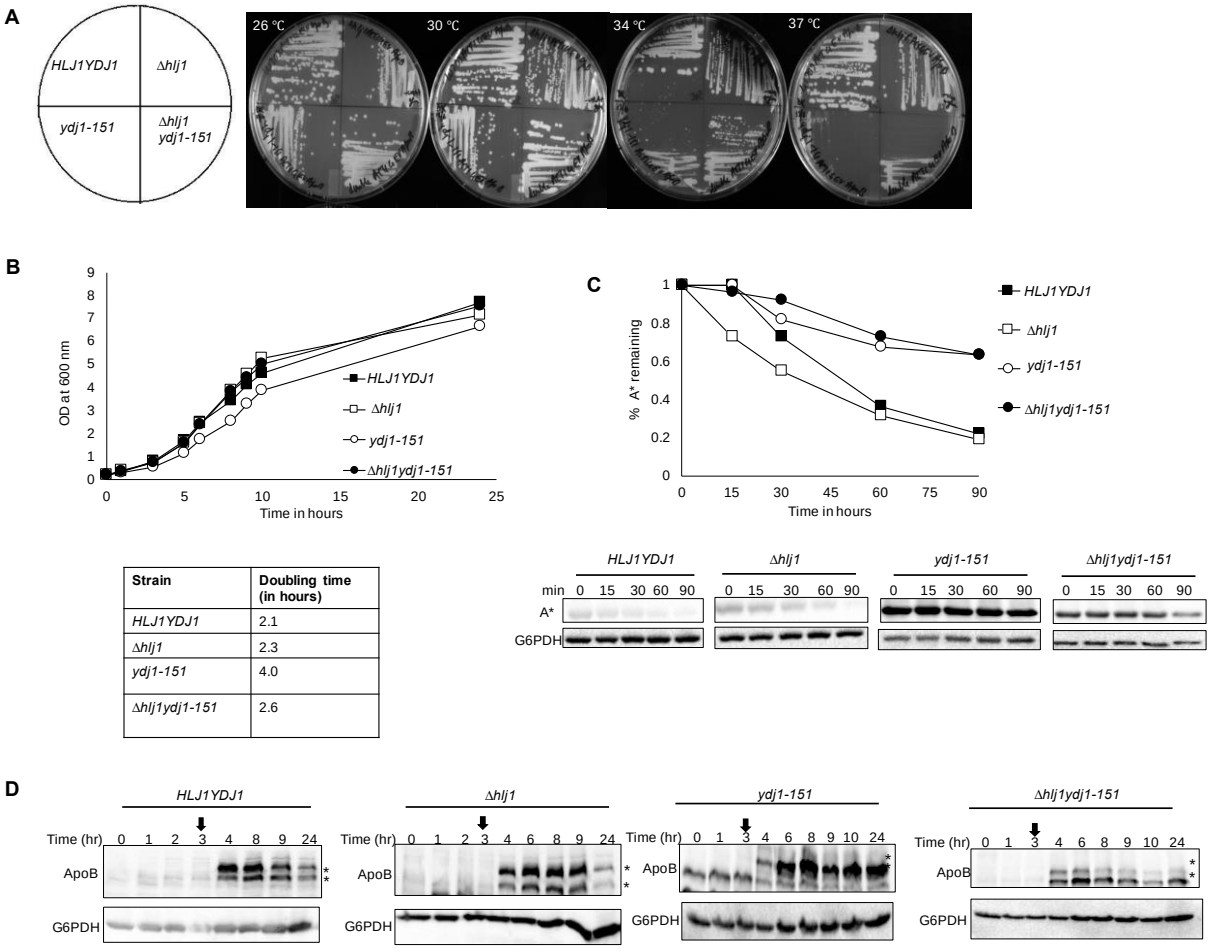

Strain	Doubling time (in hours)
HLJ1YDJ1	2.1
Δhlj1	2.3
ydj1-151	4.0
Δhlj1ydj1-151	2.6

Figure 8. Inducible expression of ApoB29 in yeast mutated for ER-associated Hsp40s.

A. The temperature sensitivity of wild-type (*HLJ1YDJ1*), *ydj1-151,* Δ*hlj1,* and Δ*hlj1 ydj1-151* yeast was tested at permissible (26°C, 30°C) semi-permissible (34°C) and non-permissible (37°C) temperatures after strains containing an integrated copy of the ACT-GEV gene were isolated. B. A growth assay was conducted in the *HLJ1YDJ1* (closed squares), Δ*hlj1* (open squares), *ydj1-151* (open circles) and Δ*hlj1ydj1-151* (closed circles) strains, and growth curves were plotted and doubling times for each strain were calculated. C. A cycloheximide chase assay was conducted as described in in each strain expressing an ERAD substrate, Chimera A*, at 30°C. Cells were collected at the indicated time points and lysates were processed for SDS-PAGE and quantitative western blotting. G6PD served as a loading control, and the levels of Chimera A* were normalized to the levels of G6PD. D. ApoB29 expression was induced by the addition of 300 nM ß-estradiol after 3 hrs in culture (denoted by an arrow) to the *HLJ1YDJ1,* Δ*hlj1, ydj1-151* and Δ*hlj1ydj1-151* strains transformed with an HA-tagged ApoB29 gene under the control of the GAL promoter.

Equivalent ODs of cells were collected at each indicated time point and processed after TCA precipitation for SDS-PAGE and western blotting. ApoB29 appears as two bands representing a glycosylated species (*) and a non-glycosylated species (**) (Doonan et al., 2019).

After verifying the expected phenotypes of these strains, a plasmid containing the N-terminal 29% of the ApoB100 gene ("ApoB29") under the control of a GAL-inducible plasmid was introduced into wild-type (*HLJ1YDJ1*), *ydj1-151,* Δ*hlj1,* and Δ*hlj1 ydj1-151* yeast with the stably integrated ACT1-GEV system. ApoB29 is a naturally occurring ApoB disease isoform in humans and is the smallest ApoB variant that can successfully traffic through the secretory pathway and is regulated by lipid levels in the ER (Collins et al., 1988; Huang et al., 1989; Linton et al., 1993; McLeod et al., 1994). After the cultures were established, β-estradiol was added at a final concentration of 300 nM and 2 OD_{600} of cells were harvested at various times. As expected, ApoB29 was expressed in the strains after induction with β-estradiol with a maximal level of expression achieved after only ~1 hr in the presence of the hormone (Figure 8D). Because the ApoB protein undergoes N-linked glycosylation in the ER as well as complex glycosylation in the Golgi, it often appears as two bands, representing a glycosylated and a non-glycosylated species (Doonan et al., 2019; Grubb et al., 2012; Harazono et al., 2005; Hrizo et al., 2007).

2.3.2 Ydj1 associates with and facilitates the degradation of ApoB29 in yeast

Hsp70 was the first chaperone found to facilitate the degradation of ApoB. This discovery was made possible in an *in vitro* system using reagents prepared from mammalian cells as well as in cell culture (Fisher et al., 1997; Gusarova et al., 2001). Even though the yeast system has been used extensively to explore the contributions of several chaperones and a ubiquitin ligase during ApoB biogenesis (Doonan et al., 2019; Grubb et al., 2012; Hrizo et al., 2007; Rubenstein et al.,

2012), the role of the primary yeast Hsp70 homolog, Ssa1, on the stability of this apolipoprotein had not been examined. Therefore, I conducted cycloheximide chase assays in the *ssa1-45* strain, which lacks the homologous *SSA2*, *SSA3*, and *SSA4* genes but is viable due to the presence of a temperature sensitive version of *SSA1* (Becker et al., 1996). An analogous strain containing a wild-type copy of *SSA1* served as a control. After ACT1-GEV versions of these strains were generated, a cycloheximide chase assay was performed in the yeast after they had been shifted to 37°C for 30 min. Consistent with the data from mammalian cells and *in vitro* experiments (see above), I found that ApoB29 was stabilized in yeast containing the thermosensitive version of Ssa1 (*ssa1-45*; Figure 9A). Interestingly, ApoB29 degradation in the *ssa1-45* strain caught-up with that seen in wild type cells at the later time points, suggesting compensatory effects of other chaperones in the absence of Ssa1.

Based on these data and because Hsp40s are obligatory co-chaperones for Hsp70 (Mayer and Bukau, 2005), I hypothesized that ApoB29 would also be stabilized in the Hsp40 mutant strains, constructed above. Interestingly, I found that ApoB29 was stabilized only in strains containing the loss-of-function mutation in Ydj1 (i.e., in the *ydi1-151* and the Δ*hlj1 ydj1-151* strains; Figure 9B). Because the deletion of Hlj1 did not alter the degradation rate of ApoB29, these data underscore the differential roles Hsp40s can play in the ERAD of a substrate (Brodsky, 2007; Cyr, 1995; Farinha et al., 2002; Guerriero et al., 2017; Han et al., 2007; Huyer et al., 2004; Meacham et al., 1999; Nakatsukasa et al., 2008; Sun and Brodsky, 2018; Zhang et al., 2002). Besides stimulating and enhancing the ATPase activity of Hsp70s, Hsp40s also aid in substrate recognition (Craig and Marszalek, 2017; Fan et al., 2003). To explore if Ydj1 identifies ApoB29 for the ERAD pathway, I next conducted a co-immunoprecipitation experiment in cells transformed with pACT-GEV1. Expression of ApoB29 was induced with ß-estradiol for 1 hr

before cells were harvested, solubilized, and ApoB29 was immunoprecipitated under native conditions. The presence of distinct chaperones was then examined by western blotting. As shown in Figure 9C, left ("IP:ApoB"), ApoB coimmunoprecipitated with both Ydj1 and Ssa1. As a

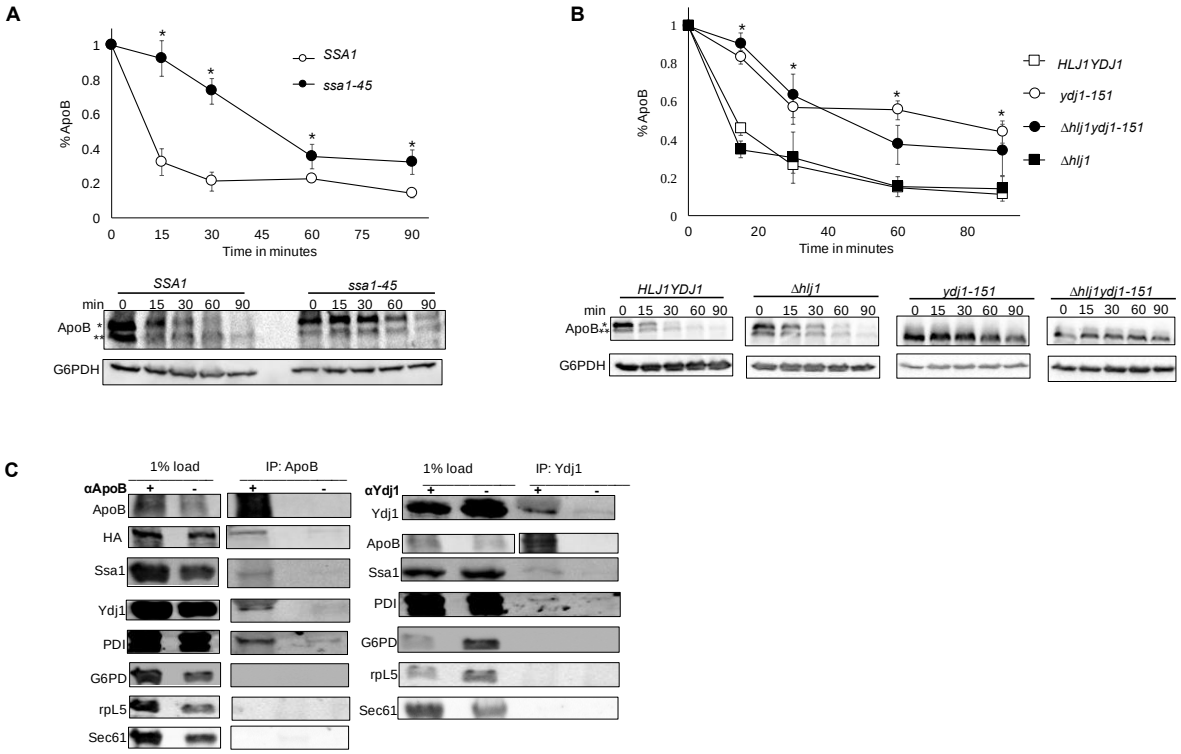

Figure 9. Ydj1 and Ssa1 associate with and facilitate the degradation of ApoB29.

A. Cycloheximide chase assays were conducted as described in the Materials and Methods. The turnover of ApoB was examined in *SSA1* (open circle) and *ssa1-45* (closed circle) strains expressing ApoB29 after cells had been shifted to 37°C for 30 min and β-estradiol was present for 1 hr. Equivalent ODs of cells were collected at each indicated time point and processed for quantitative western blotting. Data from each time point were normalized to the G6PDH loading control. Representative blots with the migration of the glycosylated (*) and unglycosylated (**) versions of ApoB29 are shown below, and GAPDH served as a loading control. The amount of ApoB29 remaining over time was plotted relative to the amount of protein at time 0. B. Cycloheximide chase assays were conducted in the *HLJ1YDJ1* (open square), Δ*hlj1* (closed square), *ydj1-151* (open circle) and Δ*hlj1ydj1-151* (closed circle) strains expressing ApoB29 as described above in Materials and Methods. Representative blots are again shown below the graph. C. Co-immunoprecipitation assays were performed as described in Materials and Methods using anti-HA conjugated beads

in wild type cells expressing ApoB29 (left), and a reciprocal immunoprecipitation was performed using an anti-Ydj1 antibody (right). Data were calculated from N=3 independent experiments, ±SE, * indicates $p<0.05$.

positive control, I also observed that PDI associated with ApoB (Grubb et al., 2012), whereas G6PDH, a cytosolic metabolic enzyme, rpL5, a ribosomal protein, and Sec61, an ER membrane protein, failed to co-immunoprecipitate with ApoB29. To confirm these data, a reciprocal co-immunoprecipitation was performed, and ApoB29 was again found associated with Ssa1 and Ydj1 (Figure 9C, right, "IP:Ydj1"). These data strongly suggest that Ydj1 interacts with and regulates the ERAD of ApoB in yeast.

To establish whether the association between ApoB and Ydj1 was direct, I next attempted to conduct a chemical crosslinking reaction in the ApoB29-expressing cells. After cells were incubated with DSP for 40 min, the cells were solubilized under denaturing (i.e., 0.1% SDS) conditions and ApoB29 was precipitated with HA-conjugated agarose. After an overnight immunoprecipitation, the samples were treated with a reductant ß-mercaptoethanol (BME) to reduce DSP cross-linked products. The lack of BME treatment was used as a control and as anticipated, addition of reductant denatured the cross-linked complex (Figure 10A). The absence of added antibody was also used as a control to detect non-specific binding. Unfortunately, although Ydj1 and Ssa1 precipitated with ApoB, they were also present in the immunoprecipitation that lacked antibody. Additional attempts to prevent the non-specific precipitation of the chaperones were unsuccessful (data not shown).

Since I noticed that the unglycosylated/deglycosylated ApoB29 species was more abundant than the glycosylated band in the *ydj1-151* strain (Figure 9B), I also asked if Ydj1 facilitated the translocation of ApoB29 into the ER. Ydj1 has been shown to assist the translocation of select proteins into the ER post-translationally (Caplan et al., 1992a; Ngosuwan et al., 2003). Even

though ApoB is known to undergo co-translational translocation into the ER, at least in higher cells (Chuck and Lingappa, 1992; Chuck et al., 1990), it was formally possible that Ydj1 contributes to ApoB29 post-translational translocation in yeast. I therefore attempted to conducted metabolic pulse chase experiments which would enable me to monitor the maturation of ApoB29 as it enters the ER.

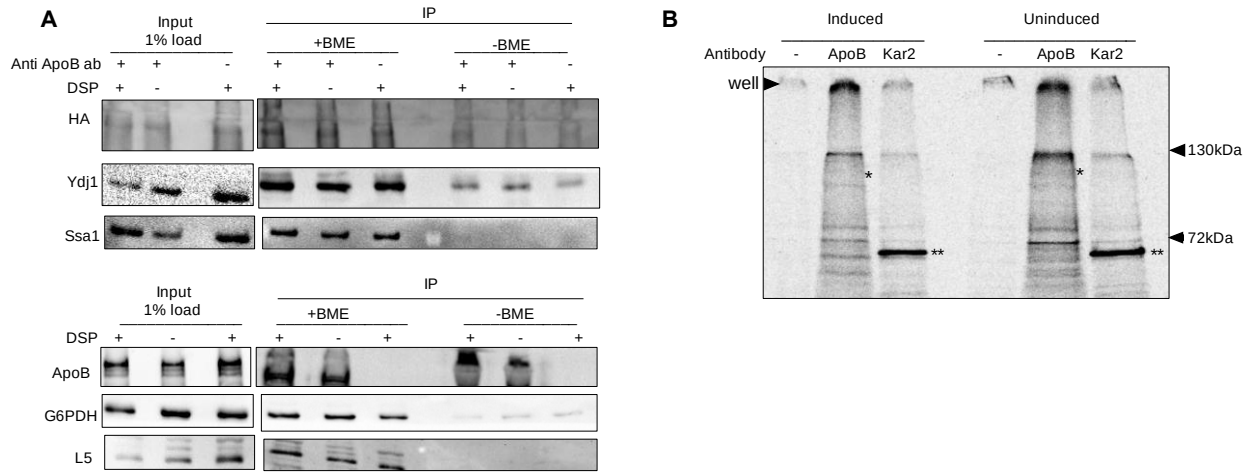

Figure 10. In vivo crosslinking and pulse chase assays in yeast expressing HA tagged ApoB29.

A. *In vivo* crosslinking using DSP was performed in yeast cells expressing ApoB29 as described in the Materials and Methods. ApoB antibody was used to pull down ApoB and samples were processed by SDS-PAGE and western blotting to detect the indicated proteins. Reductant (BME) was used to reduce the cross-linked products. No DSP, no BME and no antibody conditions were used as controls. G6PDH and L5 were used as negative controls. Top and bottom images show the same samples run on different gels. B. A pulse-chase assay was conducted in cells expressing or not expressing ApoB29 as described in Materials and Methods. ApoB29 was precipitated with an anti-ApoB antibody. * indicates the expected migration of newly translated ApoB29 species. ** indicates Kar2 which serves as a positive control.

Unfortunately, due to its size and relatively low levels of expression in yeast, attempts to identify a specific ApoB29 species in yeast after a metabolic pulse-chase were unsuccessful

(Figure 10B). As a positive control, I could however detect radiolabeled Kar2, an ER lumenal Hsp70, in the immunoprecipitate (Figure 10B).

To verify my findings on the role of Ydj1 in ApoB turnover in yeast, I then attempted to examine ApoB29 stability in another published, temperature-sensitive loss-of-function mutant strain, *ydj1C406S*. This allele encode a Ydj1 mutant that is not farnesylated and therefore is untethered to the ER membrane (Caplan et al., 1992b). However, when the stability of ApoB29 was examined in this strain compared to a wild-type strain, only a subtle difference was observed (Figure 11A). However, when I examined whether the strain was temperature sensitive, as published, robust growth was observed at 37°C (Figure 11B). This might have arisen from the presence of a suppressor mutation.

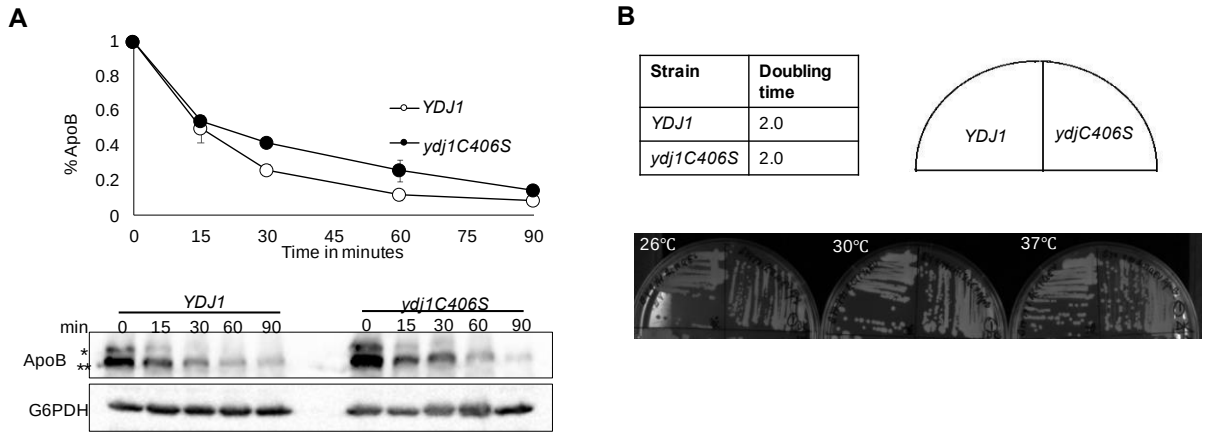

Figure 11. ApoB is marginally stabilized in ydj1C406S yeast.

A. A cycloheximide chase was conducted in the *YDJ1* and *ydj1C406S* strains at 37°C as described in Materials and Methods. B. Temperature sensitivity was conducted at 37°C, and a doubling time (in hrs) was calculated from a growth assay.

2.3.3 Optimization of ApoB100 expression and experimental conditions in McArdle Rh777 (McA) cells

Amongst the model systems utilized to study ApoB biology, McArdle Rh777 (McA) cells (ATCC CRL-1601), a rat hepatoma cell line, represent a powerful system because these cells endogenously express and secrete full-length ApoB, i.e., ApoB100, as well as ApoB48. The liver and small intestine are the primary sites of ApoB expression, and in these tissues ApoB is expressed as both the ApoB100 and ApoB48 isoforms. ApoB48 represents the N-terminal 48% of the full-length protein (Chen et al., 1987; Chen et al., 1986). In humans, ApoB100 is synthesized in the liver and is the primary structural component of VLDLs and LDLs (see Chapter 1). In contrast, ApoB48 is only expressed in the small intestine and is the primary structural component of chylomicrons. Because both isoforms are expressed in the liver of rodents, the McA liver cell line expresses both ApoB100 and ApoB48 isoforms, permitting an analysis of the contributions of specific factors on the biogenesis of two physiologically relevant species. In addition, candidate specific genes can be readily knocked down or overexpressed in McA cells and their effects on ApoB stability examined by conducting pulse chase experiments (Borchardt and Davis, 1987; Boren et al., 1992; Boren et al., 1994; Bostrom et al., 1986). Therefore, I chose to examine the role of Hsp40s in these cells.

To these ends, I first optimized basic experimental conditions. To achieve maximal lysis of cells, I used different lysis buffers and found that RIPA buffer lysed the cells optimally (Figure 12A). To optimize the number of cells needed to detect ApoB in media (i.e., after its trafficking through the secretory pathway), I seeded different number of cells ($2x10^5$ and $4x10^5$) and let them grow overnight at 37ºC. The next morning, I conducted a pulse chase experiment and collected media and cellular lysate 15 and 60 min during the chase. As expected, I observed both ApoB100

(~550 kDa) and ApoB48 (~250 kDa) in the cellular lysate at the15 and 60 min time points (Figure 12B). In contrast, I found that there was no secretion after 15 min but both species were secreted at 60 min (Figure 12B), consistent with published data (Boren et al., 1992; Boren et al., 1994; Bostrom et al., 1986; White et al., 1992) and reflective of the fact that ApoB takes ~30 min to be synthesized, folded, packaged into COPII vesicles at the ER for delivery to the

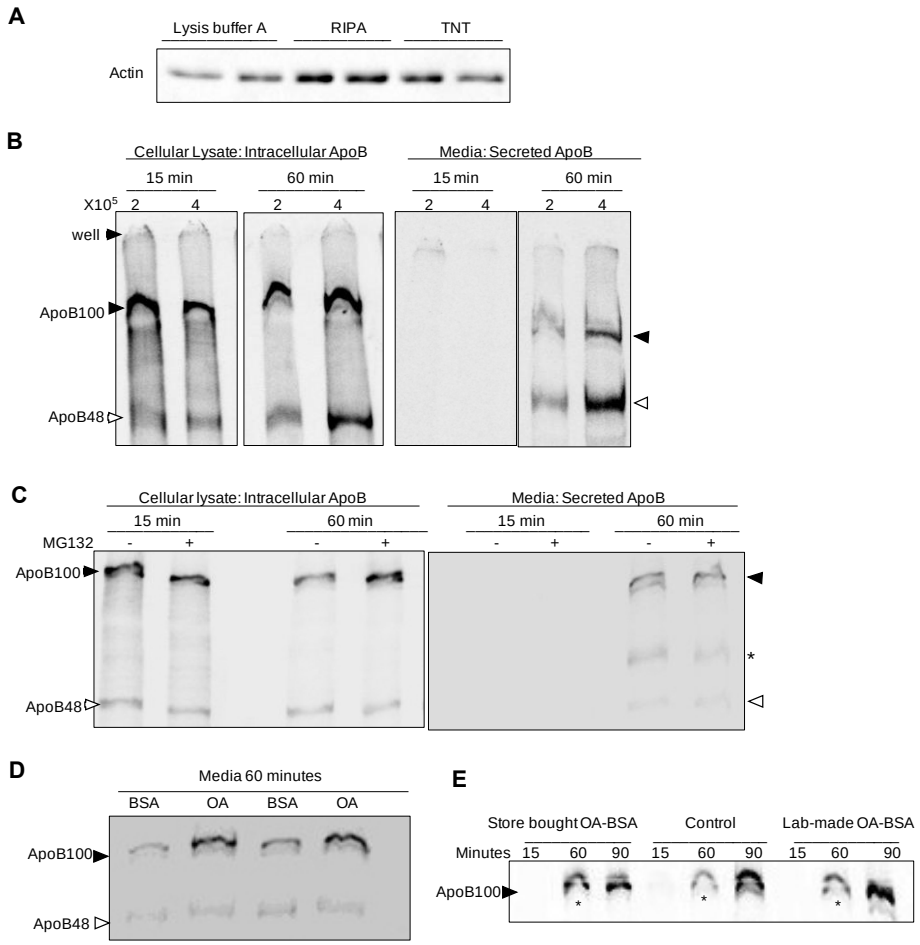

Figure 12. Optimization of experimental conditions in McA cells.

A. Equal numbers of cells were lysed using different lysis buffers and equal amounts of protein were processed for SDS-PAGE and western blotting using an anti-actin antibody. B. A pulse chase assay was conducted as described in the Materials and Methods. Different numbers of cells ($2x10^5$ and $4x10^5$) were seeded and grown overnight, and the next day the cells were starved for 1 hr and then incubated in media with radioactive amino acids for 15 min (pulse). The media was removed, the cells were washed, and an excess of unlabeled Met/Cys and cycloheximide were added

to the cells to begin the chase. The media and cells were then collected at 15 and 60 min, and ApoB was immunoprecipitated using anti-ApoB antibody and normalized counts were analyzed via SDS-PAGE and phosphorimage analysis. Arrowheads indicate the relative migrations of ApoB100 (closed arrowhead, 550 kDa) and ApoB48 (open arrowhead, 248 kDa). C. Cells were pre-incubated with 25 μM MG-132 for 1 hr and a pulse-chase assay was conducted as described above. * indicates a non-specific species in media in the 60-min sample. D. Cells were treated with 0.4 mM OA-BSA conjugate for 4 hrs and a pulse-chase assay was again conducted. E. The effects of commercially available and lab prepared OA-BSA were compared on levels of secreted ApoB100 in a pulse-chase assay. Where indicated in the text, data were quantified using imageJ.

Golgi, and ultimately secreted from cells (Benoist and Grand-Perret, 1997). Next, to examine whether I could recapitulate the proteasome-dependent degradation of ApoB (Fisher et al., 1997; Yeung et al., 1996), I incubated cells with 25μM MG-132, a proteasome inhibitor (Gaczynska and Osmulski, 2005), for 30 min prior to the addition of radioactive methionine and cysteine. I then conducted a pulse chase assay to assess the effect on ApoB levels. Consistent with reports in the literature (Cardozo et al., 2002; Fisher et al., 2008; Liang et al., 2000), proteasome inhibition enhanced intracellular ApoB100 levels at 60 min by ~2-fold (closed arrowhead, Figure 12C). Because ApoB secretion from McA cells is enhanced by the addition of an oleic acid (OA)-BSA conjugate (White et al., 1992), I also prepared OA-BSA conjugates and pre-incubated cells prior to the addition of radioactivity. As expected, ApoB100 secretion was enhanced by OA-BSA treatment (closed arrowhead, Figure 12D). This effect was more noticeable for the ApoB100 isoform, and indeed differential effects on the isoforms were also observed when MTP, the lipid loading complex, was depleted in mice (Raabe et al., 1999). To confirm this result, I also tested commercially available OA-BSA conjugates and found that the commercial and prepared OA-BSA conjugates enhanced ApoB secretion ~2-fold (Figure 12E).

2.3.4 The DNAJA1 (JA1) molecular chaperone associates with and facilitates the degradation of ApoB

After confirming ApoB expression, secretion (Figure 12B), and proteasome mediated degradation (Figure 12C), as well as oleic acid-mediated enhanced secretion of ApoB (Figure 12D 12E) in McA cells, I next investigated the role of Hsp40s during ApoB biogenesis. I first asked if DNAJA1 (JA1), the human homolog of Ydj1 (Stark et al., 2014) that shares ~46% amino acid sequence identity (Figure 13), would similarly contribute to the ERAD of ApoB.

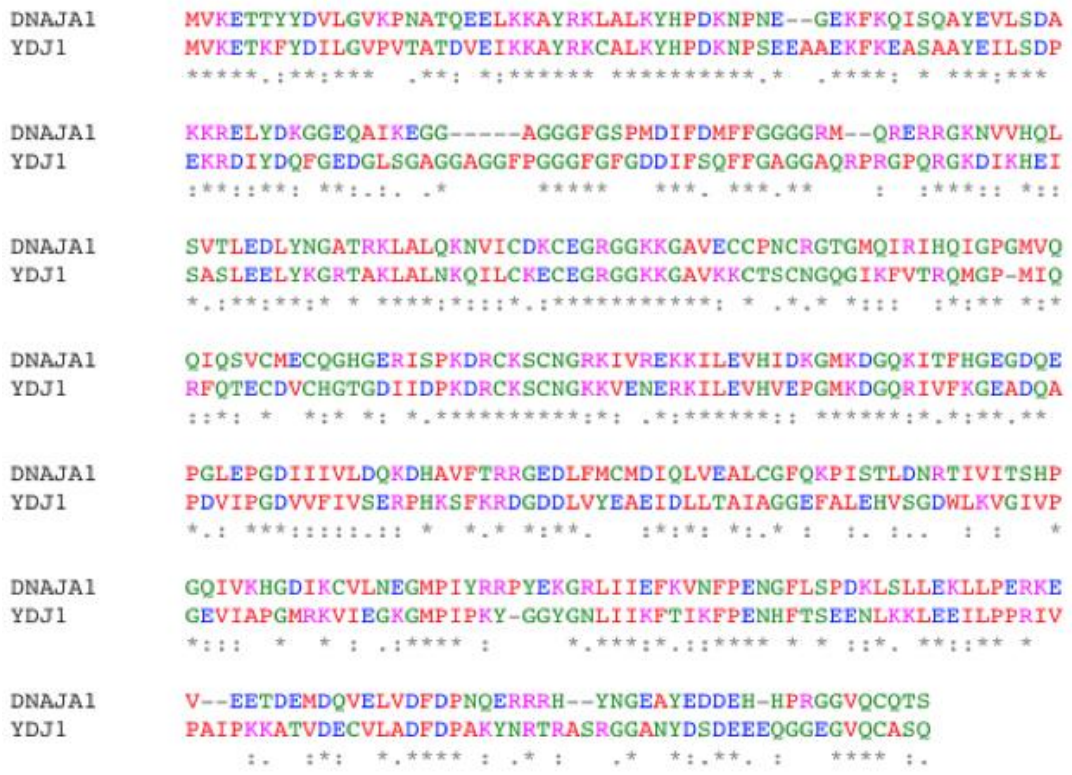

Figure 13. Ydj1p and JA1 are 46% identical.

The amino acid sequences of Ydj1p and JA1 were retrieved from NCBI database and aligned using clustal Omega. Color code represents clustal omega color scheme.

To this end, I began by knocking down JA1 in McA cells utilizing the RNAiMAX transfection reagent (Invitrogen) following the manufacturer's instructions. To optimize knockdown conditions, I used five different ORF-targeting siRNA oligonucleotides (ON-Target plus siRNA, Dharmacon, Thermo Fisher Scientific) at final concentrations of 20 nM and 30 nM. I then measured the magnitude of knockdown efficiency by conducting quantitative western blotting of JA1 from cultures 48 and 72 hr post transfection (Figure 14A). The levels of actin were measured as a loading control. I also used a fluorescently tagged scrambled siRNA (Block-It Alexa Fluor Control, Thermo Fisher Scientific) as a negative experimental control. Based on the uptake of the fluorescently tagged scrambled siRNA in cells, I calculated the transfection efficiency with both concentrations 48 hr post transfection to be >80% (data not shown). In addition, since JA1 is required for the protein quality control of select substrates in mammalian cells (Abisambra et al., 2012; De Mattos et al., 2020; Dekker et al., 2015; Okiyoneda et al., 2011; Rauch and Gestwicki, 2014), its knockdown could elicit a stress response. Therefore, I measured the levels of the cytosolic stress inducible Hsp70 chaperone but found that it was not significantly altered. In a repeat of the first experiment, I also found that select siRNAs at a final concentration of 20 nM depleted JA1 maximally to ~80% (Figure 14B). To confirm that the main product I observed was JA1,I also compared the signal with different amounts of purified JA1 (Ireland et al., 2014) (Figure

14C). Based on knockdown efficiency, the lack of a stress response, and the retained cell viability,

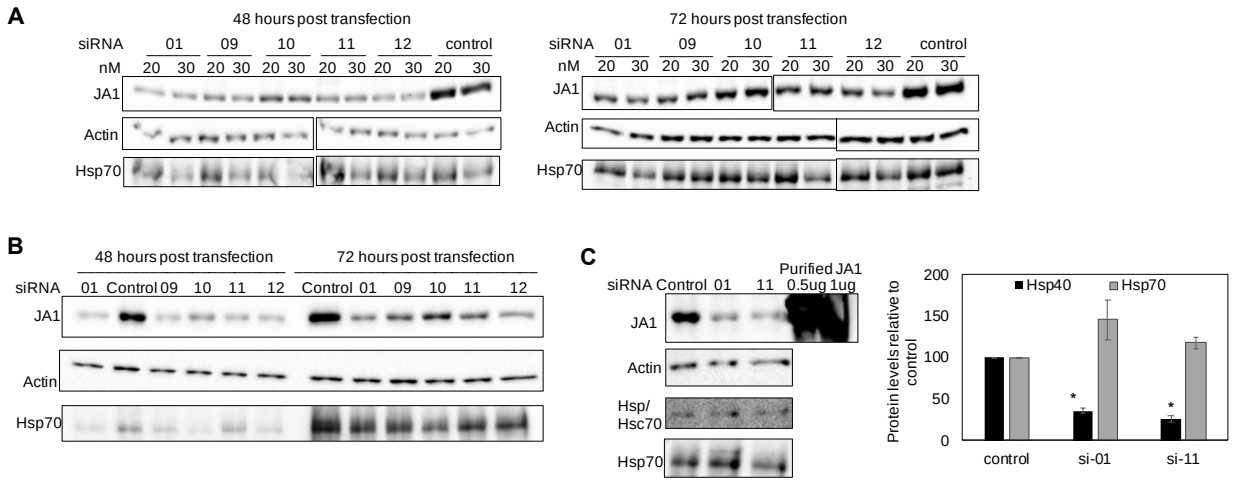

Figure 14. Optimization of JA1 knockdown conditions in McA cells.

A. McA cells were transfected with five different siRNA oligonucleotides targeting JA1 for 48 and 72 hrs at final concentrations of 20 nM and 30 nM as described in section 2.2.6. Cells were lysed in RIPA and analyzed by SDS-PAGE and western blotting using antibodies against JA1, actin, and Hsp70. B. Each siRNA was again transfected into the same number of cells, but at a final concentration of 20 nM, which were processed as described above. C. siRNAs 01 and 11 were transfected into cells at a final concentration of 20 nM; 5ug and 1ug of purified JA1 were also examined. Based on this experiment, siRNAs 01 and 11 depleted JA1 levels to >70% of the scrambled siRNA treatment and were selected for subsequent experiments. The levels of JA1, actin and Hsp70 were quantitatively analyzed via western blotting, data plotted in bar graph represent the means of N = 3 independent experiments, ±SE, and * indicates $p<0.05$.

we selected siRNA01 for subsequent experiment.

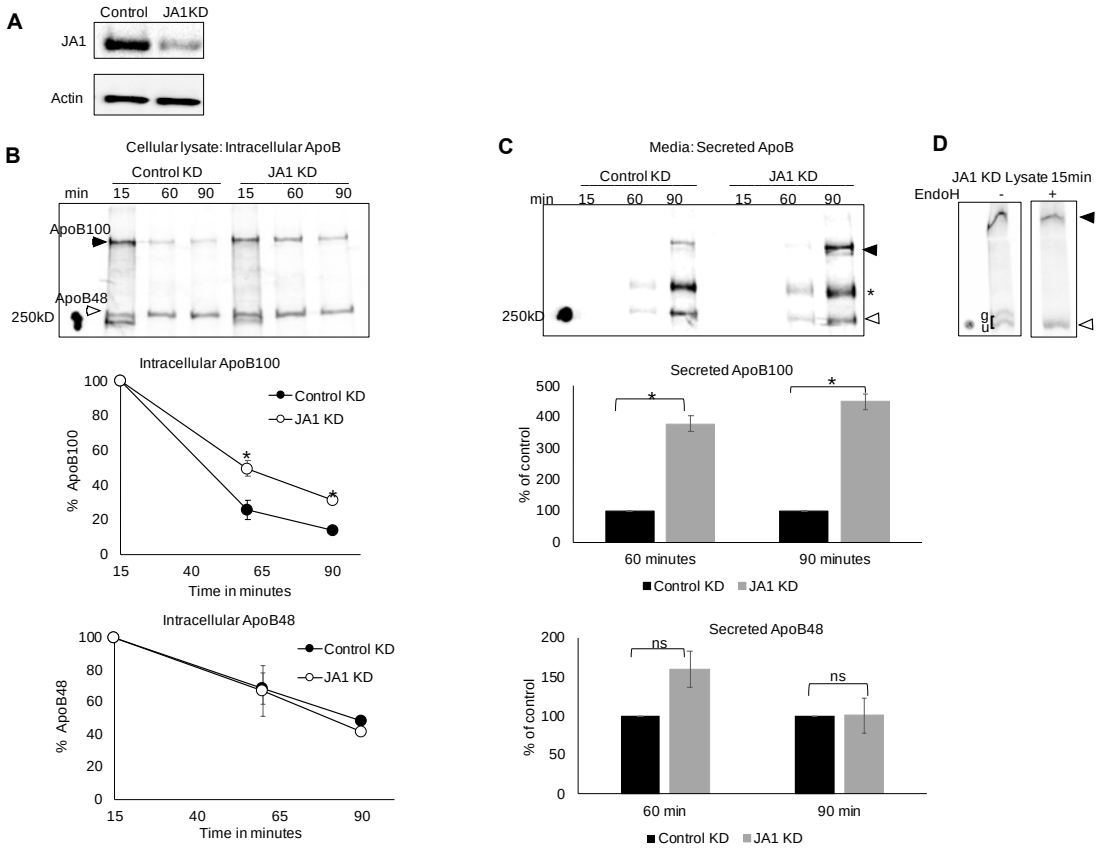

Figure 15. The JA1 molecular chaperones facilitates ApoB100 degradation.

A. McA cells were transfected with the optimized JA1 siRNA (JA1 KD) or a scrambled siRNA (control KD) for 48 hrs. A representative western blot shows JA1 and actin levels after knockdown. B. A pulse chase experiment was conducted as described in section 2.2.7. Cells were starved for 1 hr and then incubated in media with radioactive amino acids for 15 min (pulse). The media was washed, and an excess of unlabeled methionine and cysteine were added to cells to begin the chase. The media and cells were collected at 15, 60, and 90 min, and after processing ApoB was immunoprecipitated using anti-ApoB antibody and analyzed via SDS-PAGE and phosphorimaging analysis. A representative radiograph and graphs of the intracellular ApoB100 (closed arrowhead) and ApoB48 (open arrowhead) levels are shown. C. A representative radiograph and graphs show levels of secreted ApoB100 (closed arrowhead) and ApoB48 (open arrowhead). * indicates a non-specific band. D. Samples from lysate 15-min time point were subjected to EndoH digestion. The radiograph shows the collapse of the ApoB48 upper band (glycosylated, g) to the

lower band (unglycosylated, u) upon EndoH digestion. Data represent the means of N = 5 independent experiments, ±SE; * indicates $p<0.05$, ns indicates $p>0.05$.

To investigate the effect of JA1 ablation on ApoB, I conducted pulse-chase experiments after knocking down JA1 (Figure 15A). In accordance with the data obtained in *ydj1-151* yeast (Figure 9B), JA1 knockdown enhanced both intracellular and secreted ApoB100 levels when compared to the scrambled siRNA control (closed arrowheads, Figure 15B, 15C).

Similar results were also obtained with a second set of siRNAs (data not shown). In some experiments, ApoB48 migrated as a doublet. Based on EndoH treatment, these represent a core ER-glycosylated and unglycosylated species, since the glycosylated (g) species collapsed to the lower unglycosylated (u) species after treatment (Figure 15D). Regardless, the levels of ApoB48 (open arrowheads) were unaltered upon JA1 knockdown (but see below). Because ApoB48 represents the N-terminal 48% of ApoB100, it is possible that JA1 acts on the C-terminal portion of ApoB100 to facilitate its degradation. As mentioned previously, ApoB48 has also been shown to be differentially affected when MTP is inactivated (Raabe et al., 1999), consistent with the fact that ApoB100 and ApoB48 can be regulated by distinct pathways. Thus, it is also formally possible that the absence of the chaperone regulates a factor in one of these pathways that in turn differentially regulates ApoB100 compared to ApoB48.

Surprisingly, in one of my biological replicates for pulse chase experiment, I noticed there was a differential effect of JA1 knockdown on the ApoB isoforms. Whereas ApoB100 levels (closed arrowhead) increased, the levels of ApoB48 (open arrowhead) appeared to decrease (Figure 16A). Because ApoB48 is the product of an mRNA-editing event catalyzed by the Apobec1 enzyme (Blanc and Davidson, 2010), I asked if JA1 ablation alters the levels of Apobec1, which might give rise to the observed loss of ApoB48. However, after I knocked down JA1 and

compared the levels of the Apobec1 protein, no difference in the amount of this enzyme was noted (Figure 16B). Since this differential effect was observed only once and was inconsistent, it was not pursued further.

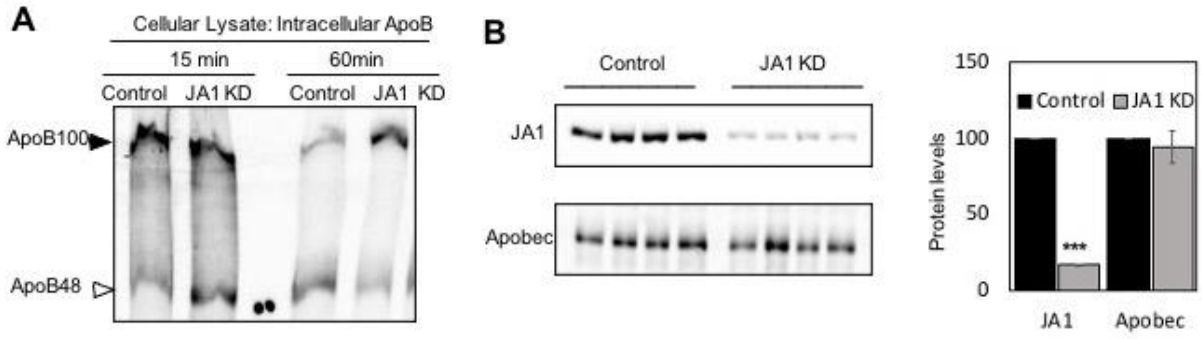

Figure 16. JA1 depletion does not alter Apobec1 levels.

A. Pulse chase was conducted as described in 2.2.7 and Figure 15. Cells were treated with scrambled siRNA (control) or JA1 siRNA (JA1 KD) for 48 hrs. Cells were starved for 1 hr and then incubated in media with radioactive amino acids for 15 min (pulse). The media was washed, and an excess of unlabeled methionine and cysteine were added to cells to begin the chase. The media and cells were collected at 15, and 60 min, and after processing ApoB was immunoprecipitated using anti-ApoB antibody and analyzed via SDS-PAGE and phosphorimaging analysis. The radiograph shows the intracellular ApoB100 (closed arrowhead) and ApoB48 (open arrowhead) levels. Double dots represent the 250 kD marker. B. A Western blot analysis was conducted to examine Apobec levels in cells transfected with scrambled siRNA (control) or JA1 siRNA (JA1 KD). JA1 levels were also examined. Data represent the means of N = 4 independent experiments, ±SE, and * indicates $p<0.05$.

I next asked if the degree of ApoB100 stabilization was comparable to the effect of proteasome inhibition, or whether there would be an additive effect of JA1 depletion and proteasome inhibition on ApoB levels. As shown in Figure 17A-B, the presence of the proteasome inhibitor, MG-132, failed to increase the amount of ApoB100 beyond that observed upon JA1 knockdown (~2.5 fold), and there was no additive effect when the two conditions were combined (~2.5 fold). These results are consistent with the notion that JA1 contributes to the targeting of

ApoB to the ERAD pathway.

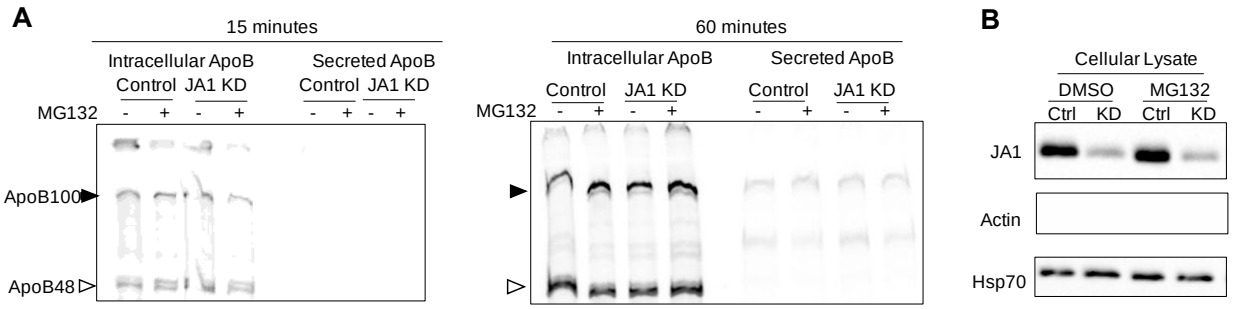

Figure 17. Proteasome inhibition and JA1 knockdown phenocopy one another.

A. JA1 was either knocked down and/or cells were treated with MG-132 for 1 hr before a pulse chase analysis was conducted as described in section 2.2.7 and Figure 15. A representative radiograph shows ApoB100 and ApoB48 levels under each condition after 15 and 60 min of the chase. B. A western blot analysis was performed to confirm the extent of JA1 knockdown. Actin and Hsp70 levels in the lysate after JA1 knockdown or under control conditions were also examined.

Because Ydj1 appeared to associate with ApoB29 in yeast (Figure 9C), I next asked if JA1 associates with ApoB in McA cells. Therefore, co-immunoprecipitations were conducted in detergent-solubilized cells followed by western blot analysis. Consistent with findings in yeast, JA1 co-precipitated with ApoB100 (Figure 18A). I then conducted cross-linking experiments by treating cells with DSP, a membrane permeable cross-linker (Mattson et al., 1993), and after the cells were solubilized under denaturing conditions, ApoB100 was immunoprecipitated and protein partners were identified by western blotting. As expected, JA1 also crosslinks with ApoB, further

validating their association (Figure 18B).

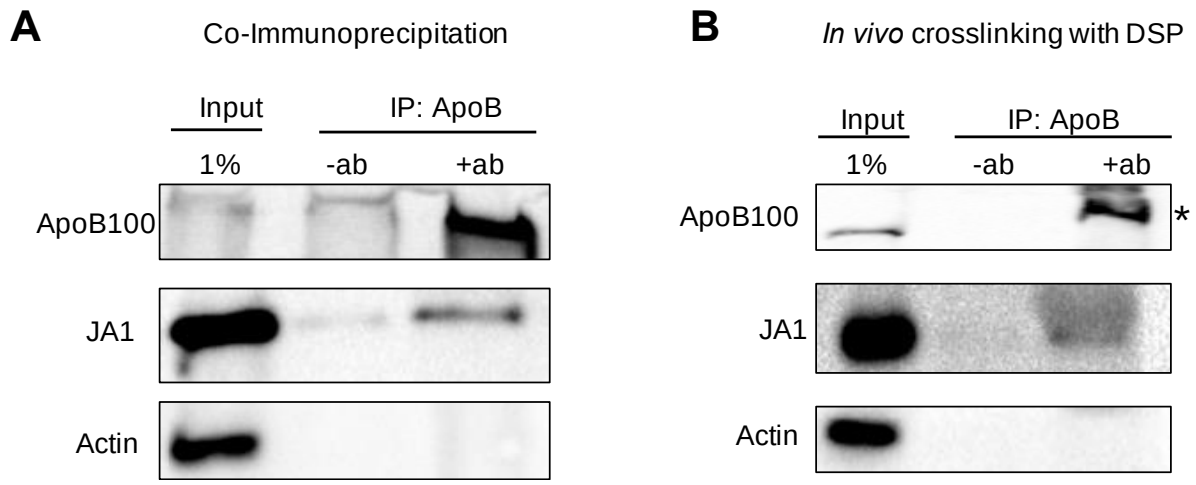

Figure 18. JA1 co-immunoprecipitates and crosslinks with ApoB100.

A. Co-immunoprecipitation assays were performed as described in section 2.2.8 using anti-ApoB beads and detergent solubilized cellular lysate. B. Chemical crosslinking was performed as described in section 2.2.8 after cells were treated with 2 mM DSP for 30 min. Crosslinking was quenched with 1 M Tris-Cl, pH 7.5, the cells were lysed, and ApoB was immunoprecipitated and the crosslinks were broken in urea sample buffer supplemented with 20 mM DTT and heating at 37°C for 30 min. Input (1 %) and immunoprecipitated fractions were processed for SDS-PAGE and western blotting. Actin was used as a negative control. Crosslinked immunoprecipitated ApoB100 migrating at a slower rate indicates incomplete reduction of the crosslinked complex in the immunoprecipitated fraction (denoted with a *).

2.3.5 The solubility of ApoB is unchanged by the loss of JA1

Based on the action of other Hsp40s (Kampinga et al., 2019) and JA1's association with ApoB100 (Figure 18), I proposed that JA1 might act as a "holdase" to maintain the solubility of ApoB as it retrotranslocates from the ER, which may be crucial given the highly hydrophobic character of this apolipoprotein (Segrest et al., 1992). To test this hypothesis, I conducted detergent solubility assays using a non-ionic detergent, dodecyl maltoside (DDM), which can solubilize

membrane bound proteins but not aggregated proteins (Calcutta et al., 2012). After I incubated cells in which JA1 had been knocked down or treated with a control (scrambled) siRNA with multiple concentrations of DDM, the samples were centrifuged at 100,000g, the soluble (supernatant) and insoluble (pellet) fractions were processed, and the presence of ApoB100 was examined by western blot analysis. Contrary to my hypothesis, depletion of JA1 had no effect on ApoB solubility (Figure 19A). Ribophorin, an integral ER membrane protein (Crimaudo et al., 1987), was also solubilized by this treatment. In contrast, when I expressed CFTR, a well-known aggregation-prone protein in McA cells (Estabrooks and Brodsky, 2020; Strickland et al., 1997), CFTR resided primarily in the insoluble fraction (Figure 19B).

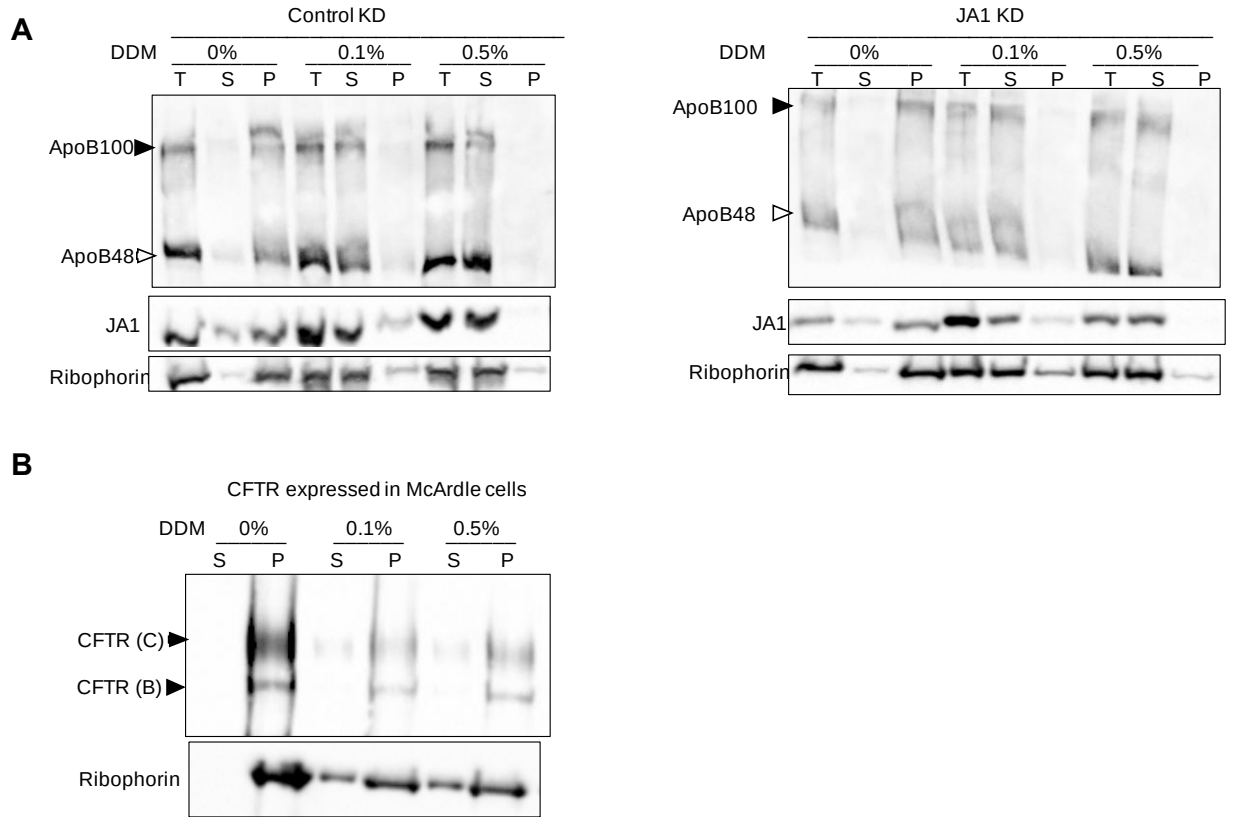

Figure 19. The loss of JA1 has no effect on ApoB solubility.

A. A detergent solubility assay was performed as described in section 2.2.8 using various concentrations of DDM in control and JA1 knockdown cells. T represents the total solubilized fraction prior to centrifugation. The efficiency of

JA1 knockdown was examined and ribophorin was used as a control. S represents the soluble fraction (supernatant), and P represents the insoluble fraction (pellet). B. Detergent solubility was conducted in McA cells overexpressing CFTR to demonstrate the efficacy of DDM to resolve soluble versus aggregated proteins. Arrowheads indicate bands B and C of CFTR, which respectively represent the ER and post-ER resident forms of the protein.

I next utilized a published protocol in which sequential incubations of lysate with different detergents, interrupted by centrifugation, was used to confirm these results. In this case, digitonin (0.1%), NP40 (1%), and SDS (0.1%) were used in order to extract increasingly aggregated species (Holden and Horton, 2009). Here too, I failed to notice any difference in the aggregation of ApoB upon JA1 knockdown (Figure 20A).

Because these experiments were conducted under steady state conditions, I wondered if the depletion of JA1 might selectively help maintain nascent ApoB in an aggregation-free state. To this end, I radioactively pulsed cells and performed the same detergent solubilization experiment. I then immunoprecipitated ApoB100 from each fraction and analyzed the material after SDS-PAGE and phosphorimager analysis. As shown in Figure 20B, JA1 knockdown did not lead to increased aggregation of nascent ApoB since—in both cases—most of the protein remained in the 1% NP40 fraction. Therefore, while JA1 associates with and facilitates the degradation of ApoB, the chaperone may not maintain the solubility of ApoB100 during ERAD. However, the lack of an effect could also be due to the following reasons. First, there could be compensatory effects of other Hsp40s when a single member of this family is silenced. Second, JA1 might be a dispensable

member of a multi protein disaggregase complex. Since the knockdown is not 100%,

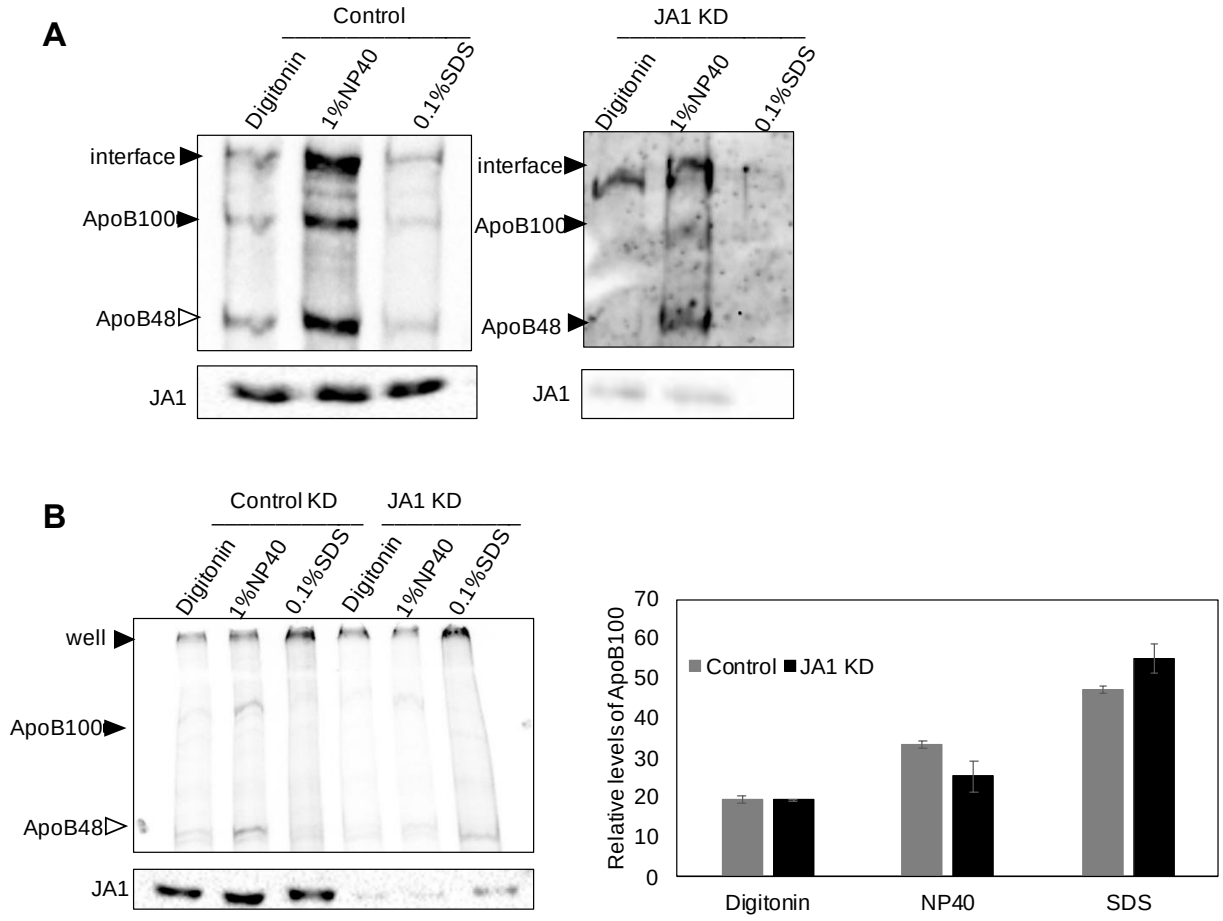

Figure 20. ApoB solubility is maintained independent of JA1 function.

A. A sequential detergent solubility assay was performed with McA cells in which a scrambled control or an siRNA directed against JA1 was used. Lysate was then treated sequentially with 0.1% digitonin, 1% NP-40 and 0.1% SDS for one hr, and in between each step, the solution was centrifuged at 7000 g for 10 min at 4°C (see 2.2.8). B. McA cells were treated with an siRNA against JA1 or a scrambled control (control KD) and were then pulsed with radioactive Met/Cys for 15 min. The media was changed, and an excess of unlabeled amino acids was provided. The cells were collected after 60 min into the chase and lysate was subjected to sequential analysis with digitonin, NP-40 and SDS, as in part A. ApoB100 was precipitated from each fraction using anti-ApoB antibody and samples were processed for SDS-PAGE and phosphorimage analysis. Data represent the means of N = 3 independent experiments, ±SE.

a residual amount of JA1 or another chaperone might be sufficient to keep ApoB in a soluble conformation.

2.4 JA1 depletion hyper-lipidates secreted ApoB100

Both levels of intracellular and secreted ApoB100 rose when JA1 was knocked down (Figure 15). Because the secreted ApoB pool contains fully lipidated lipoprotein particles (Boren et al., 1994), I asked if the enhanced secretion of ApoB I observed upon JA1 knockdown produces poorly lipidated lipoproteins that might have escaped ERAD. To examine this hypothesis, I followed a published protocol and conducted a sucrose gradient ultra-centrifugation assay (Boren et al., 1992; Boren et al., 1994). First, JA1 was knocked down or cells were treated with a scrambled siRNA control as described in section 2.2.8. This was then followed by a pulse chase analysis. Next, media was collected after 90 min into the chase. Normalized radioactive counts from this fraction were diluted and overlaid on top of the sucrose gradient, an after centrifugation, 12 fractions were collected and ApoB was immunoprecipitated from each fraction to determine its

density and thus lipidation state.

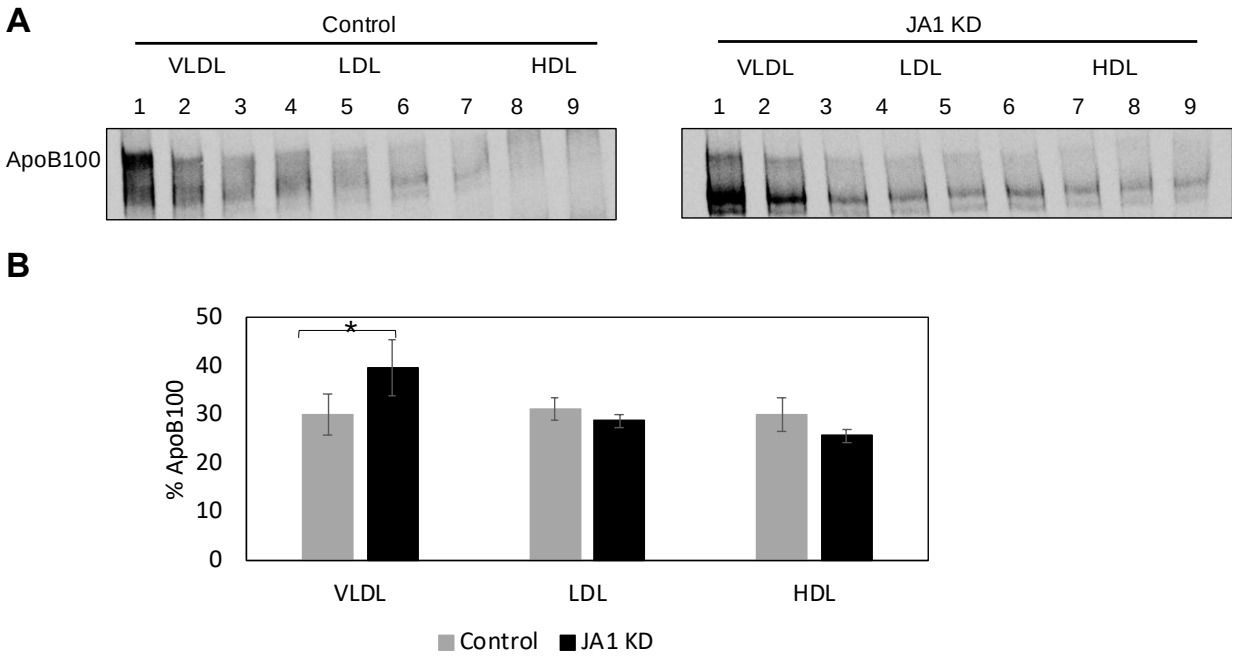

Figure 21. Depletion of JA1 hyperlipidates secreted ApoB100 in McA cells.

A. McA cells were treated with an siRNA against JA1 or a scrambled control, pulse labeled with radioactive Met/Cys for 15 min, and after the media was changed, an excess of unlabeled amino acids was provided. The media was then collected after 90 min into the chase and subjected to sucrose gradient ultracentrifugation (see section 2.2.8) before fractions were collected and ApoB100 was precipitated from each fraction and processed for SDS PAGE and phosphorimage analysis. **B.** Graph represents the means of N = 3 independent experiments, ±SE.

Interestingly, JA1 depletion led to the production of more buoyant, lipid-rich particles (i.e., VLDLs) when compared to the control (Figure 21). Since JA1 facilitates the degradation of ApoB100 (Figure 15), its depletion could alter the membrane topology of ApoB100 by increasing the extent of co-translational translocation, folding, and/or assembly. This might in turn augment MTP association and thus lipid loading (also see Discussion).

2.4.1 JA1 ablation leads to ApoB enrichment in intracellular compartments

To ascertain the intracellular enrichment of ApoB in McA cells upon JA1 knockdown, I also visualized ApoB levels by indirect immunofluorescence (IF) (see section 2.2.9). ApoB has been shown to form puncta and localizes both in the ER and post-ER compartments (Butkinaree et al., 2014; Fisher et al., 1997; Mitchell et al., 1998). Consistent with my pulse chase data, I observed that depletion of JA1 leads to an apparent increase in the number of ApoB puncta (Figure 22). However, unlike select previous reports, I did not notice significant overlap between ApoB puncta and HMGCR. It is likely that ApoB puncta were localized in pre-Golgi intermediate, ER-Golgi Intermediary Complex (ERGIC) or Golgi. Using other ER (rough ER), ERGIC or Golgi markers might help identify the subcellular localization of ApoB.

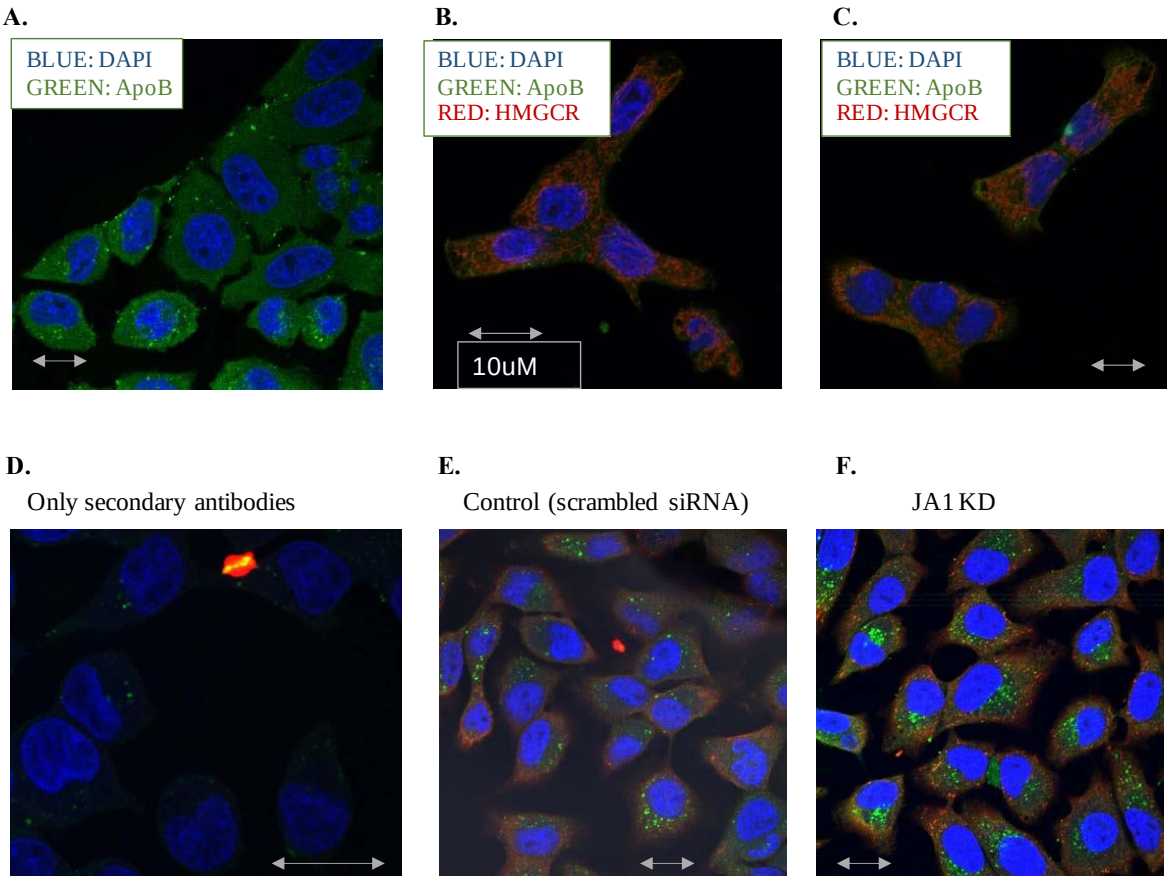

Figure 22. Depletion of JA1 leads to more ApoB puncta in McA cells.

A.Confocal indirect immunofluorescence images from McA cells probed with an antibody to ApoB (green). Nuclei were stained with DAPI (blue) B. C. Images showing McA cells probed with antibodies to ApoB (green), ER marker HMGCR (red). D. Image showing control conditions, treatment with only Alexa dye conjugated secondary antibodies. E. Cells were treated with control (scrambled siRNA) and siRNA targeted JA1 KD. IF was conducted as described in 1.2.9 and cells were probed with antibodies to ApoB (green), ER marker HMGCR (red). Arrow shows 10 µM scale.

2.4.2 DNAJB1 (JB1) associates with and stabilizes ApoB100

Hsp70s can have multiple Hsp40 co-chaperone partners, and heterologous pairs of Hsp40 isoforms have been detected (Kirstein et al., 2017; Nillegoda et al., 2015; Nillegoda et al., 2017; Nillegoda et al., 2018). Moreover, interclass JDP complexes can function with Hsp70 and Hsp110 family members and act as components of protein disaggregases (Nillegoda et al., 2017; Nillegoda

et al., 2018). In yeast, one potential disaggregase for ApoB is Hsp104, the major cytosolic disaggregase in yeast (Parsell et al., 1994), and indeed prior work in our lab showed that Hsp104 associates and facilitates the degradation of ApoB in yeast (Doonan et al., 2019). Nevertheless, because class A JDPs can function with class B JDPs, I next investigated the role of DNAJB1 (JB1), an essential class B cytosolic Hsp40, with established roles in the disaggregation of other misfolded proteins both *in vitro* and *in vivo* (Kirstein et al., 2017; Nillegoda et al., 2015; Nillegoda et al., 2017; Nillegoda et al., 2018).

As above, I first optimized JB1 knockdown conditions. JB1 knockdown in McA cells again utilized the RNAiMAX transfection reagent (Invitrogen), and four different siRNA oligonucleotides were examined at final concentrations of 20 nm (Figure 23A). The efficiency of knockdown was then measured by conducting quantitative western blotting of JB1 from cultures 48 hr post transfection. A fluorescently tagged scrambled siRNA served as a negative control. Based on the data in Figure 23A, siRNA oligonucleotide 09 was selected for further experiments (Figure 23B). Next, JB1 was knocked down and the stability of ApoB100 was examined in pulse-chase assays, as described above. Surprisingly, JB1 knockdown failed to slow ApoB100 turnover but instead destabilized ApoB100 at the 60 min time point by more than two-fold (Figure 23C). In addition, there was a pronounced decrease in the amount of secreted ApoB100 compared to the control at both the 60 and 90 min time points (Figure 23D). Interestingly, there was no effect on either intracellular or secreted ApoB48, consistent with the distinct models of ApoB48 regulation by JA1 (Figure 15) and the differential effects of MTP inhibition on ApoB48 and ApoB100 (Raabe et al., 1999). A direct effect of this alternate JPD was further supported by the fact that JB1, like JA1, also crosslinked with ApoB (Figure 23E). Thus, in contrast to the role that JA1 plays in enhancing degradation, JB1 might instead facilitate the folding ApoB100 in the ER. While initially

unexpected, this result is consistent with the functional diversity noted amongst different Hsp40s. For example, JA1 and JB1 aid in the folding of CFTR but JB12 and JC5 facilitate its degradation (Farinha et al., 2002; Schmidt et al., 2009; Zhang et al., 2002).

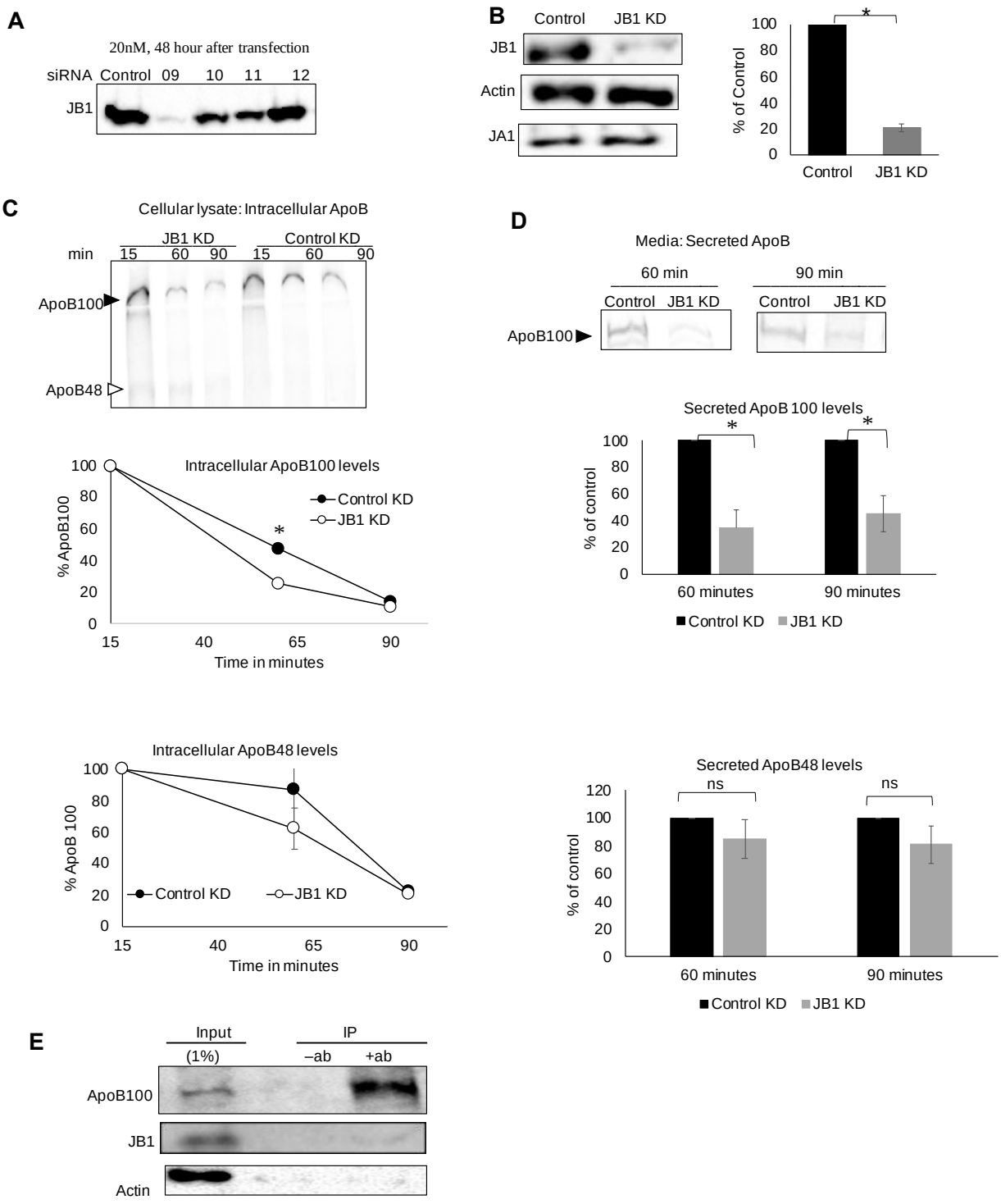

Figure 23. Knockdown of the JB1 molecular chaperone enhances ApoB100 degradation.

A. McA cells were transfected with four different siRNA oligonucleotides targeting JB1 for 48 hrs and at a final concentration of 20 nM. Cells were lysed and normalized amounts of protein were analyzed by SDS-PAGE and western blotting. Only ~20% of the chaperone remained after siRNA treatment. B. McA cells were transfected with

siRNA 09 (JB1 KD) or a scrambled siRNA control for 48 hrs. In addition to JB1, a representative western blot shows JA1 and actin levels after knockdown. C. A pulse-chase experiment was conducted as described in Materials and Methods. Cells were starved for 1 hr, incubated in media with radioactive amino acids for 15 min (pulse), and after the media was washed, an excess of unlabeled methionine and cysteine were added to begin the chase. The media and cells were then collected after 15, 60, and 90 min, and ApoB was immunoprecipitated using anti-ApoB antibody and analyzed via SDS-PAGE and phosphorimaging analysis. A representative radiograph and quantitative graphs of the intracellular ApoB100 (closed arrowhead) and ApoB48 (open arrowhead) levels are shown. D. A representative radiograph and graphs show the levels of secreted ApoB100 (closed arrowhead) and ApoB48 (open arrowhead). * indicates a non-specific band. Data represent the means of N = 3 independent experiments, ±SE; * indicates $p<0.05$, ns indicates $p>0.05$. E. Chemical crosslinking was performed as described in section 2.2.8 and Figure 18.

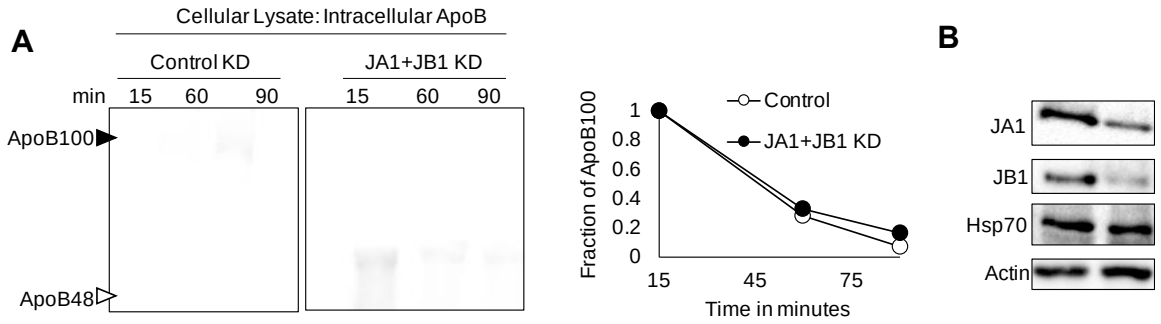

Figure 24. Double knockdown of JA1 and JB1 does not alter ApoB100 levels.

A. McA cells were transfected with siRNAs targeting both JA1 and JB1 or a scrambled siRNA (control KD) for 48 hrs. A pulse-chase analysis was then performed as described in section 2.2.7 and Figure 15. Representative radiograph and quantitative graph show intracellular ApoB100 levels upon double knockdown of JA1 and JB1. N=2. B. A representative blot shows JA1, JB1, Hsp70, and actin levels.

After observing the contrasting effects of JA1 and JB1, I was curious what effects the depletion of both JA1 and JB1 would have on ApoB, or if the depletion of one Hsp40 would be dominant. To this end, I performed a trial experiment and knocked down both of these genes and then again conducted a pulse chase assay. ApoB levels were unaffected (Figure 24A, 24B), suggesting that the effects of these JDPs either cancel out one another, or because both of the

Hsp40s play critical roles in several biological processes, their combined knockdown may elicit a more severe stress response or off-target effects (Zarouchlioti et al., 2018). Thus, under these conditions, other Hsp40s may also come into play to compensate for the absence of these chaperones.

2.4.3 DNAJC19 (JC19) does not participate in ApoB biogenesis

To control for these knockdown experiments and ensure that the loss of a JPD that does not reside in the cytosol would not artefactually alter ApoB biogenesis, I asked whether a class C JDP that resides in another cellular compartment affects ApoB levels. One class C Hsp40, JC19, resides in the inner mitochondrial membrane (Heinemeyer et al., 2019). Therefore, I followed the same experimental methods outlined above and optimized JC19 knockdown conditions (data not shown). I then selected a single siRNA for my studies (Figure 25A) and conducted pulse-chase analyses. As shown in Figure 25B-C, JC19 knockdown had no effect on ApoB levels, even though knockdown was nearly absolute. Chemical crosslinking with DSP also indicated that JC19 fails to associate with ApoB (data not shown), as anticipated.

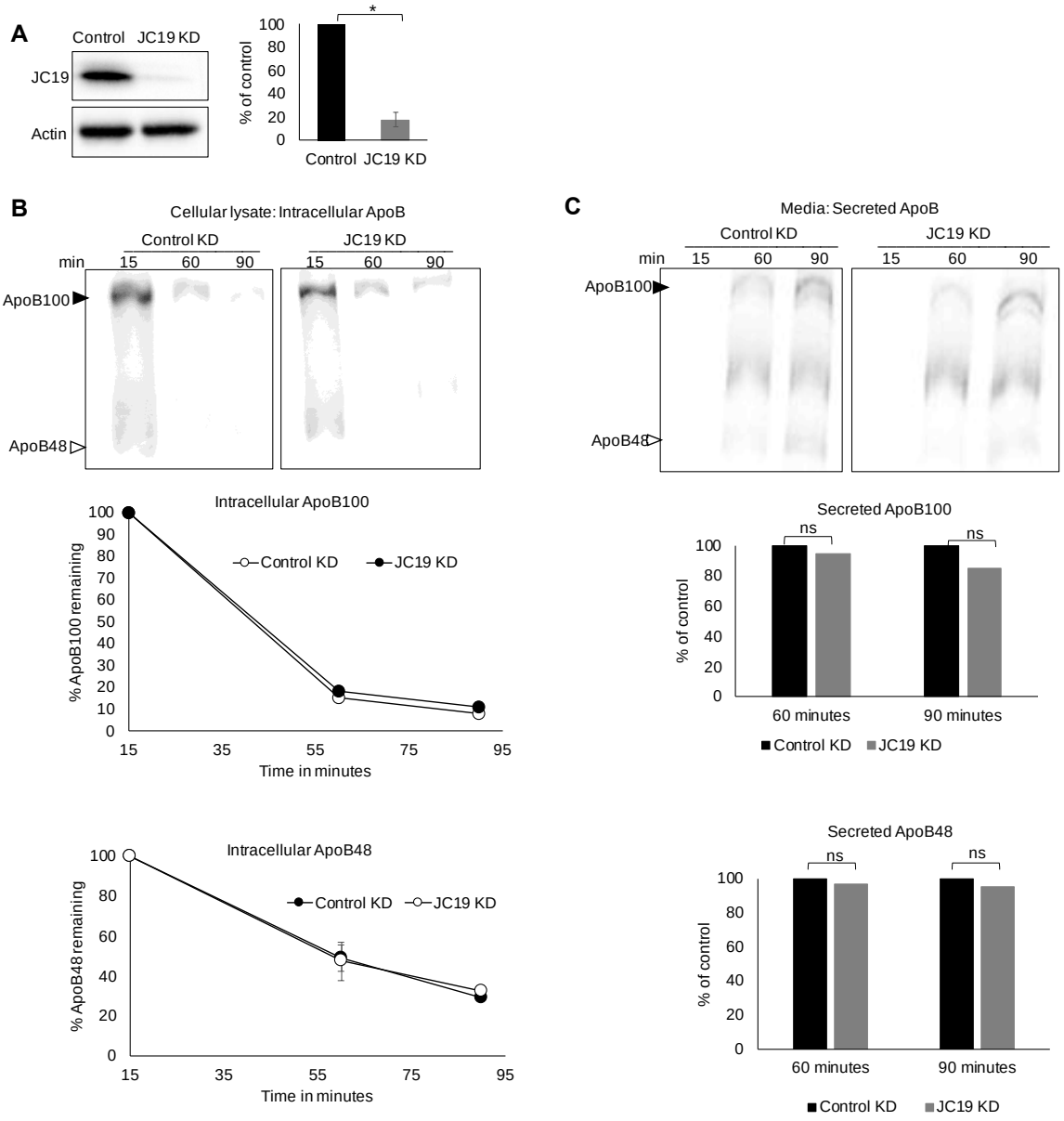

Figure 25. JC19 does not contribute to ApoB biogenesis.

A. McA cells were transfected with a scrambled siRNA (control KD) or an siRNA directed against JC19 (JC19 KD) that depleted JC19 levels to ~80% of the control after 48 hrs. Both JC19 and actin levels after knockdown are shown. B. A pulse chase was performed as described in section 2.2.7 and Figure 15. A representative radiograph and graph show intracellular ApoB100. Data represent the means of N = 3 independent experiments, ±SE. C. Representative radiographs and graph showing secreted ApoB100 and ApoB48. Data represent the means of N = 3 independent experiments, ±SE.

2.4.4 Hsp40s play differential roles in the ubiquitination of ApoB

Hsp40s act early during the selection of ERAD substrates, so the loss of Hsp40 function has been correlated with the absence of substrate ubiquitination (Preston and Brodsky, 2017). In fact, Parrales et al. found that JA1 inhibited the ubiquitination of a mutant p53 by the CHIP E3 ubiquitin ligase (Parrales et al., 2016). To determine if JA1, which facilitates ApoB100 degradation (Figure 15), also acts prior to ApoB100 ubiquitination, the level of protein ubiquitination was examined in cells transfected with HA tagged ubiquitin and that were incubated in the presence or absence of MG-132. The cells were then lysed, ApoB was immunoprecipitated, and the levels of ubiquitinated ApoB were analyzed by western blotting.

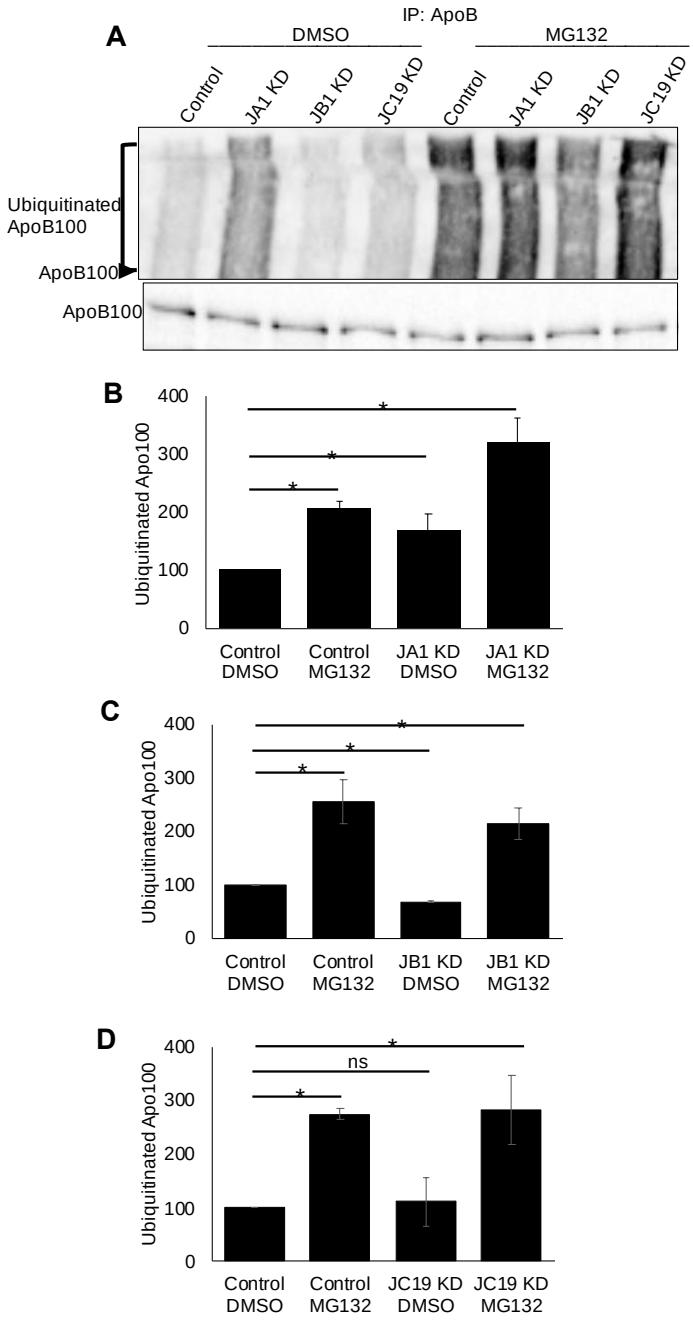

Figure 26. Differential effects of Hsp40 knockdown on the levels of ubiquitinated ApoB.

A. The level of ApoB ubiquitination was assayed in cells expressing HA-tagged ubiquitin in the absence or presence of an siRNA directed to JA1, JB1, or JC19 as described in Materials and Methods. Where indicated, cells were pre-treated with DMSO or MG-132 for 1 hr before cells were lysed and ApoB was immunoprecipitated. The levels of ubiquitinated ApoB100 were detected via SDS-PAGE and western blotting against ApoB and HA (to detect the ubiquitinated protein). A representative western blot shows the levels of ubiquitinated Apo100 **B.C.D.** Graphs

represent the levels of ubiquitinated ApoB100 normalized to the corresponding levels of ApoB100 in the presence of DMSO and that had been treated with the scrambled (control) siRNA. The arrowhead denotes the migration of unmodified ApoB100. Data represent the means of N = 3 independent experiments, ±SE.

As shown in Figure 26, JA1 knockdown led to the accumulation of ubiquitinated ApoB in the absence of MG-132, suggesting that JA1 acts after substrate ubiquitination since the loss of this chaperone slows ERAD (Figure 15). Thus, JA1 might help deliver ubiquitinated ApoB to the proteasome. In contrast to the effect of JA1 ablation—and in accordance with the fact that JA1 and

JB1 play opposing roles on ApoB100 stability—JB1 knockdown decreased the levels of ubiquitinated ApoB100 (Figure 26). Of note, JB1 was implicated in the ubiquitination of Mitogen Inducible Gene 6 (MIG6), a tumor suppressor protein (Park et al., 2015). As a control for these experiments, the levels of ubiquitinated ApoB were again unaffected by depletion of JC19 (Figure 26A, 26D). Under all conditions, proteasome inhibition upon the addition of MG-132 also led to a rise in the amount of ubiquitinated ApoB100, as expected.

2.5 Hrd1 targets ApoB100 for degradation

Human cells are predicted to express ~600 E3 ligases, which conjugate ubiquitin onto substrates (Li et al., 2008). To date, gp78 is the only ubiquitin ligase implicated in ApoB degradation (Fisher et al., 2011; Liang et al., 2003). Because ubiquitin ligases function redundantly, because some ubiquitin ligases are known to act sequentially during ERAD (Jo et al., 2011a; Menzies et al., 2018; Morito et al., 2008; Younger et al., 2006), and because ApoB is a large, multi-domain protein, I hypothesized that additional E3 ubiquitin ligases might

target ApoB for degradation. For example, Hrd1, which like gp78, is a mammalian homolog of yeast Hrd1, is also an ER membrane protein (Bays et al., 2001; Kikkert et al., 2004). Moreover, ApoB29 was reported to be ubiquitinated by Hrd1 in yeast (Rubenstein et al., 2012), and in human hepatoma cells Hrd1 resided in a multi-protein complex with ApoB100 (Rutledge et al., 2009).

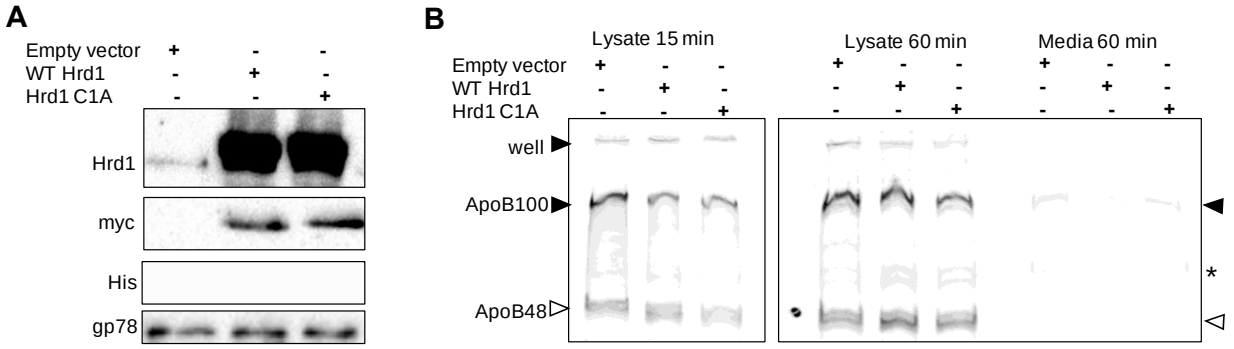

Figure 27. Over expression of wild-type or a dominant negative version of Hrd1 does not alter ApoB levels.

A. Plasmids encoding myc- and His-tagged wild type (WT) Hrd1 and a dominant negative Hrd1 mutant (Hrd1C1A) were transfected into McA cells. After 20 hrs, the cells were lysed, and western blotting was performed to detect the indicated proteins. B. McA cells were transfected with an empty vector or the WT Hrd1 or C1AHrd1 expression vectors and a pulse-chase assay was conducted. ApoB was then immunoprecipitated as described in Materials and Methods from intracellular lysate and media and the samples were processed for SDS-PAGE and phosphorimager analysis. A representative radiograph shows ApoB100 (closed arrowhead) and ApoB48 (empty arrowhead), and a dot represents the 250 kDa marker. * indicates a non-specific band.

Figure 28. Optimization of Hrd1 knockdown conditions.

A. McA cells were transfected with four different siRNA oligonucleotides at final concentrations of 20 nM and 30 nM that target Hrd1. After 48 and 72 hrs, the cells were lysed and Hrd1 and actin levels were analyzed by SDS PAGE and western blotting. B. siRNA 1 was transfected into McA cells at a final concentration of 20 nM and lysates were prepared as above after 48 hrs. Hrd1 and actin levels were quantified. Under these conditions, Hrd1 levels were depleted to 30% of the control. Data represent the means of N = 3 independent experiments, ±SE and * indicates $p<0.05$.

To begin to examine the role of Hrd1 in ApoB degradation, we obtained plasmids encoding myc- and His-tagged wild-type Hrd1 and a dominant negative Hrd1 variant (Hrd1C1A) that lacks the E3 ubiquitin ligase activity (Chen et al., 2016). I first confirmed Hrd1 overexpression by western blotting for Hrd1, the myc tag, and the hexa-His motif (Figure 27A). I also examined the levels of gp78, which seemed unaltered upon overexpression of Hrd1 (Figure 27A). After confirming expression, I conducted a pulse-chase assay to examine effects on ApoB stability. However, the overexpression of neither wild-type Hrd1 nor the dominant negative Hrd1C1A variant affected ApoB levels (Figure 27B). This lack of effect might be due to protein overload.

Based on these data, I instead knocked down endogenous Hrd1 and therefore optimized Hrd1 knockdown conditions following the same method as mentioned in the previous sections (see e.g., Figure 28A, 28B).

Next, I conducted pulse-chase experiments after knocking down Hrd1 and again collected intracellular and secreted ApoB at various times during the chase (Figure 29A). Consistent with my hypothesis, Hrd1 knockdown significantly increased the levels of both intracellular and secreted ApoB100 (Figure 29B, 29C). However, similar to experiments in which JA1 and JB1 were knocked down (Figure 15, Figure 23), there was no effect on ApoB48 levels in either cell lysate or in the media. These results suggest that Hrd1 might act on the C-terminal portion of

ApoB100, and that this ubiquitin ligase might then act on ApoB100 to target it for ERAD.

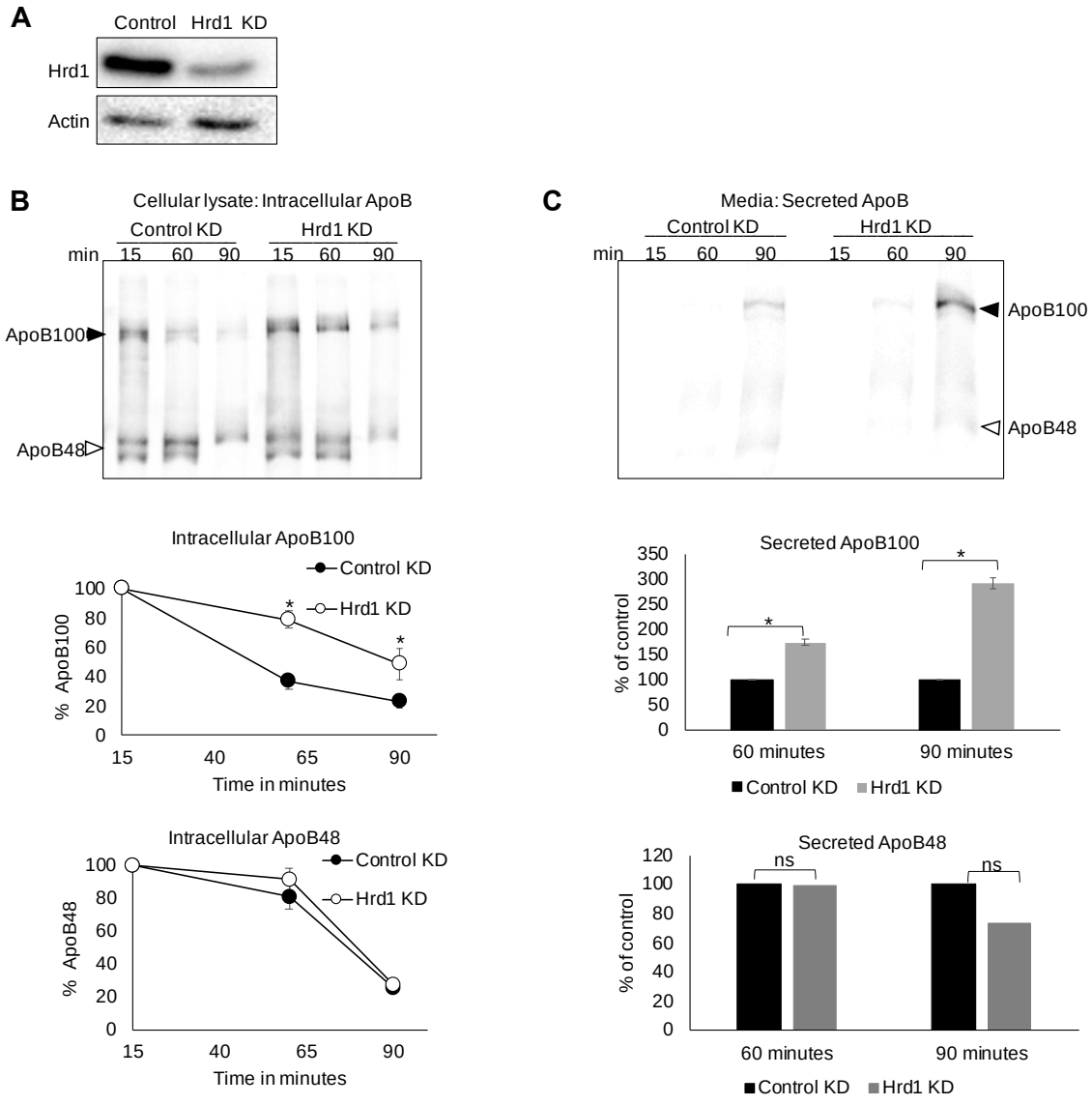

Figure 29. Hrd1 facilitates the degradation of ApoB100.

A. McA cells were transfected with an siRNA directed against Hrd1 (Hrd1 KD) or a scrambled siRNA control for 48 hrs. Hrd1 and actin levels after knockdown are shown. **B.** A pulse chase experiment was conducted after knocking down Hrd1 as described in the Materials and Methods and in Figures. ApoB was immunoprecipitated using anti-ApoB antibody and analyzed via SDS-PAGE and phosphorimaging analysis. A representative radiograph and graphs of the intracellular ApoB100 (closed arrowhead) and ApoB48 (open arrowhead) levels are shown. **C.** A representative radiograph and quantitative graphs show levels of secreted ApoB100 (closed arrowhead) and ApoB48 (open

arrowhead). Data represent the means of N = 5 independent experiments, ±SE. * indicates $p<0.05$, and ns indicates not significant.

Based on its function as a ubiquitin ligase, I next asked whether Hrd1 ubiquitinates ApoB. To test this hypothesis, I conducted ubiquitination assay after knocking Hrd1 down. Interestingly, no difference in the levels of total ubiquitinated ApoB upon Hrd1 KD was evident (Figure 30).

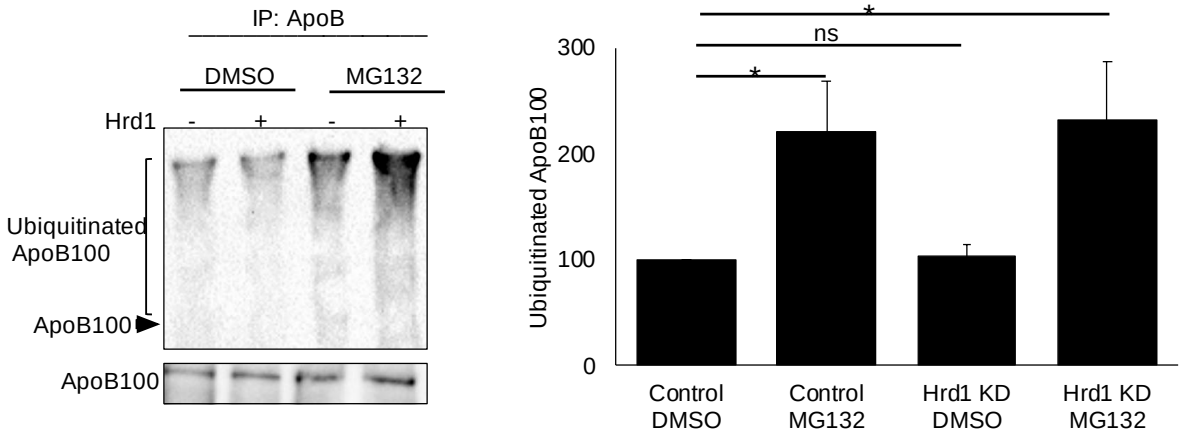

Figure 30. Hrd1 knockdown does not alter the levels of ubiquitinated ApoB100.

A. ApoB was immunoprecipitated from McA cells expressing HA-tagged ubiquitin in the presence of a Hrd1-targeted siRNA or a scrambled control. As indicated, cells were either pre-treated with DMSO or MG-132 for 1 hr before ApoB was immunoprecipitated and ubiquitin was detected via SDS-PAGE and western-blotting against the HA tag. Normalized amounts of protein were used for the immunoprecipitation. A representative western blot is shown. The arrowhead denotes the migration of unmodified ApoB100. B. The graph depicts the relative levels of ubiquitinated ApoB upon Hrd1 knockdown in the absence or absence of MG-132. Data represent the means of N = 3 independent experiments, ±SE.

Although the lack of Hrd1-dependent ubiquitination may point to the redundancy among E3 ubiquitin ligases, knockdown led to significant stabilization of ApoB100. However, it is also possible that Hrd1 regulates ApoB indirectly or that its action is primarily as a result of its function as a retrotranslocation channel (Baldridge and Rapoport, 2016; Carvalho et al., 2010; Peterson et

al., 2019). Another hypothesis is that Hrd1 only acts on nascent ApoB100. To test this hypothesis, I conducted a ubiquitination assay with sequential immunoprecipitation of radioactively labelled nascent ApoB with anti HA antibody followed by anti ApoB antibody. Interestingly Hrd1 ablation did not alter levels of ubiquitinated nascent ApoB100 (Figure 31). Thus, Hrd1 might not be responsible for targeting ApoB for ubiquitination and proteasomal degradation (see Discussion).

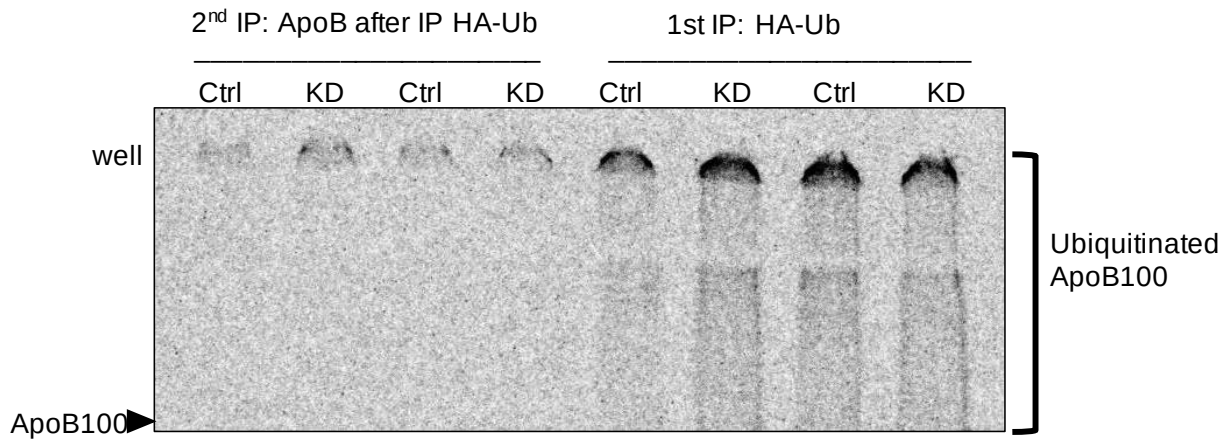

Figure 31. Hrd1 knockdown does not alter the levels of ubiquitinated nascent ApoB100.

Hrd1 was knocked down and pulse chase was conducted as described in section 2.2.7 and Figure 15. Cells collected at 90minute time point were lysed with RIPA buffer and IP was set with anti HA antibody conjugated beads. Next day, IPs were washed, and bound samples were eluted by boiling beads in 2% SDS for 4 min. SDS concentration was then adjusted to 0.1% and 10% was this was saved as input. A second overnight IP was set up with anti ApoB antibody. Finally, samples were processed and developed by SDS PAGE and phosphorimaging. Closed arrowhead denotes the migration of unmodified ApoB100.

As noted above, gp78 is the only E3 ubiquitin ligase reported to ubiquitinate ApoB (Fisher et al., 2011; Liang et al., 2003). Therefore, as a positive control, I also examined the effect of gp78 knockdown on ApoB stability. I first optimized gp78 knockdown conditions (Figure 32A, B) and then conducted pulse-chase assay after knocking down the protein to ~35% of the control (Figure

32B).

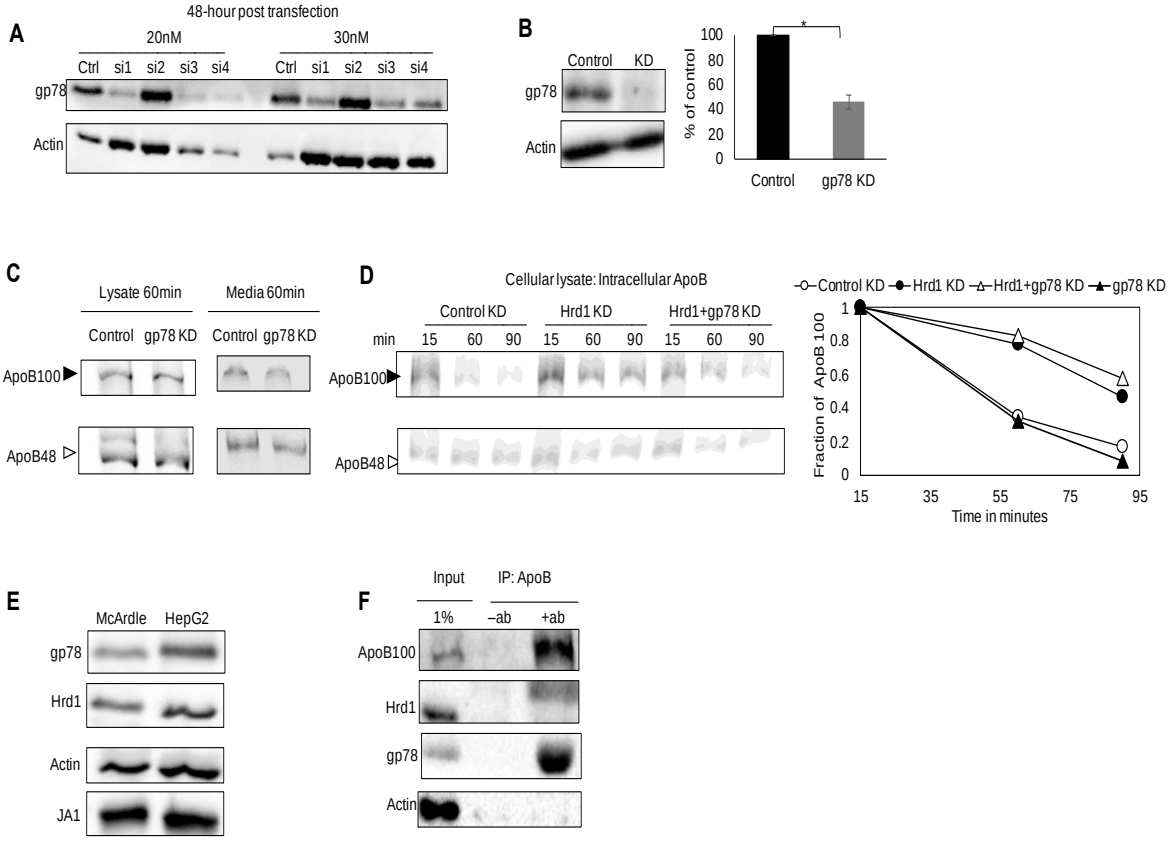

Figure 32. ApoB levels are unaltered by the loss of gp78 in McA cells.

A. McA cells were transfected with four different siRNA oligonucleotides targeting gp78 for 48 hrs and at final concentrations of 20 nM and 30 nM as described in sections 2.2.6. Cells were lysed in RIPA and analyzed by SDS-PAGE and western blotting using antibodies against gp78 and actin. B. siRNA 1 was selected to knock down gp78 and depleted gp78 levels to 35% of the control. C. A pulse chase experiment was conducted as described in section 2.2.7 and Figure 15. Cells were starved for 1 hr and then incubated in media with radioactive amino acids for 15 min (pulse). The media was washed, and an excess of unlabeled methionine and cysteine were added to begin the chase before the media and cells were collected at the indicated times and cells were lysed. ApoB was immunoprecipitated using anti-ApoB antibody and analyzed via SDS-PAGE and phosphorimaging analysis. A representative radiograph and graphs of the intracellular ApoB100 (closed arrowhead) and ApoB48 (open arrowhead) levels are shown. D. A pulse chase analysis was conducted after knocking gp78 (closed triangle), Hrd1 (open triangle), both Hrd1 and gp78 (closed circle), or in the presence of the scrambled siRNA control (open circle). Radiograph and quantitative blot show intracellular ApoB100 (closed arrowhead) and ApoB48 (open arrowhead). Data represent the means of N = 5

independent experiments, ±SE. * indicates $p<0.05$. E. McA and HepG2 cells were lysed and normalized levels of protein were processed by SDS PAGE and western blotting. The levels of gp78, Hrd1, Actin and JA1 were detected by western blotting. F. DSP based *in vivo* crosslinking was performed in McA cells and ApoB was immunoprecipitated. Samples were processed by SDS PAGE and ApoB100, Hrd1, gp78 and actin were detected by Western Blot. Actin was used as a negative control.

Surprisingly and in contrast to previous studies (Fisher et al., 2011; Liang et al., 2003), the loss of gp78 had no effect on the turnover of either intracellular ApoB100 or ApoB48 (Figure 32C). To explore if Hrd1 and gp78 act synergistically, I conducted pulse chase after depleting both Hrd1 and gp78 ligases, but I again failed to note any additive effect of gp78 knockdown on ApoB levels (Figure 32D, gp78 KD (closed triangle), Hrd1 KD (closed circle), gp78+Hrd1 double KD (open triangle), scrambled siRNA (open circle)).

Although the lack of an effect of gp78 knockdown was initially concerning, prior studies in which the role of gp78 on ApoB stability was assessed were conducted in human hepatoma (HepG2) cells and not in McA cells (Fisher et al., 2011; Liang et al., 2003).

To assess if the difference between the effects of gp78 silencing on ApoB stability arises from distinct levels of endogenous gp78 in HepG2 and McA cells, I examined the steady-state levels of gp78 in both lines. I found that gp78 is elevated in HepG2 cells compared to McA cells (Figure 32E). Therefore, the loss of this more abundant and potentially functionally redundant ubiquitin ligase likely has a more profound effect in HepG2 cells. Consistent with this model, I found that the enriched Hrd1 ligase in McA cells contributes more substantially to ApoB degradation.

As mentioned earlier, Hrd1 appears to associate with ApoB in HepG2 cells (Rutledge et al., 2009). To examine whether ApoB similarly associates with Hrd1 in McA cells, I conducted

chemical crosslinking assays using DSP and discovered that Hrd1 co-immunoprecipitates with ApoB as well as gp78 in McA cells (Figure 32F). These data corroborate the role of Hrd1 in regulating ApoB.

2.6 Discussion

ApoB is an atypical ERAD substrate. The protein is ~550 kDa, it is highly hydrophobic yet resides in the lymphatic and circulatory systems, it contains pause-transfer sequences, it is ubiquitinated co-translationally, and it is regulated by pre-secretory degradation via the ERAD pathway (Benoist and Grand-Perret, 1997; Boren et al., 1992; Boren et al., 1994; Fisher et al., 1997; Sakata et al., 1999; Yeung et al., 1996). Even though cytoplasmic Hsp70 has long been known to regulate ApoB turnover (Fisher et al., 1997; Gusarova et al., 2001), cytoplasmic Hsp40s required for ERAD selection had not been reported,

In this study, I identified and characterized the roles of two cytosolic Hsp40s that regulate the biogenesis of ApoB. I began by conducting a candidate-based screen in a yeast ApoB expression system and discovered that Ydj1, a Class A Hsp40, contributes to ApoB ERAD (Figure 9). In accordance with these data, I found that JA1, the mammalian Ydj1 homolog, associates with and facilitates the ERAD of ApoB in a mammalian liver cell line that synthesizes and secretes ApoB (Figure 15). Interestingly, JA1 depletion led to the secretion of more buoyant, lipid-rich particles when compared to mock transfected cells (Figure 21; also see below). Because Hsp40s regulate ERAD either before or after ubiquitination (Preston and Brodsky, 2017), I next examined whether ApoB was ubiquitinated when JA1 was depleted. Because the loss of JA1 led to the accumulation of ubiquitinated ApoB (Figure 26), I conclude that this chaperone acts after gp78

and Hrd1 have ubiquitinated the substrate. In addition, because chaperones, including Hsp40s, play critical roles in maintaining protein solubility, I examined whether JA1 depletion alters ApoB solubility, but no change in solubility was noted (Figures 19, 20). These data suggest that JA1 is dispensable for ApoB disaggregation and plays another role during ApoB turnover and/or that there are compensatory disaggregases. However, some redundancy amongst different Hsp40s may also underlie this phenomenon.

To examine if JA1 is member of an interclass J domain protein complex (Kirstein et al., 2017; Nillegoda et al., 2015; Nillegoda et al., 2017; Nillegoda et al., 2018), I next sought to investigate the role of DNAJB1 (JB1), a class B Hsp40, in regulating ApoB stability. I anticipated that JB1 would also facilitate the degradation of ApoB by being a member of an interclass JDP complex. Contrary to my hypothesis, I found that JB1 knockdown accelerated ApoB turnover, suggesting that this chaperone instead stabilizes ApoB (Figure 23). As observed with JA1, JB1 also crosslinks to ApoB (Figure 23), but in contrast to JA1 and consistent with its stabilizing role, JB1 depletion decreased ApoB ubiquitination (Figure 26). These data highlight the differential roles Hsp40s can play during the ERAD of a substrate.

The decision to either degrade or secrete ApoB is made at the ER/cytosol interface and is tightly regulated. This mechanism represents a "tug-of-war" between ER lumenal factors that favor lipoprotein assembly (e.g. Hsp110) and some cytosolic components that target ApoB for degradation (e.g. Hsp70, Hsp90, Hsp104, $p58^{IPK}$) (Benoist and Grand-Perret, 1997; Boren et al., 1992; Boren et al., 1994; Doonan et al., 2019; Fisher et al., 1997; Grubb et al., 2012; Gusarova et al., 2001; Hrizo et al., 2007). Since ApoB achieves a bitopic orientation while undergoing co-translational translocation at the ER membrane, the apolipoprotein remains in close proximity to JA1, which is anchored to the ER membrane via a farnesyl group (Becker et al., 1996; Beilharz et

al., 2003; Costanzo et al., 2001; Cyr et al., 1992; Hoe et al., 1998; Terada and Mori, 2000; Walsh et al., 2004; Xu et al., 2019). Because p97/VCP co-IPs with ApoB and also facilitates its degradation (Fisher et al., 2008; Rutledge et al., 2009), it is possible that JA1 assists p97/VCP during the retrotranslocation and degradation of ApoB. In turn, the depletion of JA1 may increase the extent of co-translational translocation, folding, and lipidation by the MTP complex, thus favoring transit into and residence in the lumen. Indeed, this might explain the fact that JA1 knockdown increased the buoyancy of secreted ApoB.

In general terms, the Hsp40 J domain stimulates the ATPase activity Hsp70 and uses a C-terminal region for substrate binding (Craig and Marszalek 2017; Fan, et al. 2003). JA1 is a type A Hsp40 that consists of the N-terminal signature J domain (~1-70 residues), a glycine phenylalanine rich region (GF), a zinc finger like region (ZFLR) followed by two structurally similar beta barrel C-terminal domains (CTD) 1 and 2, and a dimerization domain (Jiang et al., 2019; Kityk et al., 2018; Qian et al., 1996). The J domain forms a secondary structure consisting of four helices, and the highly conserved tripeptide HPD motif, situated between its second and third helices, is responsible for binding the interface between the nucleotide binding and substrate binding domains of Hsp70, thereby enhancing its ATPase activity (Jiang et al., 2019; Kityk et al., 2018; Qian et al., 1996). In turn, the ZFLR binds and can aid in the folding of substrates (Jiang et al., 2019; Lu and Cyr, 1998), and the CTDs are responsible for substrate binding, yet recent studies have emphasized the roles of other domains in substrate recognition (Kampinga and Craig, 2010; Schilke et al., 2017; Yu et al., 2015a; Yu et al., 2015b). In contrast, type B Hsp40s lack the ZFLR and therefore may not present as many binding interfaces to a substrate as type A Hsp40s. Moreover, a recent study reported that type B Hsp40s exhibit a unique autoinhibitory mechanism so that the Hsp70 binding sites are blocked by a short regulatory domain. Inhibition is released

upon another interaction with the C-terminal tail of Hsp70 (Faust et al., 2020). Overall, differences in sequence and domain architecture between type A and type B Hsp40s expand substrate selectivity and sub-specialization for various Hsp70-dependent functions (Rebeaud et al., 2021).

Since I found that JA1 cross-links with ApoB along with Hsp70 (Figure 18B), I hypothesize JA1 binds ApoB through the CTD1 and then recruits Hsp70 and stimulates Hsp70 activity via its J domain, thus coupling ApoB binding to ATP hydrolysis. Thus, JA1 might require both its J domain and CTD1 in regulating ApoB biogenesis. However, the roles of the GF and ZFLR domains have also become clearer in recent years as mutations in these domains affect not only substrate binding affinity but can compromise Hsp70-dependent ATPase activity. In addition, Hsp40s act as homodimers and can also form intermolecular complexes with Hsp40s from another class via J domain-CTD1 salt bridges (Kirstein et al., 2017; Nillegoda et al., 2015; Nillegoda et al., 2017; Nillegoda et al., 2018), thereby presenting more and diverse surfaces for substrate binding. The resulting J-domain-CTD1 interface is also distinct from the surface that interacts with Hsp70. Given that ApoB is large, contains several hydrophobic surfaces for lipid bunding, and is therefore potentially aggregation prone, it is likely that ApoB binds several regions in JA1. Further studies with JA1 constructs harboring mutations in these specific domains will help determine which domains are necessary and sufficient for its role in regulating ApoB.

Even though JB1 is also a co-chaperone for Hsp70 (Blard et al., 2007; Gao et al., 2015; Michels et al., 1999), I found that JB1 instead stabilizes ApoB (Figure 23). Therefore, JB1 protects ApoB from degradation and/or aggregation, thus facilitating protein folding by disfavoring the formation of off-pathway folding intermediates. These data also indicate that chaperones within the same complex can have distinct roles, either protecting or degrading a substrate, and potentially competing with one another. Like JB1, we previously showed that an Hsp70-like chaperone in

yeast, Hsp110 (Sse1), associates with and stabilizes ApoB (Hrizo et al., 2007). Consistent with the findings in the yeast model, when Hsp110 was overexpressed in McA cells, the secretion of ApoB was enhanced (Hrizo et al., 2007). In other work, JB1 was reported to function with the mammalian Hsp110s and Hsp70 to disaggregate and refold luciferase aggregates and resolubilize aggregated alpha synuclein and tau (Deane and Brown, 2017; den Brave et al., 2020; Hageman and Kampinga, 2009; Kuo et al., 2013; Mattoo et al., 2013; Nillegoda et al., 2015; Osaki et al., 2018; Rampelt et al., 2012). In theory, JB1 could be a therapeutic target since its depletion would result in lower levels of circulating atherogenic lipoproteins, but based on its role in disaggregating toxic proteins (see above), severe secondary effects would occur if JB1 function was compromised. Nevertheless, future *in vivo* studies are needed to confirm the role of JB1 in lipoprotein and cholesterol metabolism.

Ubiquitination commits an ERAD substrate for proteasome-mediated degradation, and multiple E3 ubiquitin ligases commonly target a substrate for degradation (Jo et al., 2011a; Menzies et al., 2018; Morito et al., 2008; Younger et al., 2006). Prior to my work, gp78 was the only E3 known to act on ApoB (Fisher et al., 2011; Liang et al., 2003), but I found that Hrd1 is also required for ApoB for degradation (Figure 29). Surprisingly, I was unable to observe additive or synergistic effects of depleting both Hrd1 and gp78. The difference between my data and prior studies could be attributed to the different cell types (HepG2 cells were used in (Bakillah et al., 1997)) in which these studies were conducted. It is also worth noting that Hrd1 and gp78, though homologous to yeast Hrd1, have distinct interaction networks, most likely due to sequence variations in their membrane domains (Christianson et al., 2011; Lilley and Ploegh, 2005). However, there are ERAD substrates that require both of these E3s, whereas others may need only

one but not the other (Bernasconi et al., 2010; Christianson et al., 2011; Fang et al., 2001; Ishikura et al., 2010; Menzies et al., 2018; Song et al., 2005; Zhang et al., 2015a).

Interestingly, no change in the levels of ubiquitinated ApoB were noted in the absence of Hrd1 (Figures 30 and 31), suggesting that ApoB might not be a substrate for Hrd1's catalytic activity. However, it is also established that Hrd1 acts a retrotranslocation channel for some misfolded proteins (Baldridge and Rapoport 2016; Peterson, et al. 2019).

Does ApoB undergo retrotranslocation though the Hrd1 channel? Prior work has shown that ApoB retrotranslocates through Sec61 channel (Chen et al., 1998; Mitchell et al., 1998), but if ApoB retrotranslocation also requires Hrd1, how does a biogenic intermediate within Sec61 channel then enter Hrd1 channel? It is possible that lack of lipidation of ApoB might recruit luminal factors that then direct luminal ApoB segments to the Hrd1 channel. Hrd1 complex is a multi-spanning transmembrane protein with its catalytic domain facing the cytosol, and consistent with this model, Hrd1 cross-links with ApoB (Rutledge et al, Figure 28) as well as with luminal and cytosolic factors including VCP/p97 and BiP. Moreover, VCP/p97 and luminal factors like BiP and p58IPK facilitate ApoB degradation (Qiu et al 2005, Oyadomari et al 2006). Additionally, the existence of a composite retrotranslocation channel consisting of more than one protein (i.e., both Sec61 and Hrd1) cannot be ruled out. In other words, Hrd1 and Sec61 may form a transient mixed retrotranslocon to move ApoB back to the cytosol. Future work will also investigate if Hrd1 acts downstream of Hsp40s since Sel1L, the Hrd1 cofactor, assists the ER lumenal Hsp40 ERdj5 via its J domain to facilitate cholera toxin retrotranslocation (Williams et al., 2013).

Although McA cells are a standard model used to study ApoB and are relatively easy to manipulate and maintain, they are a hepatoma cell line that has been immortalized and passaged repetitively. These cells may harbor abnormal genetic expression patterns when compared to

primary hepatocytes. Additionally, McA cells, which derive from rodents, express the ApoB48 isoform, in contrast to the human liver. Therefore, McA cells may possess additional mechanisms or machinery needed to regulate ApoB48 compared to a human liver. Moreover, cell line-based discrepancies or inconsistencies present a challenge to the field when considering which cell line is more reliable. Although McA cells represent a valuable model for preliminary experiments, the results from this study must be validated in primary hepatocytes or whole animal models.

In sum, as overabundance of the atherogenic ApoB-containing particles is a major risk factor for CAD, a better understanding of the mechanism underlying the regulation of ApoB will help combat CAD. Through his study, I have identified and characterized the roles of select contributors that regulate ApoB. Because drugs are in development that target these contributors (Assimon et al., 2013; Koishi et al., 1992; Lu et al., 2020; McConnell and McAlpine, 2013; Park et al., 2020; Shevtsov et al., 2019; Soti et al., 2005; Yokota et al., 2000), my work serves as a first step toward the development of improved or complementary methods to treat CAD. Regardless, future work to validate these findings in murine models will provide more physiologically relevant findings.

3.0 CONCLUSION

An imbalance in the circulating levels of ApoB containing lipoprotein particles can cause dyslipidemia. Whereas lower levels can cause hypocholesterolemia, higher levels are atherogenic and cause CAD, which is the most common form of cardiovascular disease that kills millions of people every year. The oldest treatment for CAD includes statins that inhibit cholesterol synthesis. However, side effects and resistance to the drug force some patients to stop taking their medication. Discovery of additional, alternative therapies include an antisense oligonucleotide-based drug called Mipomersen that inhibits assembly and transport of lipoprotein particles by targeting ApoB. However, this drug is prescribed to a select group of patients and is very expensive. Thus, the search for alternative therapeutic targets to combat CAD has motivated our lab to better define the machinery involved in the regulation of ApoB. Through my research, I have identified and characterized select cytosolic Hsp40s and an E3 ubiquitin ligase that regulate the biogenesis of ApoB and that could potentially serve as therapeutic targets.

3.1 Hsp40s in ApoB ERAD

Hsp40s, also known as J proteins, are a class of co-chaperones that assist Hsp70s in protein folding by enhancing Hsp70 ATPase activity through their J domain and facilitating substrate selectivity though their C-terminal substrate binding domain. Hsp40s play essential roles in many processes, including protein folding, transport, prevention of aggregation, and degradation. Based on their sequence and architecture, Hsp40s are categorized in to three classes A, B and C. Members

of all three classes possess the J domain that harbors the HPD tripeptide motif responsible for stimulating the ATPase activity of Hsp70. Hsp40s form the largest family of Hsps with more than 50 members in mammals. Several of these homologs have been investigated for their roles in the biogenesis of proteins that enter and traffic through the secretory pathway, such as CFTR. For example, both JA1 and JB1 bind and aid the folding of wild type CFTR (Farinha et al., 2002; Meacham et al., 1999). However, JA1 assists CHIP dependent degradation of CFTR sub-domains *in vitro* (Younger et al., 2006). In yeast, both Ydj1 and Hlj1 play redundant roles in the degradation of CFTR (Youker et al., 2004). Other Hsp40s, including DNAJC5 (cysteine string protein) and DNAJB12, enhance degradation of CFTR by recruiting E3 ubiquitin ligases (Grove et al., 2011; Schmidt et al., 2009; Yamamoto et al., 2010; Zhang et al., 2002; Zhang et al., 2006; Zhang et al., 2001). Thus, the various distinct roles Hsp40s play in the biogenesis of CFTR underscores the functional diversity of Hsp40s towards an ERAD substrate.

The role of Hsp40s in the regulation of ApoB, to date, is poorly explored. One study showed that the knockout of a luminal Hsp40, $p58^{IPK}$ (DNAJC3/Erdj6) (Barber et al., 1994), stabilized ApoB in primary mouse hepatocytes (Oyadomari et al., 2006). It was speculated that $p58^{IPK}$ most likely assists BiP during the translocation of ApoB.

Since the fate of ApoB (secretion or degradation) is determined while it undergoes co-translational translocation at the ER-cytosol interface, I instead investigated the roles of two ER membrane anchored Hsp40s in yeast with previously established roles in the ERAD of CFTR, Ydj1 and Hlj1. Interestingly I found that Ydj1, a class A Hsp40, associates with and expedites the degradation of ApoB, whereas Hlj1, a class B Hsp40 plays no role in ApoB biogenesis, highlighting the differential roles Hsp40s can play in the ERAD of a substrate (Figure 9).

To investigate the role of Hsp40s in a standard mammalian cell line that endogenously synthesizes and secretes ApoB, I depleted JA1 (the human homolog of Ydj1) and monitored the levels of both intracellular and secreted ApoB by conducting metabolic pulse chase assays. As expected, JA1, like its yeast counterpart, also associated with and accelerated the degradation of ApoB. To better understand the role of JA1, I assessed the lipidation status of the enhanced secreted ApoB species. Interestingly, I found that JA1 depletion shifted the lipoprotein particles to more buoyant, lipid rich particles (Figure 21). Additionally, JA1 ablation also led to the accumulation of ubiquitinated ApoB (Figure 26), suggesting that JA1 might be accelerating the delivery of ubiquitinated ApoB to the proteasome. However, depletion of JA1 on its own did not alter the soluble state of ApoB as ApoB remained detergent sensitive when JA1 was knocked down (Figures 19, 20).

Has ApoB been shown to aggregate in any of the standard cell lines used in the field? Assessing puncta formation by indirect fluorescence showed that the addition of PUFAs led to co-localization of ApoB with LC-3, an autophagosome marker. This species was suggested to be aggregated (Fisher and Williams, 2008), however the aggregation state of ApoB had not been tested biochemically with different detergents of various strengths. I also questioned if the lack of an effect of JA1 depletion on the aggregation of ApoB might be a cell line-dependent phenotype. I therefore expressed CFTR in McA cells and found that it fractionated with the insoluble fraction (Figure 19). Therefore, it is likely that JA1 does not play a role in maintaining the solubility of ApoB.

Future efforts should investigate the aggregation state of ApoB in yeast lacking Ydj1. Hsp40s Ydj1 and Sis1 have been shown to maintain the solubility of select substrates before proteasomal degradation (Guerriero et al., 2013; Park et al., 2007; Park et al., 2013). A lack of an

effect on this property may confirm that Ydj1/JA1 are not required to disaggregate ApoB. However, an observed effect will be intriguing, since mammalian cells have almost double the number (>50) of Hsp40s than yeast (>22) and therefore disaggregation in mammalian cells might be more complex and substrate-specific. Of note, yeast also have Hsp104, which is a major ATP-dependent disaggregase. However, we showed that Hsp104 does not affect the aggregation state of ApoB but instead assists in the retrotranslocation of ApoB (Doonan et al 2019).

As mentioned above, there are ~50 Hsp40s in mammalian cells. There are 7 Hsp40s in the ER lumen (Erdj1-7) (Melnyk et al., 2015). As stated earlier, $p58^{IPK}$ (DNAJC3/Erdj6) has been shown to play a pro-degradative role during the biogenesis of ApoB in primary hepatocytes. The roles of the of the other Erdjs remains unknown. Do JA1 and $p58^{IPK}$ (DNAJC3/Erdj6) act synergistically to degrade ApoB? A double knockdown of JA1 and $p58^{IP}$ will provide information on the relative contributions of these Hsp40s. As a control, ApoB levels should be examined after knocking DNAJC3, as reported in Chapter 2.

Hsp40s use their J domains to stimulate Hsp70s ATPase activity and C-terminus for substrate binding. Is the role of JA1 in ApoB biogenesis J domain dependent? Future experiments should determine which domain of JA1 is required to regulate ApoB. siRNA-resistant tagged J domain mutant (HPD motif mutant) or C-terminal mutants (including truncation mutants) should be transfected into cells and the rescue of the defect caused by JA1 knockdown would be monitored by pulse chase assay. It is likely that both domains are required to assist Hsp70 in the biogenesis of ApoB. Nevertheless, there are several Hsp40s both in yeast and mammals with J domain independent roles (for a recent review, see (Ajit Tamadaddi and Sahi, 2016)). Functional assays using HPD motif mutants or truncations of the J domain have found that the following Hsp40s do not require their J domains: Swa2p, which assists in clathrin coat assembly in yeast, and in

mammalian cells, DNAJA1, which assists in the replication of Influenza A virus replication, $p58^{IPK}$, which assists in the inhibition of PKR (interferon-induced protein kinase), DNAJB8, which remains partially functional in disaggregating polyglutamine residues, and DNAJB11, which prevents client aggregation (Cao et al., 2014; Hageman et al., 2010; Sahi et al., 2010; Shen and Hendershot, 2005; Xiao et al., 2006; Yan et al., 2002).

In contrast to JA1, JB1, a class B Hsp40, stabilizes ApoB (Figure 23). This effect was significant at only one timepoint for the intracellular ApoB pool but at two time points in the secreted population. These contrasting roles of JA1 and JB1 emphasize the differential effects Hsp40s can play in determining the fate of ApoB, like in CFTR as stated earlier. When I next depleted both JA1 and JB1, I observed no effect on ApoB levels. The effects might either have been canceled out or their knockdown would have caused a severe stress response or off-target effects. In addition, compensatory role of other Hsp40s cannot be ruled out.

Since I found that two Hsp40s, each from different classes, play contrasting roles in ApoB biogenesis, it will be intriguing to identify the timing of their interaction with ApoB. The following metabolic pulse chase experiment could be performed: synchronize translation with the addition of puromycin, treat cells with a cross-linker at specific times during the chase, and follow this by sequential immunoprecipitation with anti ApoB antibody followed by anti-JA1 or JB1 secondary precipitations. This will reveal which Hps40 binds to ApoB in the early versus later phases of biogenesis. Additionally, different ApoB truncations can also be expressed in McA cells or cells that do not endogenously express ApoB, and cross-linking experiments could be performed to determine the preferential binding of JA1/JB1 to different biogenic ApoB intermediates.

3.2 E3 ubiquitin ligases in ApoB ERAD

The Hrd1 E3 ubiquitin ligase ubiquitinated and helped degrade ApoB in yeast (Rubenstein et al., 2012). Additionally, Hrd1 co-immunoprecipitated with ApoB100 in human hepatoma cells (Rutledge et al., 2009). Therefore, I investigated the role of Hrd1 in ApoB biogenesis in McA cells. Hrd1 depletion significantly stabilized ApoB levels (Figure 29) but did not alter levels of ubiquitinated ApoB (Figures 30, 31), suggesting that it might function as a retrotranslocation channel (Baldridge and Rapoport, 2016; Carvalho et al., 2010; Peterson et al., 2019). Lack of lipidation may lead to the recognition of unlipidated and potentially aggregation prone ApoB by the lumenal factors which might direct it for Hrd1-mediated retrotranslocation. Additionally, the retrotranslocation channel might consist of more than one protein (i.e., both Sec61 and Hrd1). In other words, Hrd1 and Sec61 may form a transient mixed retrotranslocon to move ApoB back to the cytosol.

Surprisingly and in contrast to previous studies (Fisher et al., 2011; Liang et al., 2003), the loss of gp78 had no effect on the turnover of either intracellular ApoB100 or ApoB48 in McA cells (Figure 32). I did not observe any differences upon double knockdown of both Hrd1 and gp78. Upon assessing endogenous levels of protein, gp78 was somewhat higher in HepG2 cells compared to McA (Figure 32). Thus, loss of gp78 led to an effect on ApoB levels in HepG2 cells. Similarly, higher levels of Hrd1 in McA cells is responsible for ApoB ERAD. Genetic variability and cell line-based discrepancy can lead to inconsistent effects as has been observed when gp78's effect on HMGCR was examined (Tsai et al., 2012) (see section 1.2.3.4.) .

3.3 The ribosomal associated complex (RAC) in ApoB biogenesis

The RAC consists of Ssz1 (a non-canonical Hsp70), Zuotin or DNAJC2 (Hsp40), and Listerin (an E3 ubiquitin ligase) (Preissler and Deuerling, 2012), and together they facilitate Ribosome Quality Control, which is involved in the degradation of nascent polypeptides in the event of a translational stall. Interestingly, Listerin's role in co-translational degradation was recently revealed by the Hegde lab, where by using an *in vitro* system they found that Ltn1 ubiquitinates a co-translational translocating protein that stalls at the Sec61 channel (von der Malsburg et al., 2015). In accordance with a potential role for the RAC in ApoB biogenesis, ApoB has amphipathic stretches which interact with the Sec61 protein channel, and this interaction impedes translocation and thus the ribosome-ApoB complex is stalled on the Sec-61 translocon (Chuck and Lingappa, 1992; Chuck et al., 1990; Yamaguchi et al., 2006). In addition, ApoB has been observed to undergo ubiquitination at the Sec61 translocon before it is completely translated (Rutledge et al., 2009; Zhou et al., 1998). DNAJC2 is in proximity to the ApoB nascent polypeptide, thereby most suitably placed to target ApoB for degradation. Thus, it is very likely that the members of RAC, due to their proximity to the paused ApoB nascent polypeptide, might ubiquitinate ApoB and target it for degradation. This hypothesis should be addressed in future studies.

3.4 The guided entry of tail (GET) anchored protein complex in ApoB biogenesis

Nearly one-third of all proteins enter the secretory pathway (Braakman and Bulleid, 2011; Ghaemmaghami et al., 2003; Kanapin et al., 2003). This begins with the translocation of these

proteins into the ER. Translocation is a complex process and can either occur co-translationally or post-translationally (Brodsky, 1998; Chang et al., 2012; Chartron et al., 2012; Liou et al., 2007; Schuldiner et al., 2008). When the nascent polypeptide has a signal sequence at its N-terminus, like ApoB, it usually undergoes co-translational translocation after recognition by the Signal Sequence Recognition Particle (SRP). However, the protein needs to be in a Sec61 competent conformation, i.e., it should not misfold and should be kept soluble before entering the ER through the Sec61 pore. However, another family of proteins translocates in a Sec61-independent manner. This family of proteins requires the GET complex, a highly conserved set of factors that bind nascent polypeptides and target them to an alternative ER membrane protein complex (Chang, et al. 2012; Chartron, et al. 2012; Liou, et al. 2007; Schuldiner, et al. 2008). GET proteins maintain the solubility of ER targeted hydrophobic proteins by binding and protecting the transmembrane domains of tail anchored proteins while they move to the ER (Brodsky, 1998; Chang et al., 2012; Chartron et al., 2012; Liou et al., 2007; Schuldiner et al., 2008). Additionally, GET proteins also contribute to the degradation of misfolded or untranslocated proteins (Brodsky 1998; Chang, et al. 2012; Chartron, et al. 2012; Liou, et al. 2007; Schuldiner, et al. 2008). Because ApoB is hydrophobic and must be maintained in solution in an aggregation free state, both while translocating and after retrotranslocation, it is possible that some GET family members might stabilize and facilitate ApoB translocation.

In yeast, Sgt2 (SGTA in mammals) is a peripheral GET member and binds to the transmembrane domain of a nascent polypeptide, thereby acting as a chaperone. This Sgt2-polyypeptide complex is delivered to the ER through several steps that are mediated by core members of the GET family, namely, Get3, Get4, and Get5 (Brodsky 1998; Chang, et al. 2012; Chartron, et al. 2012; Liou, et al. 2007; Schuldiner, et al. 2008). ApoB has hydrophobic domains

throughout its entire sequence. Thus, Sgt2 may recognize these domains in the nascent ApoB polypeptide, bind to them, keep it in a translocation competent conformation, and carry ApoB to the ER. Moreover, several studies have found that GET proteins work in association with the Hsps, which include Hsp70 and Hsp40. Strikingly, Liou and colleagues found that Ydj1 interacts with Sgt2 in yeast (Liou et al., 2007). Additionally, one study conducted in HeLa cells found that SGTA-Hsp70 complex interacts with J proteins while mediating translocation of a viral protein into the ER Ref. Thus, Ydj1 may facilitate the translocation of ApoB by collaborating with Sgt2.

3.5 Limitations of the model system

I began my studies by investigating the role of Hsp40s in ApoB biogenesis by conducting a candidate-based screen in yeast (Figure 9). Yeast have been extensively used to study roles of chaperones and E3 ubiquitin ligases in the ERAD of several mammalian proteins, including ApoB (Ahner et al., 2007; Doonan et al., 2019; Grubb et al., 2012; Hrizo et al., 2007; McClellan et al., 2005; Ravid et al., 2006; Youker et al., 2004). Yeast do not endogenously express ApoB, but the conservation of chaperones, the established characterization and conserved nature of the ERAD machinery, the ease of genetic manipulations, and the availability of temperature-sensitive strains make yeast a useful tool to study ERAD. Additionally, past results were consistent when recapitulated in mammalian cells ((Ahner et al., 2007; Gusarova et al., 2001; Meacham et al., 1999) and for a recent review, see (Needham et al., 2019)). Consistent with this history of using the yeast model, data from yeast on Hsp40s in this study were consistent in McA cells (Figure 15), underscoring the advantages of using yeast as a model system to study ApoB ERAD, particularly for conducting a preliminary screen. In fact, after my initial screen, I conducted my studies and

confirmed my results in McA cells, which are a standard model in the field. For example, the secreted lipoprotein profile of McA cells is more similar to a human liver despite its rat origin (Boren et al., 1994), and rat and human ApoB100 are ~70% identical. Whereas the ~30% non-identical regions are interspersed in the entire protein, a higher percent of non-identical region exists in the C-terminal region between residues 3677-4271, which span the β_2 (2571-4032) -α_3 (4017-4515) regions (see section 1.1.2). The other cell systems used to study ApoB are HepG2 and Huh7 cells, which are human hepatoma cells (Simon et al., 1982) HepG2 cells, despite being human in origin, secrete lipid poor particles, unlike the human liver and McA cells, which secrete buoyant lipid rich particles. The defective lipoprotein particle secretion profile in HepG2 cells has been attributed to a hyperactive MEK-ERK signaling pathway. When this pathway is inhibited, the lipid status of the secreted lipoproteins shifts to more buoyant state (Tsai et al., 2007). Huh7 cells have also been used in some studies but are no better than HepG2 cells when the assembly or secretion of ApoB particles is examined (Meex et al., 2011).

3.6 Concluding remarks

ApoB is an unusual ERAD substrate; no other ERAD substrate among the ~80 known disease associated substrates is targeted for degradation co-translationally, like ApoB. Knowledge of the contributing factors in ApoB regulation will not only provide novel insights into the identification of potential therapeutic candidates that may be targeted to treat CAD but also better define how ApoB—and likely other uncharacterized proteins—are targeted for ERAD. The discoveries from my project provide new insight into the cellular 'machines' that change the stability of ApoB in the cell. The results of this study may also have direct implications on the

development of drugs to treat heart disease, and more specifically, CAD. Since drugs are in development that target many of the factors I have investigated (Assimon et al., 2013; Koishi et al., 1992; Lu et al., 2020; McConnell and McAlpine, 2013; Park et al., 2020; Shevtsov et al., 2019; Soti et al., 2005; Yokota et al., 2000), these data should be translated into animal models in future efforts, which will allow the testing of these new drugs.

APPENDIX A: INVESTIGATE THE ROLES OF JA1 IN APOB BIOGENESIS IN "HUMANIZED" McA CELLS

Appendix A.1 Introduction

The model system I have used for my studies are McA cells, a rat hepatoma cell line that synthesizes and secretes both ApoB100 and ApoB48 isoforms. ApoB48 is the product of a unique RNA editing process by the Apobec1 enzyme. Deamidation of a cytidine residue (CAA) converts Glutamine (UAA) to a stop codon, producing ApoB48 mRNA (Blanc and Davidson, 2010). ApoB48, synthesized only in higher mammals, is responsible for the transport of dietary cholesterol and lipids synthesized in intestine in chylomicron particles.

During my investigations, I failed to observe any differences in the levels of ApoB48 upon JA1, JB1, Hrd1 knockdown (Figures 15, 23, 29). To simplify the interpretation of my result and explore the effect of JA1 knockdown exclusively on ApoB100, we received "humanized" McA cells from the Fisher lab in which the Apobec1 enzyme was knocked-out using the Cre Lox system; these cells, like the human hepatoma cell line, express only ApoB100 (and not ApoB48). These cells will henceforth be referred to as "Apobec KO" cells.

Appendix A.2 Materials and methods

Pulse Chase assays, JA1 knockdown and ubiquitination assays were conducted as described in 2.2.7 and in Figures 15, 23.

Appendix A.3 Results and discussion

I first conducted a pulse chase experiment in Apobec KO cells to confirm the absence of ApoB48 (Figure 33A). To verify proteasome mediated degradation, I pre-incubated cells with 25 µM MG-132 for an hour before

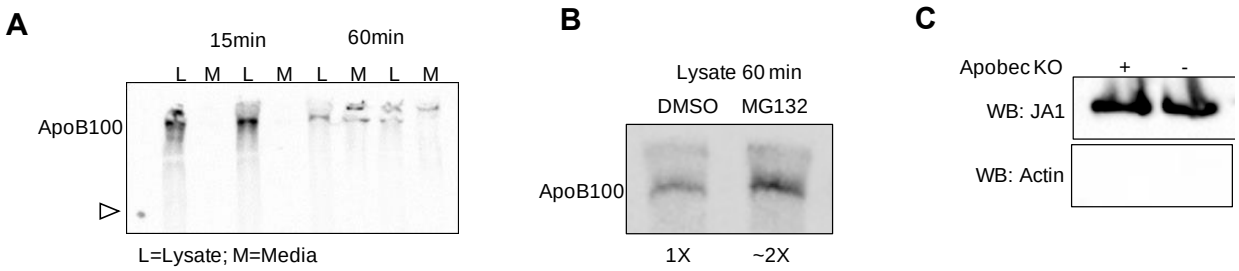

Figure 33. Apobec KO McA cells do not express ApoB48 and MG132 increases the levels of secreted ApoB100. A. A pulse chase was conducted as described in section 2.2.7. Radiograph shows lysate (L) and media (M) samples from two replicates at 15 and 60 min respectively. Open arrowhead shows the 250 kDa marker and the point of expected migration of ApoB48. B. Cells were incubated with MG132 (25µM) or DMSO and pulse chase was conducted. C. Apobec KO cells and McA cells were lysed and normalized amounts of protein were loaded. Levels of JA1 and actin were examined by SDS PAGE and western blotting.

conducting the pulse chase assay. Consistent with findings from McA cells, I observed a ~2-fold increase in ApoB100 (Figure 33B). I also compared the endogenous levels of JA1 and actin in Apobec KO McA and McA cells. The levels of both proteins were similar in the two cell lines (Figure 33C). Next, to explore the effect of JA1 on ApoB100 levels in Apobec KO McA cells, I conducted a pulse chase experiment after knocking down JA1 (Figure 34A). Interestingly, I did not observe any effect of JA1 knockdown on ApoB100 levels (Figure 34B). To investigate if JA1 knockdown altered the extent of Apob100 ubiquitination, I conducted ubiquitination assay as described in section 2.2.7. I observed a minor (~1.5x) increase in the levels of ubiquitinated

ApoB100 (Figure 34C).

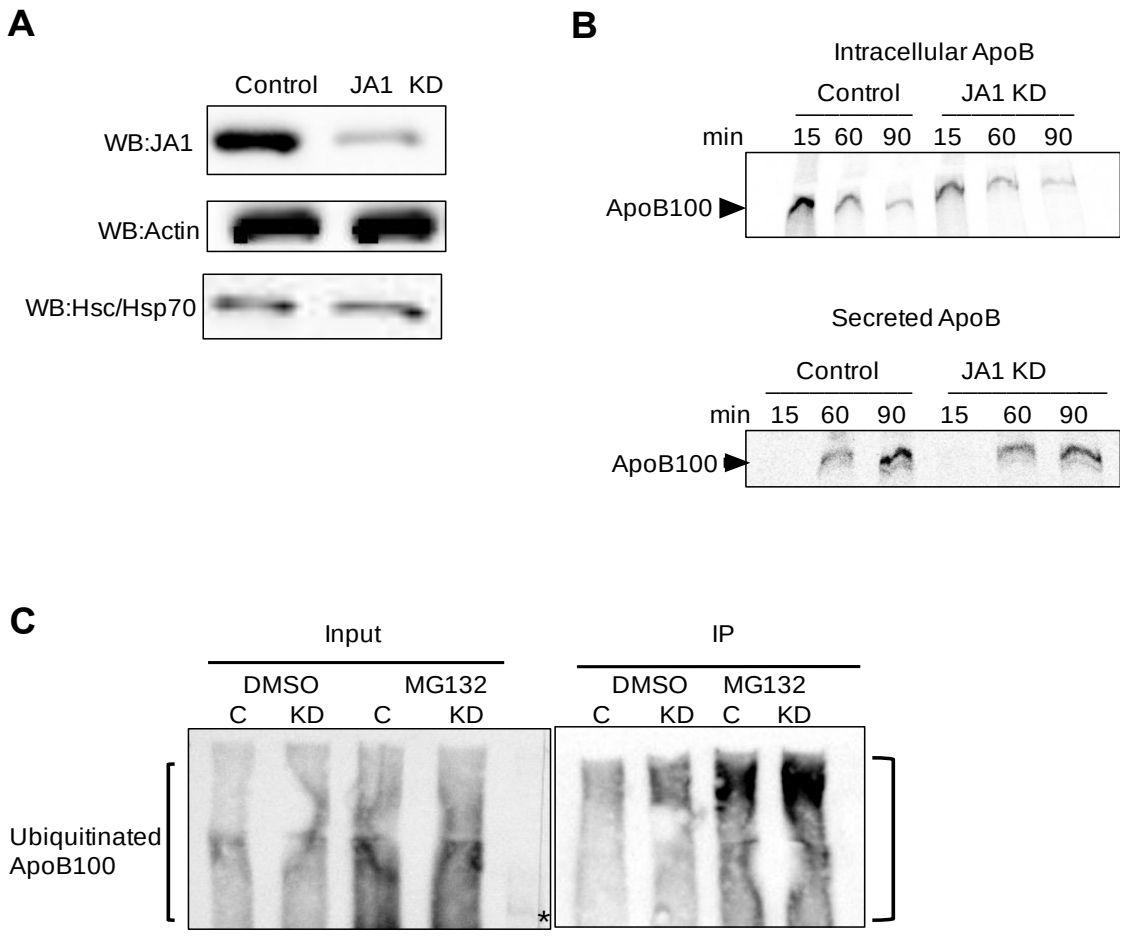

Figure 34. JA1 knockdown does not affect ApoB100 levels in Apobec KO McA cells.

A. Cells were transfected with siRNA targeting JA1 or mock transfected with scrambled siRNA (control) as described in Materials and Methods. Levels of JA1, Actin, and Hsc/Hsp70 were measured by SDS PAGE and western blotting. B. After JA1 knockdown, a pulse chase was conducted as described in the Materials and Methods. Representative radiographs show intracellular (top) and secreted (bottom) ApoB100. C. Levels of ubiquitinated ApoB100 were measured in cells expressing HA-tagged ubiquitin in mock transfected (C) and JA1 KD (KD) cells as described in Figure 20. Where indicated, cells were treated with DMSO or MG-132 (25 μM) for an hour. The asterisk denotes the migration of unmodified ApoB100.

The lack of an effect of JA1 knockdown in Apobec KO cells on ApoB100 secretion/stability might be due to several reasons. First, ApoB mRNA is probably the most well

characterized target of Apobec1. However, it has other targets, including neurofibromatosis-1, and its absence may disrupt global RNA stability and editing (Anant and Davidson, 2000; Conticello, 2008; Morgan et al., 2004; Rosenberg et al., 2011). Thus, it is likely that Apobec KO in McA cells resulted in activation or inactivation of key pathways that elicited stress responses or/and secondary effects (Roberts et al., 2013; Yamanaka et al., 1997). Second, the Apobec KO McA cells I used for my experiments did not appear as healthy (more rounded cells) as McA cells, so knockdown of JA1, a critical Hsp40, could have exacerbated the stress response. In addition, only two out of six aliquots of frozen cells that we received from the Fisher lab survived (they were also not confluent). It is therefore possible that a select group of cells survived, were selected for, and then clonally expanded. This might have led to physiological changes. Further experiments on additional clones may reveal if the effect of JA1 is consistent in these cells, and additional derived cells are being examined in the Fisher lab.

APPENDIX B: INTERROGATING THE ROLE OF KELCH LIKE PROTEIN 12 (KLHL12) IN APOB BIOGENESIS

Appendix B.1 Introduction

ApoB100-containing VLDL particles are significantly larger than nearly all other cargo of the COPII machinery (Gusarova et al., 2003; Rahim et al., 2012), and therefore may depend on adapter proteins that aid their packaging and transport. Kelch-like protein 12 (KLHL12) is a substrate specific adapter involved in the COP-II mediated ER exit of large cargo, including pro-collagen and VLDL particles (Gusarova et al., 2003; Jin et al., 2012; Siddiqi et al., 2003). KLHL12 is a member of the Cullin3-based (CUL3) ubiquitin ligase complex that plays key roles in mammalian cell differentiation (Dubiel et al., 2018). The Fisher lab at NYU School of Medicine showed that ablation of KLHl12 significantly lowered intracellular and secreted ApoB100 levels in McA cells (Butkinaree et al., 2014). Interestingly, depletion of KLHL12 enriched the ER localized ApoB100 fraction, suggesting disruption in post-ER trafficking of ApoB100. Consistent with this finding, overexpression of KLHL12 increased levels of secreted ApoB100, indicating that the endogenous levels of KLHL12 may limit the trafficking of ApoB100-VLDL particles (Butkinaree et al., 2014). Based on these data, I asked if exogenously expressing ApoB100 in HEK cells would cause a transcriptional upregulation of KLHL12. To this end, I examined KLHL12 mRNA levels in HEK cells in the presence or absence of ApoB100 expression. I anticipated an increase in KLHL12 mRNA levels upon expression of ApoB.

Appendix B.2 Materials and methods

HEK cells were seeded at 2×10^5 cells/well in six-well plates and grown overnight. Cells were transfected with the plasmid encoding ApoB100 as described in section 2.2.6. After 24 hours, RNA was extracted using the RNeasy Mini Kit (Qiagen 74104) following the manufacturer's instructions. RNA concentration and purity were measured using the NanoDrop spectrophotometer. RNA was then reverse transcribed into cDNA according to the instructions of the manufacturer. Next, an RT PCR was set up using Syber Green Master Mix in the StepOnePlus system and primers amplifying KLHL12 (Applied Biosystems, Thermo Fisher Scientific). Beta actin was used as the internal control.

Appendix B.3 Results and discussion

To achieve maximal expression of ApoB100, I transfected HEK cells with 1, 2, 4 µg of pcDNA3.1-ApoB100 plasmid. Optimal expression was observed when cells were transfected with 4 µg of the plasmid (Figure 35A). I then extracted RNA (Figure 35B) and conducted RT PCR to measure the levels of KLHL12 when ApoB100 was expressed. Interestingly, I found a slight but statistically insignificant increase in the mRNA expression of KLHL12 (Figure 35C).

HEK cells are not a standard or widely used model to study ApoB biogenesis. However, this was a proof of principle experiment. It is unknown if ApoB containing VLDL particles assemble and traffic similarly in HEK cells as in McA cells. Cell line-based inconsistency or discrepancy has been observed before in the processing of an FH causing mutant of the PCSK9 enzyme, which is responsible for the lysosomal degradation of LDL receptors (Dubiel et al., 2018;

Sun et al., 2005). Whereas the mutant enzyme underwent cleavage in McA or HepG2 cells, it was not cleaved in HEK cells, corroborating the limitation of using different cell lines in studying lipid metabolism. It is also possible that the endogenous native level of KLHL12 was sufficient for ApoB packaging, and therefore I did not observe any increase in KLHL12 mRNA levels.

The Fisher lab also found that KLHL12 overexpression caused secretion of more buoyant ApoB in McA cells, suggesting conditions that favor lipidation and secretion (Butkinaree et al., 2014). Since inhibition of the autophagy pathway when KLHL12 was overexpressed increased intracellular (but not secreted) ApoB levels, the authors speculated that ApoB might be subjected to ER-phagy which is a specialized organelle-specific autophagy pathway targets damaged parts of ER that shelter misfolded proteins to the lysosome (Bernales et al., 2007; Ferro-Novick et al., 2021; Scott et al., 1989). The Fisher lab is currently investigating if KLHL12 mediated degradation of ApoB occurs via the ER-phagy pathway.

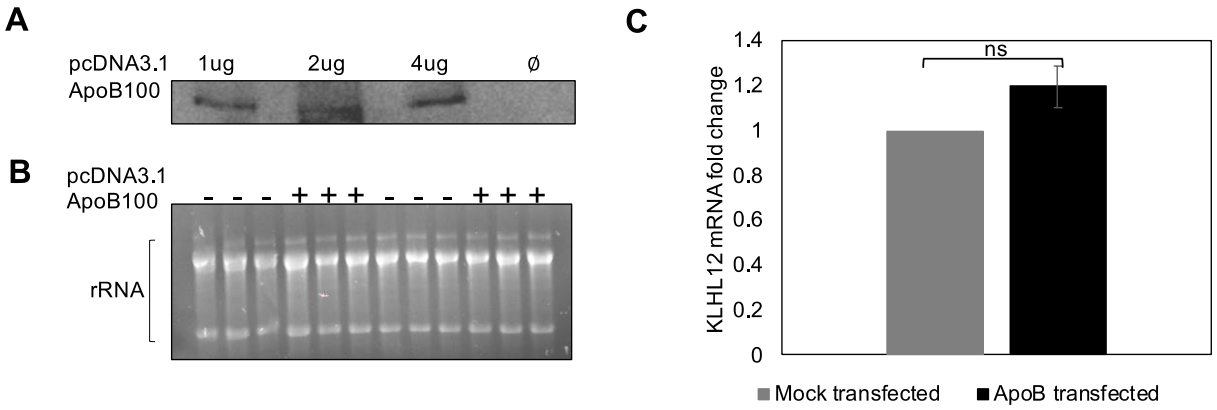

Figure 35. ApoB100 expression does not alter KLHL12 mRNA levels in HEK293 cells.

A. HEK293 cells were transfected with three different concentrations of pcDNA3.1-ApoB100 as described in Materials and Methods. Levels of ApoB100 were examined by SDS PAGE and western blotting. B. RNA was extracted from cells transfected with pcDNA3.1 control vector or pcDNA3.1 containing ApoB100. An agarose gel showing RNA from two biological replicates where each had three technical replicates. C. The mean ± SE fold-

change between mock transfected and ApoB100 transfected cells was determined by qPCR. Data are the means of three biological replicates, with three technical replicates. P value = 0.090

APPENDIX C: EXAMINE THE ROLE OF N-GLYCANASE 1 (NGLY1) ENZYME IN APOB BIOGENESIS

Appendix C.1 Introduction

The NGLY1 gene in humans encodes the N-Glycanase protein (NGLY1) or PNGase, a cytosolic enzyme responsible for removal of N-linked glycans from misfolded proteins following retrotranslocation but before degradation (Enns et al., 2014; Hirsch et al., 2003; Katiyar et al., 2005). Several ERAD substrates including, T cell receptor and MHC Class I, have been shown to be deglysolyated by PNGase (de Virgilio et al., 1998; Hughes et al., 1997; Suzuki et al., 1997; Yu et al., 1997). Deficiency of NGLY1 causes congenital disorder of deglycosylation, symptomized by developmental delay, peripheral neuropathy and microencephaly (Need et al., 2012; Suzuki et al., 2016).

ApoB has 19 glycosylation sites (Harazono et al., 2005). I asked if inhibition of NGLY1 would increase levels of intracellular ApoB since glycosylated ApoB would fail to be degraded by the proteasome. To this end, I used a drug called ZYVAD-FMK (Misaghi et al., 2004) to inhibit NGLY1 and conducted pulse chase assays.

Appendix C.2 Materials and methods

To optimize the concentration of the inhibitor to be used in pulse chase assays, I conducted CellTitre-Glo luminescent viability assays. To this end, ~10,000 cells were seeded in collagen

coated 96 well plates. ZYVAD-FM (Selleck Chemicals) was resuspended in DMSO to a final concentration of 10 mM and the following concentrations were added to cells: 20 uM, 10 uM, 5 uM, 2.5 µM and 1.25 µM in triplicates. Concentrations were selected over a range to generate a sigmoidal curve. Only DMSO and only media were used as control treatments. After drug treatment for 24 hours, 67 µl of CellTiter-Glo solution was added to each well and imaged using the BioRad imager. An IC_{50} was calculated using Image J Protein analyzer tool. For subsequent pulse chase experiments, cells were treated overnight with 20 µM of the inhibitor. To enhance secretion of ApoB, cells were preincubated with 4mM oleic acid-BSA conjugate for 3 hours where indicated.

Appendix C.3 Results and discussion

I found that NGLY1 inhibition via the application of ZYVAD-FM, an inhibitor of this enzyme (Misaghi et al., 2004), did not affect ApoB levels either in the cellular lysate or media (Figure 36A, B). Whereas oleic acid treatment, as expected, enhanced levels of secreted ApoB100. This result, however, is not completely unexpected since Dr. Lynley Doonan, a previous graduate student in our lab, found that deletion of *PNG1* (which encodes PNGase) in yeast did not affect ApoB levels. Moreover, there is growing evidence that NGLY1-dependent deglycosylation is not required for all ERAD substrates (Galeone et al., 2020; Kario et al., 2008). Additionally, the drug might not have been as effective in inhibiting the enzyme. Future work could examine ApoB levels after depleting NGLY1 by siRNA-mediated knockdown

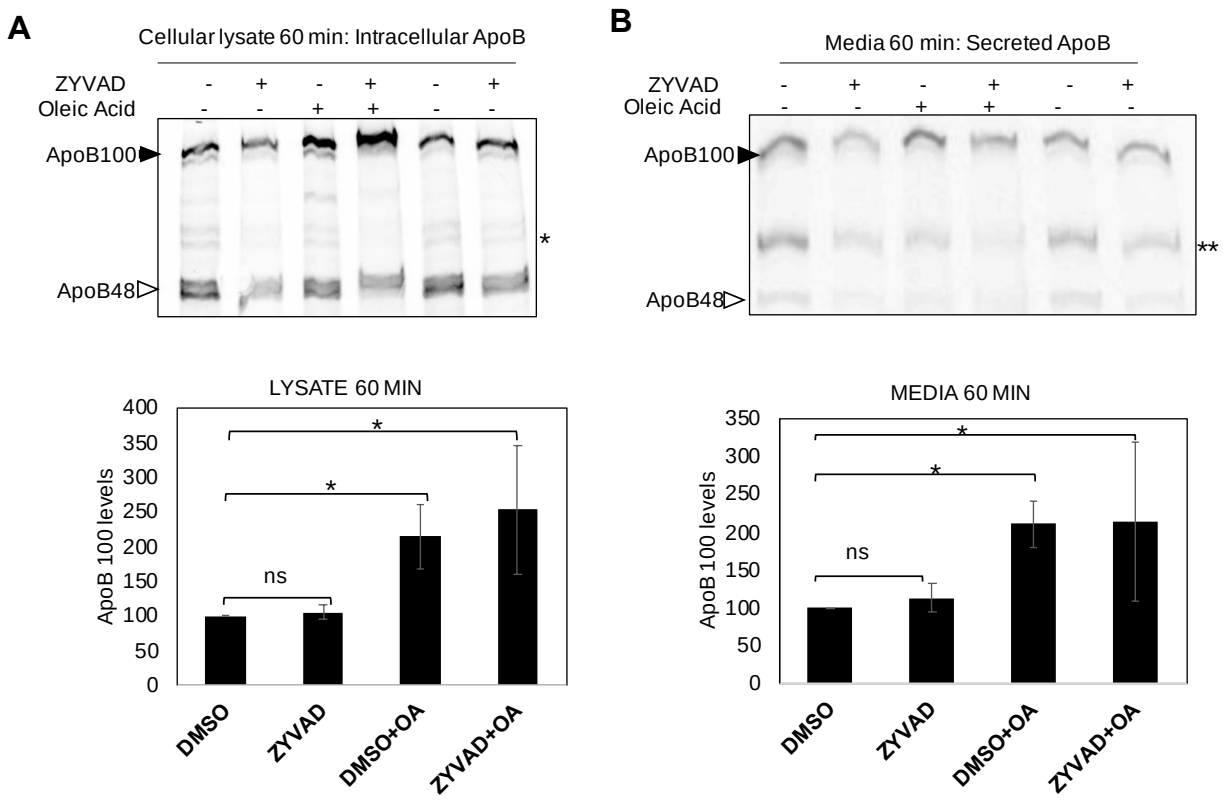

Figure 36. Inhibition of NGLY1 does not affect ApoB levels.

Cells were treated with DMSO or ZYVAD-FMK (20μM) overnight and where indicated were preincubated with 4mM OA for 4 hours before pulse chase experiments were performed as described in section 2.2.7 and Figure 15. Samples were normalized to the amount of radioactivity, and ApoB was immunoprecipitated. Data were analyzed by SDS-PAGE, phosphorimaging, and Image J, and are the means of three biological replicates, each with two technical replicates. A. Representative radiograph and quantitative graph showing intracellular levels of ApoB. B. A Representative radiograph and quantitative graph showing secreted levels of ApoB. Ns= non-significant, * indicates p value <0.05.

APPENDIX D: HOW DOES BAP 31 CONTRIBUTE TO THE BIOGENESIS OF APOB

Appendix D.1 Introduction

BAP31 is an ER integral membrane protein that associates with the translocon and Derlin and assists in the retro-translocation and ERAD of CFTR (Lambert et al., 2001; Wang et al., 2008). The yeast homolog of BAP31 also assists in the biogenesis of membrane proteins (Annaert et al., 1997; Paquet et al., 2004; Schamel et al., 2003). Preliminary unpublished work from our lab by Dr. Sarah Grubb has shown that Bap31 contributes to ApoB ERAD in McA cells. To continue investigating the role of BAP31 in ApoB biogenesis, I began with optimizing Bap31 knockdown conditions in these cells.

Appendix D.2 Materials and methods

siRNA mediated knockdown was performed using Lipofectamine RNAimax reagent as described in section 2.2.6.

Appendix D.3 Results and discussion

I began knockdown optimization with two siRNAs (si5 and si6) that Dr. Sarah Grubb successfully used in her experiments. I treated cells with 10 nM, 20 nM and 30 nM of scrambled siRNA (ctrl) for 48 hrs. I then lysed cells and examined levels of Bap31 by SDS PAGE and western

blotting. Surprisingly, I did not observe any depletion in BAP31 levels (Figure 37A). These siRNAs were shown to ablate BAP31 by Dr. Sarah Grubb at higher concentrations (100 nM) but since such high concentrations can elicit severe stress response, I chose to use lower concentrations. I then ordered a set of four new individual siRNAs (9, 10, 11, 12) from Horizon/Dharmacon and used 10 nM (Figure 37B) and 30 nM (Figure 37C) for 48 and 72 hr. I again failed to observe any silencing with the new siRNAs (Figure 37B, C). I next wondered if combining these siRNAs would deplete BAP31. Thus, I combined si5+si6 (5+6, 10 nM each) and siRNAs 9+10+11+12 (pool, 10 nM each) and transfected cells for 48 and 72 hr. Again, I failed to observe any BAP31 depletion (Figure 37D). I then used higher concentrations, treatment 1 (50 nM each of si5 and si6) and 2 (25 nM each of si9, si10, si11, si12), and transfected cells for 48 hrs. After 48 hrs, I added the same concentrations of siRNAs and lysed cells after a total transfection duration of 72 hours (Figure 37E). These conditions also failed to knock down BAP31 (Figure 37E). Next, I wondered if a shorter transfection of 24 hr might work, but as before observed no effect on BAP31 levels (Figure 37F).

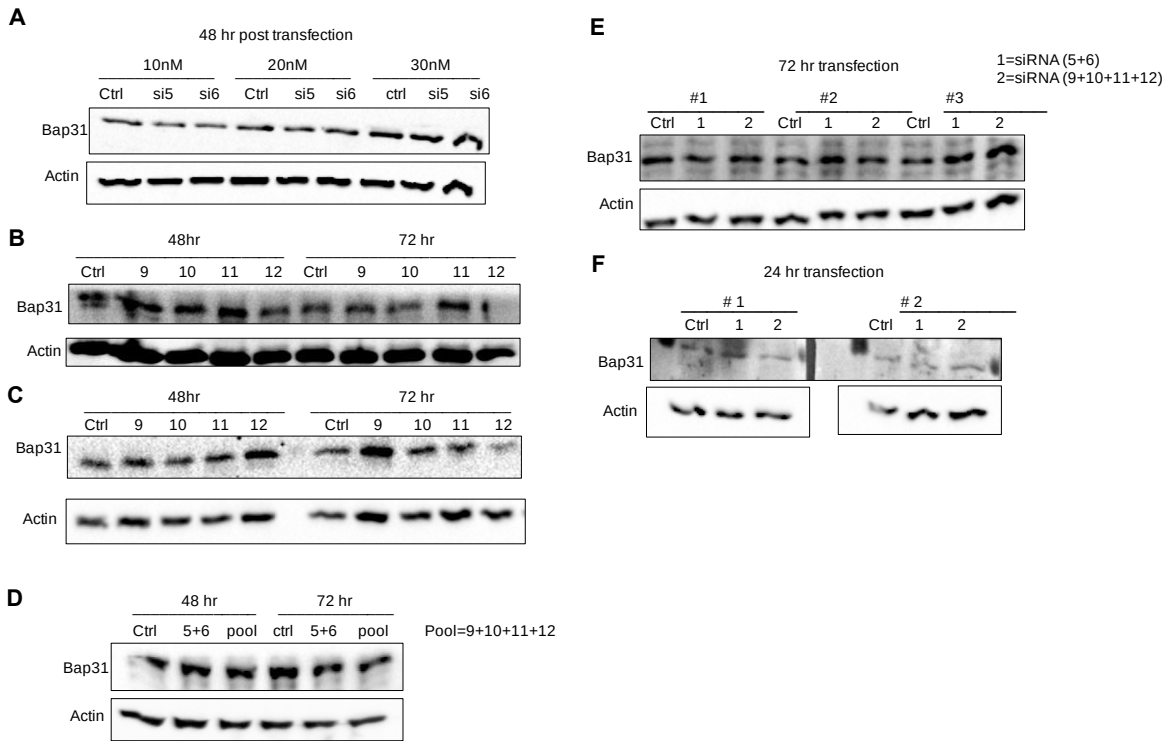

Figure 37. siRNA knockdown did not lower BAP31 protein levels.

A. Cells were transfected with 10, 20, 30 nM of control (ctrl, mock transfected), siRNA 5 (si5), siRNA 6 (si6), for 48 hrs. I then lysed cells and examined levels of Bap31 by SDS PAGE and western blotting. B.C. A set of four new individual siRNAs (9, 10, 11, 12) at 10 nM (B) and 20 nM (C) were transfected in for 48, 72 hrs respectively. D. si5+si6 (5+6, 10nM each) and siRNAs 9+10+11+12 (pool, 10nM each) and transfected cells for 48 and 72 hr. E. Higher concentrations (100 nM total) of the following combinations 1 (50 nM each of si5 and si6) and 2 (25 nM each of si9, si10, si11, si12) were transfected in cells for 48 and 72 hrs respectively. F. Higher concentrations (100 nM total) of the following combinations 1 (50 nM each of si5 and si6) and 2 (25 nM each of si9, si10, si11, si12) were transfected in cells for 24 hrs.

Since none of my attempts could succeed at knocking down BAP31 protein levels, I questioned if the siRNAs were silencing the transcript. Thus, I conducted RT PCR to examine the levels of BAP31 mRNA. Interestingly, I observed that the combination of siRNA 5+6 at 50 nM each knocked down mRNA levels by ~80% and ~70% after 48 and 72 hrs of transfection, whereas

the siRNA pool of 9-12 at 25 nM each silenced the message by less than 50% (Figure 38A); however, the protein levels were not significantly lowered, indicating that the protein is very stable. Since the first set (siRNAs 5+6) lowered mRNA levels, I next wondered if transfecting a fewer number of cells with the same siRNAs would lower protein levels since the protein would be diluted following every cell division. This approach again failed to work (Figure 38B). In sum, it is worth noting that BAP31 is one of the most abundant proteins in the ER (Cacciagli et al., 2013; Quistgaard, 2021), and that Dr. Sarah Grubb also had difficulty in knocking BAP31 down.

A

mRNA levels

	48 hours	**72 hours**
siRNA 5+6	~80% Knockdown	~70% Knockdown
siRNA 9-12	~40% knockdown	~25% knockdown

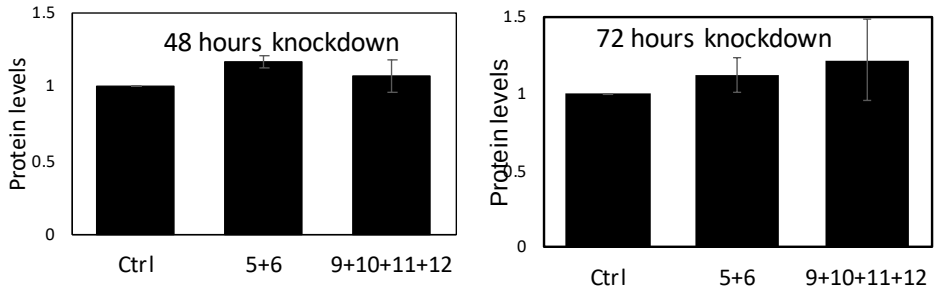

B

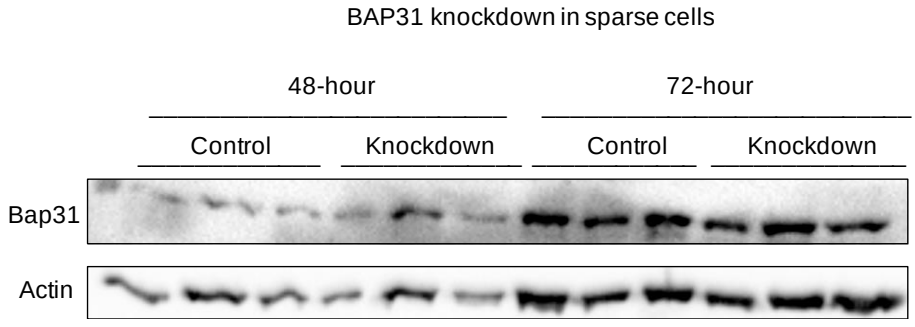

Figure 38. Decreased BAP31 mRNA levels upon siRNA treatment, but protein levels remain unchanged.

A. Cells were transfected with siRNAs (5+6), 50 nM each, and siRNA (9-12), 25 nM each, for 48 and 72 hours. RNA was extracted and RT PCR was conducted as described in Appendix B.2. Actin levels were used as an internal control.

The table shows the mRNA levels and graphs below represent the corresponding protein levels after transfection. B. Cells (10,000) were seeded and transfected with scrambled (Control) or siRNAs (5+6), 50 nM each (Knockdown). Cells were processed by SDS PAGE and western blotting.

REFERENCES

Abisambra, J.F., Jinwal, U.K., Suntharalingam, A., Arulselvam, K., Brady, S., Cockman, M., Jin, Y., Zhang, B., and Dickey, C.A. (2012). DnaJA1 antagonizes constitutive Hsp70-mediated stabilization of tau. J Mol Biol *421*, 653-661.

Abul-Husn, N.S., Manickam, K., Jones, L.K., Wright, E.A., Hartzel, D.N., Gonzaga-Jauregui, C., O'Dushlaine, C., Leader, J.B., Lester Kirchner, H., Lindbuchler, D.M., *et al.* (2016). Genetic identification of familial hypercholesterolemia within a single U.S. health care system. Science *354*.

Adams A, K.C. (1997). Methods in yeast genetics : a Cold Spring Harbor Laboratory course manual.

Adams, B.G. (1972). Induction of galactokinase in Saccharomyces cerevisiae: kinetics of induction and glucose effects. J Bacteriol *111*, 308-315.

Adhyaru, B.B., and Jacobson, T.A. (2018). Safety and efficacy of statin therapy. Nat Rev Cardiol *15*, 757-769.

Adle, D.J., and Lee, J. (2008). Expressional control of a cadmium-transporting P1B-type ATPase by a metal sensing degradation signal. J Biol Chem *283*, 31460-31468.

Adle, D.J., Wei, W., Smith, N., Bies, J.J., and Lee, J. (2009). Cadmium-mediated rescue from ER-associated degradation induces expression of its exporter. Proc Natl Acad Sci U S A *106*, 10189-10194.

Ahner, A., Nakatsukasa, K., Zhang, H., Frizzell, R.A., and Brodsky, J.L. (2007). Small heat-shock proteins select deltaF508-CFTR for endoplasmic reticulum-associated degradation. Mol Biol Cell *18*, 806-814.

Ajit Tamadaddi, C., and Sahi, C. (2016). J domain independent functions of J proteins. Cell Stress Chaperones *21*, 563-570.

Alzayady, K.J., Panning, M.M., Kelley, G.G., and Wojcikiewicz, R.J. (2005). Involvement of the p97-Ufd1-Npl4 complex in the regulated endoplasmic reticulum-associated degradation of inositol 1,4,5-trisphosphate receptors. J Biol Chem *280*, 34530-34537.

Anant, S., and Davidson, N.O. (2000). An AU-rich sequence element (UUUN[A/U]U) downstream of the edited C in apolipoprotein B mRNA is a high-affinity binding site for Apobec-1: binding of Apobec-1 to this motif in the 3' untranslated region of c-myc increases mRNA stability. Mol Cell Biol *20*, 1982-1992.

Anderson, T.A., Levitt, D.G., and Banaszak, L.J. (1998). The structural basis of lipid interactions in lipovitellin, a soluble lipoprotein. Structure *6*, 895-909.

Annaert, W.G., Becker, B., Kistner, U., Reth, M., and Jahn, R. (1997). Export of cellubrevin from the endoplasmic reticulum is controlled by BAP31. J Cell Biol *139*, 1397-1410.

Assimon, V.A., Gillies, A.T., Rauch, J.N., and Gestwicki, J.E. (2013). Hsp70 protein complexes as drug targets. Curr Pharm Des *19*, 404-417.

Au, C.S., Wagner, A., Chong, T., Qiu, W., Sparks, J.D., and Adeli, K. (2004). Insulin regulates hepatic apolipoprotein B production independent of the mass or activity of Akt1/PKBalpha. Metabolism *53*, 228-235.

Bakillah, A., Zhou, Z., Luchoomun, J., and Hussain, M.M. (1997). Measurement of apolipoprotein B in various cell lines: correlation between intracellular levels and rates of secretion. Lipids *32*, 1113-1118.

Balch, W.E., Morimoto, R.I., Dillin, A., and Kelly, J.W. (2008). Adapting proteostasis for disease intervention. Science *319*, 916-919.

Baldridge, R.D., and Rapoport, T.A. (2016). Autoubiquitination of the Hrd1 Ligase Triggers Protein Retrotranslocation in ERAD. Cell *166*, 394-407.

Barber, G.N., Thompson, S., Lee, T.G., Strom, T., Jagus, R., Darveau, A., and Katze, M.G. (1994). The 58-kilodalton inhibitor of the interferon-induced double-stranded RNA-activated protein kinase is a tetratricopeptide repeat protein with oncogenic properties. Proc Natl Acad Sci U S A *91*, 4278-4282.

Bays, N.W., Gardner, R.G., Seelig, L.P., Joazeiro, C.A., and Hampton, R.Y. (2001). Hrd1p/Der3p is a membrane-anchored ubiquitin ligase required for ER-associated degradation. Nat Cell Biol *3*, 24-29.

Becker, J., Walter, W., Yan, W., and Craig, E.A. (1996). Functional interaction of cytosolic hsp70 and a DnaJ-related protein, Ydj1p, in protein translocation in vivo. Mol Cell Biol *16*, 4378-4386.

Beilharz, T., Egan, B., Silver, P.A., Hofmann, K., and Lithgow, T. (2003). Bipartite signals mediate subcellular targeting of tail-anchored membrane proteins in Saccharomyces cerevisiae. J Biol Chem *278*, 8219-8223.

Benayoun, L., Granot, E., Rizel, L., Allon-Shalev, S., Behar, D.M., and Ben-Yosef, T. (2007). Abetalipoproteinemia in Israel: evidence for a founder mutation in the Ashkenazi Jewish population and a contiguous gene deletion in an Arab patient. Mol Genet Metab *90*, 453-457.

Benjamin, E.J., Muntner, P., Alonso, A., Bittencourt, M.S., Callaway, C.W., Carson, A.P., Chamberlain, A.M., Chang, A.R., Cheng, S., Das, S.R., *et al.* (2019). Heart Disease and Stroke Statistics-2019 Update: A Report From the American Heart Association. Circulation *139*, e56-e528.

Benoist, F., and Grand-Perret, T. (1997). Co-translational degradation of apolipoprotein B100 by the proteasome is prevented by microsomal triglyceride transfer protein. Synchronized translation studies on HepG2 cells treated with an inhibitor of microsomal triglyceride transfer protein. J Biol Chem *272*, 20435-20442.

Bernales, S., Schuck, S., and Walter, P. (2007). ER-phagy: selective autophagy of the endoplasmic reticulum. Autophagy *3*, 285-287.

Bernasconi, R., Galli, C., Calanca, V., Nakajima, T., and Molinari, M. (2010). Stringent requirement for HRD1, SEL1L, and OS-9/XTP3-B for disposal of ERAD-LS substrates. J Cell Biol *188*, 223-235.

Biederer, T., Volkwein, C., and Sommer, T. (1997). Role of Cue1p in ubiquitination and degradation at the ER surface. Science *278*, 1806-1809.

Bittencourt, M.S., and Cerci, R.J. (2015). Statin effects on atherosclerotic plaques: regression or healing? BMC Med *13*, 260.

Blanc, V., and Davidson, N.O. (2010). APOBEC-1-mediated RNA editing. Wiley Interdiscip Rev Syst Biol Med *2*, 594-602.

Blard, O., Feuillette, S., Bou, J., Chaumette, B., Frebourg, T., Campion, D., and Lecourtois, M. (2007). Cytoskeleton proteins are modulators of mutant tau-induced neurodegeneration in Drosophila. Hum Mol Genet *16*, 555-566.

Boekholdt, S.M., Hovingh, G.K., Mora, S., Arsenault, B.J., Amarenco, P., Pedersen, T.R., LaRosa, J.C., Waters, D.D., DeMicco, D.A., Simes, R.J., *et al.* (2014). Very low levels of atherogenic lipoproteins and the risk for cardiovascular events: a meta-analysis of statin trials. J Am Coll Cardiol *64*, 485-494.

Borchardt, R.A., and Davis, R.A. (1987). Intrahepatic assembly of very low density lipoproteins. Rate of transport out of the endoplasmic reticulum determines rate of secretion. J Biol Chem *262*, 16394-16402.

Boren, J., Graham, L., Wettesten, M., Scott, J., White, A., and Olofsson, S.O. (1992). The assembly and secretion of ApoB 100-containing lipoproteins in Hep G2 cells. ApoB 100 is cotranslationally integrated into lipoproteins. J Biol Chem *267*, 9858-9867.

Boren, J., Lee, I., Zhu, W., Arnold, K., Taylor, S., and Innerarity, T.L. (1998). Identification of the low density lipoprotein receptor-binding site in apolipoprotein B100 and the modulation of its binding activity by the carboxyl terminus in familial defective apo-B100. J Clin Invest *101*, 1084-1093.

Boren, J., Rustaeus, S., and Olofsson, S.O. (1994). Studies on the assembly of apolipoprotein B-100- and B-48-containing very low density lipoproteins in McA-RH7777 cells. J Biol Chem *269*, 25879-25888.

Bostrom, K., Wettesten, M., Boren, J., Bondjers, G., Wiklund, O., and Olofsson, S.O. (1986). Pulse-chase studies of the synthesis and intracellular transport of apolipoprotein B-100 in Hep G2 cells. J Biol Chem *261*, 13800-13806.

Braakman, I., and Bulleid, N.J. (2011). Protein folding and modification in the mammalian endoplasmic reticulum. Annu Rev Biochem *80*, 71-99.

Bradbury, P., Mann, C.J., Kochl, S., Anderson, T.A., Chester, S.A., Hancock, J.M., Ritchie, P.J., Amey, J., Harrison, G.B., Levitt, D.G., *et al.* (1999). A common binding site on the microsomal triglyceride transfer protein for apolipoprotein B and protein disulfide isomerase. J Biol Chem *274*, 3159-3164.

Brodsky, J.L. (1998). Translocation of proteins across the endoplasmic reticulum membrane. Int Rev Cytol *178*, 277-328.

Brodsky, J.L. (2007). The protective and destructive roles played by molecular chaperones during ERAD (endoplasmic-reticulum-associated degradation). Biochem J *404*, 353-363.

Brodsky, J.L. (2012). Cleaning up: ER-associated degradation to the rescue. Cell *151*, 1163-1167.

Brodsky, J.L., and Fisher, E.A. (2008). The many intersecting pathways underlying apolipoprotein B secretion and degradation. Trends Endocrinol Metab *19*, 254-259.

Brodsky, J.L., Gusarova, V., and Fisher, E.A. (2004). Vesicular trafficking of hepatic apolipoprotein B100 and its maturation to very low-density lipoprotein particles; studies from cells and cell-free systems. Trends Cardiovasc Med *14*, 127-132.

Brodsky, J.L., Lawrence, J.G., and Caplan, A.J. (1998). Mutations in the cytosolic DnaJ homologue, YDJ1, delay and compromise the efficient translation of heterologous proteins in yeast. Biochemistry *37*, 18045-18055.

Brown, M.S., and Goldstein, J.L. (1975). Regulation of the activity of the low density lipoprotein receptor in human fibroblasts. Cell *6*, 307-316.

Brown, M.S., and Goldstein, J.L. (1976). Receptor-mediated control of cholesterol metabolism. Science *191*, 150-154.

Brown, M.S., Herz, J., and Goldstein, J.L. (1997). LDL-receptor structure. Calcium cages, acid baths and recycling receptors. Nature *388*, 629-630.

Buck, T.M., Zeng, X., Cantrell, P.S., Cattley, R.T., Hasanbasri, Z., Yates, M.E., Nguyen, D., Yates, N.A., and Brodsky, J.L. (2020). The Capture of a Disabled Proteasome Identifies Erg25 as a Substrate for Endoplasmic Reticulum Associated Degradation. Mol Cell Proteomics *19*, 1896-1909.

Butkinaree, C., Guo, L., Ramkhelawon, B., Wanschel, A., Brodsky, J.L., Moore, K.J., and Fisher, E.A. (2014). A regulator of secretory vesicle size, Kelch-like protein 12, facilitates the secretion of apolipoprotein B100 and very-low-density lipoproteins--brief report. Arterioscler Thromb Vasc Biol *34*, 251-254.

Butler, M.G. (2010). Genetics of hypertension. Current status. J Med Liban *58*, 175-178.

Cacciagli, P., Sutera-Sardo, J., Borges-Correia, A., Roux, J.C., Dorboz, I., Desvignes, J.P., Badens, C., Delepine, M., Lathrop, M., Cau, P., *et al.* (2013). Mutations in BCAP31 cause a severe X-linked phenotype with deafness, dystonia, and central hypomyelination and disorganize the Golgi apparatus. Am J Hum Genet *93*, 579-586.

Calcutta, A., Jessen, C.M., Behrens, M.A., Oliveira, C.L., Renart, M.L., Gonzalez-Ros, J.M., Otzen, D.E., Pedersen, J.S., Malmendal, A., and Nielsen, N.C. (2012). Mapping of unfolding states of integral helical membrane proteins by GPS-NMR and scattering techniques: TFE-induced unfolding of KcsA in DDM surfactant. Biochim Biophys Acta *1818*, 2290-2301.

Cao, M., Wei, C., Zhao, L., Wang, J., Jia, Q., Wang, X., Jin, Q., and Deng, T. (2014). DnaJA1/Hsp40 is co-opted by influenza A virus to enhance its viral RNA polymerase activity. J Virol *88*, 14078-14089.

Caplan, A.J., Cyr, D.M., and Douglas, M.G. (1992a). YDJ1p facilitates polypeptide translocation across different intracellular membranes by a conserved mechanism. Cell *71*, 1143-1155.

Caplan, A.J., and Douglas, M.G. (1991). Characterization of YDJ1: a yeast homologue of the bacterial dnaJ protein. J Cell Biol *114*, 609-621.

Caplan, A.J., Tsai, J., Casey, P.J., and Douglas, M.G. (1992b). Farnesylation of YDJ1p is required for function at elevated growth temperatures in Saccharomyces cerevisiae. J Biol Chem *267*, 18890-18895.

Cardozo, C., Wu, X., Pan, M., Wang, H., and Fisher, E.A. (2002). The inhibition of microsomal triglyceride transfer protein activity in rat hepatoma cells promotes proteasomal and nonproteasomal degradation of apoprotein b100. Biochemistry *41*, 10105-10114.

Carvalho, A.F., Pinto, M.P., Grou, C.P., Alencastre, I.S., Fransen, M., Sa-Miranda, C., and Azevedo, J.E. (2007). Ubiquitination of mammalian Pex5p, the peroxisomal import receptor. J Biol Chem *282*, 31267-31272.

Carvalho, P., Stanley, A.M., and Rapoport, T.A. (2010). Retrotranslocation of a misfolded luminal ER protein by the ubiquitin-ligase Hrd1p. Cell *143*, 579-591.

Chang, Y.W., Lin, T.W., Li, Y.C., Huang, Y.S., Sun, Y.J., and Hsiao, C.D. (2012). Interaction surface and topology of Get3-Get4-Get5 protein complex, involved in targeting tail-anchored proteins to endoplasmic reticulum. J Biol Chem *287*, 4783-4789.

Chartron, J.W., Clemons, W.M., Jr., and Suloway, C.J. (2012). The complex process of GETting tail-anchored membrane proteins to the ER. Curr Opin Struct Biol *22*, 217-224.

Chen, P.F., Marcel, Y.L., Yang, C.Y., Gotto, A.M., Jr., Milne, R.W., Sparrow, J.T., and Chan, L. (1988). Primary sequence mapping of human apolipoprotein B-100 epitopes. Comparisons of trypsin accessibility and immunoreactivity and implication for apoB conformation. Eur J Biochem *175*, 111-118.

Chen, Q., Zhong, Y., Wu, Y., Liu, L., Wang, P., Liu, R., Cui, F., Li, Q., Yang, X., Fang, S., *et al.* (2016). HRD1-mediated ERAD tuning of ER-bound E2 is conserved between plants and mammals. Nat Plants *2*, 16094.

Chen, S.H., Habib, G., Yang, C.Y., Gu, Z.W., Lee, B.R., Weng, S.A., Silberman, S.R., Cai, S.J., Deslypere, J.P., Rosseneu, M., *et al.* (1987). Apolipoprotein B-48 is the product of a messenger RNA with an organ-specific in-frame stop codon. Science *238*, 363-366.

Chen, S.H., Yang, C.Y., Chen, P.F., Setzer, D., Tanimura, M., Li, W.H., Gotto, A.M., Jr., and Chan, L. (1986). The complete cDNA and amino acid sequence of human apolipoprotein B-100. J Biol Chem *261*, 12918-12921.

Chen, Y., Le Caherec, F., and Chuck, S.L. (1998). Calnexin and other factors that alter translocation affect the rapid binding of ubiquitin to apoB in the Sec61 complex. J Biol Chem *273*, 11887-11894.

Chirieac, D.V., Davidson, N.O., Sparks, C.E., and Sparks, J.D. (2006). PI3-kinase activity modulates apo B available for hepatic VLDL production in apobec-1-/- mice. Am J Physiol Gastrointest Liver Physiol *291*, G382-388.

Christiano, R., Nagaraj, N., Frohlich, F., and Walther, T.C. (2014). Global proteome turnover analyses of the Yeasts S. cerevisiae and S. pombe. Cell Rep *9*, 1959-1965.

Christianson, J.C., Olzmann, J.A., Shaler, T.A., Sowa, M.E., Bennett, E.J., Richter, C.M., Tyler, R.E., Greenblatt, E.J., Harper, J.W., and Kopito, R.R. (2011). Defining human ERAD networks through an integrative mapping strategy. Nat Cell Biol *14*, 93-105.

Christianson, J.C., and Ye, Y. (2014). Cleaning up in the endoplasmic reticulum: ubiquitin in charge. Nat Struct Mol Biol *21*, 325-335.

Chua, N.K., Coates, H.W., and Brown, A.J. (2020). Squalene monooxygenase: a journey to the heart of cholesterol synthesis. Prog Lipid Res, 101033.

Chua, N.K., Hart-Smith, G., and Brown, A.J. (2019a). Non-canonical ubiquitination of the cholesterol-regulated degron of squalene monooxygenase. J Biol Chem *294*, 8134-8147.

Chua, N.K., Scott, N.A., and Brown, A.J. (2019b). Valosin-containing protein mediates the ERAD of squalene monooxygenase and its cholesterol-responsive degron. Biochem J *476*, 2545-2560.

Chuck, S.L., and Lingappa, V.R. (1992). Pause transfer: a topogenic sequence in apolipoprotein B mediates stopping and restarting of translocation. Cell *68*, 9-21.

Chuck, S.L., Yao, Z., Blackhart, B.D., McCarthy, B.J., and Lingappa, V.R. (1990). New variation on the translocation of proteins during early biogenesis of apolipoprotein B. Nature *346*, 382-385.

Cladaras, C., Hadzopoulou-Cladaras, M., Nolte, R.T., Atkinson, D., and Zannis, V.I. (1986). The complete sequence and structural analysis of human apolipoprotein B-100: relationship between apoB-100 and apoB-48 forms. EMBO J *5*, 3495-3507.

Collins, D.R., Knott, T.J., Pease, R.J., Powell, L.M., Wallis, S.C., Robertson, S., Pullinger, C.R., Milne, R.W., Marcel, Y.L., Humphries, S.E., *et al.* (1988). Truncated variants of apolipoprotein B cause hypobetalipoproteinaemia. Nucleic Acids Res *16*, 8361-8375.

Conticello, S.G. (2008). The AID/APOBEC family of nucleic acid mutators. Genome Biol *9*, 229.

Costanzo, M.C., Crawford, M.E., Hirschman, J.E., Kranz, J.E., Olsen, P., Robertson, L.S., Skrzypek, M.S., Braun, B.R., Hopkins, K.L., Kondu, P., *et al.* (2001). YPD, PombePD and WormPD: model organism volumes of the BioKnowledge library, an integrated resource for protein information. Nucleic Acids Res *29*, 75-79.

Craig, E.A., and Marszalek, J. (2017). How Do J-Proteins Get Hsp70 to Do So Many Different Things? Trends Biochem Sci *42*, 355-368.

Crimaudo, C., Hortsch, M., Gausepohl, H., and Meyer, D.I. (1987). Human ribophorins I and II: the primary structure and membrane topology of two highly conserved rough endoplasmic reticulum-specific glycoproteins. EMBO J *6*, 75-82.

Crooke, R.M., Graham, M.J., Lemonidis, K.M., Whipple, C.P., Koo, S., and Perera, R.J. (2005). An apolipoprotein B antisense oligonucleotide lowers LDL cholesterol in hyperlipidemic mice without causing hepatic steatosis. J Lipid Res *46*, 872-884.

Cyr, D.M. (1995). Cooperation of the molecular chaperone Ydj1 with specific Hsp70 homologs to suppress protein aggregation. FEBS Lett *359*, 129-132.

Cyr, D.M., and Douglas, M.G. (1994). Differential regulation of Hsp70 subfamilies by the eukaryotic DnaJ homologue YDJ1. J Biol Chem *269*, 9798-9804.

Cyr, D.M., Lu, X., and Douglas, M.G. (1992). Regulation of Hsp70 function by a eukaryotic DnaJ homolog. J Biol Chem *267*, 20927-20931.

Dadu, R.T., and Ballantyne, C.M. (2014). Lipid lowering with PCSK9 inhibitors. Nat Rev Cardiol *11*, 563-575.

Daida, H., Dohi, T., Fukushima, Y., Ohmura, H., and Miyauchi, K. (2019). The Goal of Achieving Atherosclerotic Plaque Regression with Lipid-Lowering Therapy: Insights from IVUS Trials. J Atheroscler Thromb *26*, 592-600.

De Loof, H., Rosseneu, M., Yang, C.Y., Li, W.H., Gotto, A.M., Jr., and Chan, L. (1987). Human apolipoprotein B: analysis of internal repeats and homology with other apolipoproteins. J Lipid Res *28*, 1455-1465.

De Mattos, E.P., Wentink, A., Nussbaum-Krammer, C., Hansen, C., Bergink, S., Melki, R., and Kampinga, H.H. (2020). Protein Quality Control Pathways at the Crossroad of Synucleinopathies. J Parkinsons Dis *10*, 369-382.

de Virgilio, M., Weninger, H., and Ivessa, N.E. (1998). Ubiquitination is required for the retro-translocation of a short-lived luminal endoplasmic reticulum glycoprotein to the cytosol for degradation by the proteasome. J Biol Chem *273*, 9734-9743.

Deane, C.A., and Brown, I.R. (2017). Components of a mammalian protein disaggregation/refolding machine are targeted to nuclear speckles following thermal stress in differentiated human neuronal cells. Cell Stress Chaperones *22*, 191-200.

DeBose-Boyd, R.A. (2008). Feedback regulation of cholesterol synthesis: sterol-accelerated ubiquitination and degradation of HMG CoA reductase. Cell Res *18*, 609-621.

Dekker, S.L., Kampinga, H.H., and Bergink, S. (2015). DNAJs: more than substrate delivery to HSPA. Front Mol Biosci *2*, 35.

den Brave, F., Cairo, L.V., Jagadeesan, C., Ruger-Herreros, C., Mogk, A., Bukau, B., and Jentsch, S. (2020). Chaperone-Mediated Protein Disaggregation Triggers Proteolytic Clearance of Intra-nuclear Protein Inclusions. Cell Rep *31*, 107680.

Di Leo, E., Lancellotti, S., Penacchioni, J.Y., Cefalu, A.B., Averna, M., Pisciotta, L., Bertolini, S., Calandra, S., Gabelli, C., and Tarugi, P. (2005). Mutations in MTP gene in abeta- and hypobeta-lipoproteinemia. Atherosclerosis *180*, 311-318.

Djousse, L., Hunt, S.C., Arnett, D.K., Province, M.A., Eckfeldt, J.H., and Ellison, R.C. (2003). Dietary linolenic acid is inversely associated with plasma triacylglycerol: the National Heart, Lung, and Blood Institute Family Heart Study. Am J Clin Nutr *78*, 1098-1102.

Doonan, L.M., Fisher, E.A., and Brodsky, J.L. (2018). Can modulators of apolipoproteinB biogenesis serve as an alternate target for cholesterol-lowering drugs? Biochim Biophys Acta Mol Cell Biol Lipids *1863*, 762-771.

Doonan, L.M., Guerriero, C.J., Preston, G.M., Buck, T.M., Khazanov, N., Fisher, E.A., Senderowitz, H., and Brodsky, J.L. (2019). Hsp104 facilitates the endoplasmic-reticulum-associated degradation of disease-associated and aggregation-prone substrates. Protein Sci *28*, 1290-1306.

Dubiel, W., Dubiel, D., Wolf, D.A., and Naumann, M. (2018). Cullin 3-Based Ubiquitin Ligases as Master Regulators of Mammalian Cell Differentiation. Trends Biochem Sci *43*, 95-107.

Elsabrouty, R., Jo, Y., Dinh, T.T., and DeBose-Boyd, R.A. (2013). Sterol-induced dislocation of 3-hydroxy-3-methylglutaryl coenzyme A reductase from membranes of permeabilized cells. Mol Biol Cell *24*, 3300-3308.

Enns, G.M., Shashi, V., Bainbridge, M., Gambello, M.J., Zahir, F.R., Bast, T., Crimian, R., Schoch, K., Platt, J., Cox, R., *et al.* (2014). Mutations in NGLY1 cause an inherited disorder of the endoplasmic reticulum-associated degradation pathway. Genet Med *16*, 751-758.

Estabrooks, S., and Brodsky, J.L. (2020). Regulation of CFTR Biogenesis by the Proteostatic Network and Pharmacological Modulators. Int J Mol Sci *21*.

Fan, C.Y., Lee, S., and Cyr, D.M. (2003). Mechanisms for regulation of Hsp70 function by Hsp40. Cell Stress Chaperones *8*, 309-316.

Fang, S., Ferrone, M., Yang, C., Jensen, J.P., Tiwari, S., and Weissman, A.M. (2001). The tumor autocrine motility factor receptor, gp78, is a ubiquitin protein ligase implicated in degradation from the endoplasmic reticulum. Proc Natl Acad Sci U S A *98*, 14422-14427.

Farinha, C.M., Nogueira, P., Mendes, F., Penque, D., and Amaral, M.D. (2002). The human DnaJ homologue (Hdj)-1/heat-shock protein (Hsp) 40 co-chaperone is required for the in vivo stabilization of the cystic fibrosis transmembrane conductance regulator by Hsp70. Biochem J *366*, 797-806.

Faust, O., Abayev-Avraham, M., Wentink, A.S., Maurer, M., Nillegoda, N.B., London, N., Bukau, B., and Rosenzweig, R. (2020). HSP40 proteins use class-specific regulation to drive HSP70 functional diversity. Nature *587*, 489-494.

Fernandez-Higuero, J.A., Etxebarria, A., Benito-Vicente, A., Alves, A.C., Arrondo, J.L., Ostolaza, H., Bourbon, M., and Martin, C. (2015). Structural analysis of APOB variants, p.(Arg3527Gln), p.(Arg1164Thr) and p.(Gln4494del), causing Familial Hypercholesterolaemia provides novel insights into variant pathogenicity. Sci Rep *5*, 18184.

Ferro-Novick, S., Reggiori, F., and Brodsky, J.L. (2021). ER-Phagy, ER Homeostasis, and ER Quality Control: Implications for Disease. Trends Biochem Sci.

Fisher, E.A., and Ginsberg, H.N. (2002). Complexity in the secretory pathway: the assembly and secretion of apolipoprotein B-containing lipoproteins. J Biol Chem *277*, 17377-17380.

Fisher, E.A., Khanna, N.A., and McLeod, R.S. (2011). Ubiquitination regulates the assembly of VLDL in HepG2 cells and is the committing step of the apoB-100 ERAD pathway. J Lipid Res *52*, 1170-1180.

Fisher, E.A., Lapierre, L.R., Junkins, R.D., and McLeod, R.S. (2008). The AAA-ATPase p97 facilitates degradation of apolipoprotein B by the ubiquitin-proteasome pathway. J Lipid Res *49*, 2149-2160.

Fisher, E.A., Pan, M., Chen, X., Wu, X., Wang, H., Jamil, H., Sparks, J.D., and Williams, K.J. (2001). The triple threat to nascent apolipoprotein B. Evidence for multiple, distinct degradative pathways. J Biol Chem *276*, 27855-27863.

Fisher, E.A., and Williams, K.J. (2008). Autophagy of an oxidized, aggregated protein beyond the ER: a pathway for remarkably late-stage quality control. Autophagy *4*, 721-723.

Fisher, E.A., Zhou, M., Mitchell, D.M., Wu, X., Omura, S., Wang, H., Goldberg, A.L., and Ginsberg, H.N. (1997). The degradation of apolipoprotein B100 is mediated by the ubiquitin-proteasome pathway and involves heat shock protein 70. J Biol Chem *272*, 20427-20434.

Foresti, O., Ruggiano, A., Hannibal-Bach, H.K., Ejsing, C.S., and Carvalho, P. (2013). Sterol homeostasis requires regulated degradation of squalene monooxygenase by the ubiquitin ligase Doa10/Teb4. Elife *2*, e00953.

Fryer, L.G., Jones, B., Duncan, E.J., Hutchison, C.E., Ozkan, T., Williams, P.A., Alder, O., Nieuwdorp, M., Townley, A.K., Mensenkamp, A.R., *et al.* (2014). The endoplasmic reticulum coat protein II transport machinery coordinates cellular lipid secretion and cholesterol biosynthesis. J Biol Chem *289*, 4244-4261.

Funato, K., Riezman, H., and Muniz, M. (2020). Vesicular and non-vesicular lipid export from the ER to the secretory pathway. Biochim Biophys Acta Mol Cell Biol Lipids *1865*, 158453.

Gaczynska, M., and Osmulski, P.A. (2005). Small-molecule inhibitors of proteasome activity. Methods Mol Biol *301*, 3-22.

Galeone, A., Adams, J.M., Matsuda, S., Presa, M.F., Pandey, A., Han, S.Y., Tachida, Y., Hirayama, H., Vaccari, T., Suzuki, T., *et al.* (2020). Regulation of BMP4/Dpp retrotranslocation and signaling by deglycosylation. Elife *9*.

Gao, X., Carroni, M., Nussbaum-Krammer, C., Mogk, A., Nillegoda, N.B., Szlachcic, A., Guilbride, D.L., Saibil, H.R., Mayer, M.P., and Bukau, B. (2015). Human Hsp70 Disaggregase Reverses Parkinson's-Linked alpha-Synuclein Amyloid Fibrils. Mol Cell *59*, 781-793.

Gardner, R.G., Swarbrick, G.M., Bays, N.W., Cronin, S.R., Wilhovsky, S., Seelig, L., Kim, C., and Hampton, R.Y. (2000). Endoplasmic reticulum degradation requires lumen to cytosol signaling. Transmembrane control of Hrd1p by Hrd3p. J Cell Biol *151*, 69-82.

Ghaemmaghami, S., Huh, W.K., Bower, K., Howson, R.W., Belle, A., Dephoure, N., O'Shea, E.K., and Weissman, J.S. (2003). Global analysis of protein expression in yeast. Nature *425*, 737-741.

Gill, S., Stevenson, J., Kristiana, I., and Brown, A.J. (2011). Cholesterol-dependent degradation of squalene monooxygenase, a control point in cholesterol synthesis beyond HMG-CoA reductase. Cell Metab *13*, 260-273.

Ginsberg, H.N. (1997). Role of lipid synthesis, chaperone proteins and proteasomes in the assembly and secretion of apoprotein B-containing lipoproteins from cultured liver cells. Clin Exp Pharmacol Physiol *24*, A29-32.

Goldstein, J.L., and Brown, M.S. (1990). Regulation of the mevalonate pathway. Nature *343*, 425-430.

Goldstein, J.L., and Brown, M.S. (2015). A century of cholesterol and coronaries: from plaques to genes to statins. Cell *161*, 161-172.

Gordon, D.A., Jamil, H., Gregg, R.E., Olofsson, S.O., and Boren, J. (1996). Inhibition of the microsomal triglyceride transfer protein blocks the first step of apolipoprotein B lipoprotein assembly but not the addition of bulk core lipids in the second step. J Biol Chem *271*, 33047-33053.

Grove, D.E., Fan, C.Y., Ren, H.Y., and Cyr, D.M. (2011). The endoplasmic reticulum-associated Hsp40 DNAJB12 and Hsc70 cooperate to facilitate RMA1 E3-dependent degradation of nascent CFTRDeltaF508. Mol Biol Cell *22*, 301-314.

Grubb, S., Guo, L., Fisher, E.A., and Brodsky, J.L. (2012). Protein disulfide isomerases contribute differentially to the endoplasmic reticulum-associated degradation of apolipoprotein B and other substrates. Mol Biol Cell *23*, 520-532.

Guerriero, C.J., and Brodsky, J.L. (2012). The delicate balance between secreted protein folding and endoplasmic reticulum-associated degradation in human physiology. Physiol Rev *92*, 537-576.

Guerriero, C.J., Reutter, K.R., Augustine, A.A., Preston, G.M., Weiberth, K.F., Mackie, T.D., Cleveland-Rubeor, H.C., Bethel, N.P., Callenberg, K.M., Nakatsukasa, K., *et al.* (2017). Transmembrane helix hydrophobicity is an energetic barrier during the retrotranslocation of integral membrane ERAD substrates. Mol Biol Cell *28*, 2076-2090.

Guerriero, C.J., Weiberth, K.F., and Brodsky, J.L. (2013). Hsp70 targets a cytoplasmic quality control substrate to the San1p ubiquitin ligase. J Biol Chem *288*, 18506-18520.

Gusarova, V., Brodsky, J.L., and Fisher, E.A. (2003). Apolipoprotein B100 exit from the endoplasmic reticulum (ER) is COPII-dependent, and its lipidation to very low density lipoprotein occurs post-ER. J Biol Chem *278*, 48051-48058.

Gusarova, V., Caplan, A.J., Brodsky, J.L., and Fisher, E.A. (2001). Apoprotein B degradation is promoted by the molecular chaperones hsp90 and hsp70. J Biol Chem *276*, 24891-24900.

Gusarova, V., Seo, J., Sullivan, M.L., Watkins, S.C., Brodsky, J.L., and Fisher, E.A. (2007). Golgi-associated maturation of very low density lipoproteins involves conformational changes in apolipoprotein B, but is not dependent on apolipoprotein E. J Biol Chem *282*, 19453-19462.

Hageman, J., and Kampinga, H.H. (2009). Computational analysis of the human HSPH/HSPA/DNAJ family and cloning of a human HSPH/HSPA/DNAJ expression library. Cell Stress Chaperones *14*, 1-21.

Hageman, J., Rujano, M.A., van Waarde, M.A., Kakkar, V., Dirks, R.P., Govorukhina, N., Oosterveld-Hut, H.M., Lubsen, N.H., and Kampinga, H.H. (2010). A DNAJB chaperone subfamily with HDAC-dependent activities suppresses toxic protein aggregation. Mol Cell *37*, 355-369.

Hamilton, R.L. (1972). Synthesis and secretion of plasma lipoproteins. Adv Exp Med Biol *26*, 7-24.

Hampton, R.Y., Gardner, R.G., and Rine, J. (1996). Role of 26S proteasome and HRD genes in the degradation of 3-hydroxy-3-methylglutaryl-CoA reductase, an integral endoplasmic reticulum membrane protein. Mol Biol Cell *7*, 2029-2044.

Hampton, R.Y., and Rine, J. (1994). Regulated degradation of HMG-CoA reductase, an integral membrane protein of the endoplasmic reticulum, in yeast. J Cell Biol *125*, 299-312.

Han, S., Liu, Y., and Chang, A. (2007). Cytoplasmic Hsp70 promotes ubiquitination for endoplasmic reticulum-associated degradation of a misfolded mutant of the yeast plasma membrane ATPase, PMA1. J Biol Chem *282*, 26140-26149.

Han, S.T., Rab, A., Pellicore, M.J., Davis, E.F., McCague, A.F., Evans, T.A., Joynt, A.T., Lu, Z., Cai, Z., Raraigh, K.S., *et al.* (2018). Residual function of cystic fibrosis mutants predicts response to small molecule CFTR modulators. JCI Insight *3*.

Harazono, A., Kawasaki, N., Kawanishi, T., and Hayakawa, T. (2005). Site-specific glycosylation analysis of human apolipoprotein B100 using LC/ESI MS/MS. Glycobiology *15*, 447-462.

Harris, W.S. (1989). Fish oils and plasma lipid and lipoprotein metabolism in humans: a critical review. J Lipid Res *30*, 785-807.

Havel, R.J. (1975). Lipoproteins and lipid transport. Adv Exp Med Biol *63*, 37-59.

Havel, R.J., Eder, H.A., and Bragdon, J.H. (1955). The distribution and chemical composition of ultracentrifugally separated lipoproteins in human serum. J Clin Invest *34*, 1345-1353.

Heinemeyer, T., Stemmet, M., Bardien, S., and Neethling, A. (2019). Underappreciated Roles of the Translocase of the Outer and Inner Mitochondrial Membrane Protein Complexes in Human Disease. DNA Cell Biol *38*, 23-40.

Heron, M. (2017). Deaths: Leading Causes for 2015. Natl Vital Stat Rep *66*, 1-76.

Hirsch, C., Blom, D., and Ploegh, H.L. (2003). A role for N-glycanase in the cytosolic turnover of glycoproteins. EMBO J *22*, 1036-1046.

Hitchcock, A.L., Auld, K., Gygi, S.P., and Silver, P.A. (2003). A subset of membrane-associated proteins is ubiquitinated in response to mutations in the endoplasmic reticulum degradation machinery. Proc Natl Acad Sci U S A *100*, 12735-12740.

Hobbs, H.H., Brown, M.S., and Goldstein, J.L. (1992). Molecular genetics of the LDL receptor gene in familial hypercholesterolemia. Hum Mutat *1*, 445-466.

Hoe, K.L., Won, M., Chung, K.S., Jang, Y.J., Lee, S.B., Kim, D.U., Lee, J.W., Yun, J.H., and Yoo, H.S. (1998). Isolation of a new member of DnaJ-like heat shock protein 40 (Hsp40) from human liver. Biochim Biophys Acta *1383*, 4-8.

Holden, P., and Horton, W.A. (2009). Crude subcellular fractionation of cultured mammalian cell lines. BMC Res Notes *2*, 243.

Hrizo, S.L., Gusarova, V., Habiel, D.M., Goeckeler, J.L., Fisher, E.A., and Brodsky, J.L. (2007). The Hsp110 molecular chaperone stabilizes apolipoprotein B from endoplasmic reticulum-associated degradation (ERAD). J Biol Chem *282*, 32665-32675.

Huang, L.S., Ripps, M.E., Korman, S.H., Deckelbaum, R.J., and Breslow, J.L. (1989). Hypobetalipoproteinemia due to an apolipoprotein B gene exon 21 deletion derived by Alu-Alu recombination. J Biol Chem *264*, 11394-11400.

Hughes, E.A., Hammond, C., and Cresswell, P. (1997). Misfolded major histocompatibility complex class I heavy chains are translocated into the cytoplasm and degraded by the proteasome. Proc Natl Acad Sci U S A *94*, 1896-1901.

Hussain, M.M., Bakillah, A., and Jamil, H. (1997). Apolipoprotein B binding to microsomal triglyceride transfer protein decreases with increases in length and lipidation: implications in lipoprotein biosynthesis. Biochemistry *36*, 13060-13067.

Hussain, M.M., Fatma, S., Pan, X., and Iqbal, J. (2005). Intestinal lipoprotein assembly. Curr Opin Lipidol *16*, 281-285.

Hussain, M.M., Iqbal, J., Anwar, K., Rava, P., and Dai, K. (2003a). Microsomal triglyceride transfer protein: a multifunctional protein. Front Biosci *8*, s500-506.

Hussain, M.M., Kancha, R.K., Zhou, Z., Luchoomun, J., Zu, H., and Bakillah, A. (1996). Chylomicron assembly and catabolism: role of apolipoproteins and receptors. Biochim Biophys Acta *1300*, 151-170.

Hussain, M.M., Shi, J., and Dreizen, P. (2003b). Microsomal triglyceride transfer protein and its role in apoB-lipoprotein assembly. J Lipid Res *44*, 22-32.

Huyer, G., Piluek, W.F., Fansler, Z., Kreft, S.G., Hochstrasser, M., Brodsky, J.L., and Michaelis, S. (2004). Distinct machinery is required in Saccharomyces cerevisiae for the endoplasmic reticulum-associated degradation of a multispanning membrane protein and a soluble luminal protein. J Biol Chem *279*, 38369-38378.

Ikeda, Y., Demartino, G.N., Brown, M.S., Lee, J.N., Goldstein, J.L., and Ye, J. (2009). Regulated endoplasmic reticulum-associated degradation of a polytopic protein: p97 recruits proteasomes to Insig-1 before extraction from membranes. J Biol Chem *284*, 34889-34900.

Inoue, S., Bar-Nun, S., Roitelman, J., and Simoni, R.D. (1991). Inhibition of degradation of 3-hydroxy-3-methylglutaryl-coenzyme A reductase in vivo by cysteine protease inhibitors. J Biol Chem *266*, 13311-13317.

Insull, W., Jr. (2009). The pathology of atherosclerosis: plaque development and plaque responses to medical treatment. Am J Med *122*, S3-S14.

Ireland, A.W., Gobillot, T.A., Gupta, T., Seguin, S.P., Liang, M., Resnick, L., Goldberg, M.T., Manos-Turvey, A., Pipas, J.M., Wipf, P., *et al.* (2014). Synthesis and structure-activity relationships of small molecule inhibitors of the simian virus 40 T antigen oncoprotein, an anti-polyomaviral target. Bioorg Med Chem *22*, 6490-6502.

Ishikura, S., Weissman, A.M., and Bonifacino, J.S. (2010). Serine residues in the cytosolic tail of the T-cell antigen receptor alpha-chain mediate ubiquitination and endoplasmic reticulum-associated degradation of the unassembled protein. J Biol Chem *285*, 23916-23924.

Jacquemyn, J., Cascalho, A., and Goodchild, R.E. (2017). The ins and outs of endoplasmic reticulum-controlled lipid biosynthesis. EMBO Rep *18*, 1905-1921.

Jaenicke, L.A., Brendebach, H., Selbach, M., and Hirsch, C. (2011). Yos9p assists in the degradation of certain nonglycosylated proteins from the endoplasmic reticulum. Mol Biol Cell *22*, 2937-2945.

Jamil, H., Gordon, D.A., Eustice, D.C., Brooks, C.M., Dickson, J.K., Jr., Chen, Y., Ricci, B., Chu, C.H., Harrity, T.W., Ciosek, C.P., Jr., *et al.* (1996). An inhibitor of the microsomal triglyceride transfer protein inhibits apoB secretion from HepG2 cells. Proc Natl Acad Sci U S A *93*, 11991-11995.

Jang, A.Y., Han, S.H., Sohn, I.S., Oh, P.C., and Koh, K.K. (2020). Lipoprotein(a) and Cardiovascular Diseases- Revisited. Circ J.

Jansson, S.E. (1970). Cytoplasmic distribution of endogenous and exogenous 5-hydroxytryptamine in rat peritoneal mast cells. Acta Physiol Scand *80*, 345-352.

Jiang, Y., Rossi, P., and Kalodimos, C.G. (2019). Structural basis for client recognition and activity of Hsp40 chaperones. Science *365*, 1313-1319.

Jin, L., Pahuja, K.B., Wickliffe, K.E., Gorur, A., Baumgartel, C., Schekman, R., and Rape, M. (2012). Ubiquitin-dependent regulation of COPII coat size and function. Nature *482*, 495-500.

Jo, Y., and Debose-Boyd, R.A. (2010). Control of cholesterol synthesis through regulated ER-associated degradation of HMG CoA reductase. Crit Rev Biochem Mol Biol *45*, 185-198.

Jo, Y., Lee, P.C., Sguigna, P.V., and DeBose-Boyd, R.A. (2011a). Sterol-induced degradation of HMG CoA reductase depends on interplay of two Insigs and two ubiquitin ligases, gp78 and Trc8. Proc Natl Acad Sci U S A *108*, 20503-20508.

Jo, Y., Sguigna, P.V., and DeBose-Boyd, R.A. (2011b). Membrane-associated ubiquitin ligase complex containing gp78 mediates sterol-accelerated degradation of 3-hydroxy-3-methylglutaryl-coenzyme A reductase. J Biol Chem *286*, 15022-15031.

Johs, A., Hammel, M., Waldner, I., May, R.P., Laggner, P., and Prassl, R. (2006). Modular structure of solubilized human apolipoprotein B-100. Low resolution model revealed by small angle neutron scattering. J Biol Chem *281*, 19732-19739.

Kamitani, T., Kito, K., Nguyen, H.P., and Yeh, E.T. (1997). Characterization of NEDD8, a developmentally down-regulated ubiquitin-like protein. J Biol Chem *272*, 28557-28562.

Kampinga, H.H., Andreasson, C., Barducci, A., Cheetham, M.E., Cyr, D., Emanuelsson, C., Genevaux, P., Gestwicki, J.E., Goloubinoff, P., Huerta-Cepas, J., *et al.* (2019). Function, evolution, and structure of J-domain proteins. Cell Stress Chaperones *24*, 7-15.

Kampinga, H.H., and Craig, E.A. (2010). The HSP70 chaperone machinery: J proteins as drivers of functional specificity. Nat Rev Mol Cell Biol *11*, 579-592.

Kanapin, A., Batalov, S., Davis, M.J., Gough, J., Grimmond, S., Kawaji, H., Magrane, M., Matsuda, H., Schonbach, C., Teasdale, R.D., *et al.* (2003). Mouse proteome analysis. Genome Res *13*, 1335-1344.

Kario, E., Tirosh, B., Ploegh, H.L., and Navon, A. (2008). N-linked glycosylation does not impair proteasomal degradation but affects class I major histocompatibility complex presentation. J Biol Chem *283*, 244-254.

Katiyar, S., Joshi, S., and Lennarz, W.J. (2005). The retrotranslocation protein Derlin-1 binds peptide:N-glycanase to the endoplasmic reticulum. Mol Biol Cell *16*, 4584-4594.

Khan, M.T., and Joseph, S.K. (2003). Proteolysis of type I inositol 1,4,5-trisphosphate receptor in WB rat liver cells. Biochem J *375*, 603-611.

Khavandi, M., Duarte, F., Ginsberg, H.N., and Reyes-Soffer, G. (2017). Treatment of Dyslipidemias to Prevent Cardiovascular Disease in Patients with Type 2 Diabetes. Curr Cardiol Rep *19*, 7.

Kikkert, M., Doolman, R., Dai, M., Avner, R., Hassink, G., van Voorden, S., Thanedar, S., Roitelman, J., Chau, V., and Wiertz, E. (2004). Human HRD1 is an E3 ubiquitin ligase involved in degradation of proteins from the endoplasmic reticulum. J Biol Chem *279*, 3525-3534.

Kirstein, J., Arnsburg, K., Scior, A., Szlachcic, A., Guilbride, D.L., Morimoto, R.I., Bukau, B., and Nillegoda, N.B. (2017). In vivo properties of the disaggregase function of J-proteins and Hsc70 in Caenorhabditis elegans stress and aging. Aging Cell *16*, 1414-1424.

Kityk, R., Kopp, J., and Mayer, M.P. (2018). Molecular Mechanism of J-Domain-Triggered ATP Hydrolysis by Hsp70 Chaperones. Mol Cell *69*, 227-237 e224.

Knott, T.J., Rall, S.C., Jr., Innerarity, T.L., Jacobson, S.F., Urdea, M.S., Levy-Wilson, B., Powell, L.M., Pease, R.J., Eddy, R., Nakai, H., *et al.* (1985). Human apolipoprotein B: structure of carboxyl-terminal domains, sites of gene expression, and chromosomal localization. Science *230*, 37-43.

Koishi, M., Hosokawa, N., Sato, M., Nakai, A., Hirayoshi, K., Hiraoka, M., Abe, M., and Nagata, K. (1992). Quercetin, an inhibitor of heat shock protein synthesis, inhibits the acquisition of thermotolerance in a human colon carcinoma cell line. Jpn J Cancer Res *83*, 1216-1222.

Krul, E.S., Parhofer, K.G., Barrett, P.H., Wagner, R.D., and Schonfeld, G. (1992). ApoB-75, a truncation of apolipoprotein B associated with familial hypobetalipoproteinemia: genetic and kinetic studies. J Lipid Res *33*, 1037-1050.

Kuhlbrandt, W. (2004). Biology, structure and mechanism of P-type ATPases. Nat Rev Mol Cell Biol *5*, 282-295.

Kuo, Y., Ren, S., Lao, U., Edgar, B.A., and Wang, T. (2013). Suppression of polyglutamine protein toxicity by co-expression of a heat-shock protein 40 and a heat-shock protein 110. Cell Death Dis *4*, e833.

Kupper, N., Ge, D., Treiber, F.A., and Snieder, H. (2006). Emergence of novel genetic effects on blood pressure and hemodynamics in adolescence: the Georgia Cardiovascular Twin Study. Hypertension *47*, 948-954.

Kwiterovich, P.O., Jr. (2000). The metabolic pathways of high-density lipoprotein, low-density lipoprotein, and triglycerides: a current review. Am J Cardiol *86*, 5L-10L.

Lambert, G., Becker, B., Schreiber, R., Boucherot, A., Reth, M., and Kunzelmann, K. (2001). Control of cystic fibrosis transmembrane conductance regulator expression by BAP31. J Biol Chem *276*, 20340-20345.

Lan, Q., Li, Y., Wang, F., Li, Z., Gao, Y., Lu, H., Wang, Y., Zhao, Z., Deng, Z., He, F., *et al.* (2021). Deubiquitinase Ubp3 enhances the proteasomal degradation of key enzymes in sterol homeostasis. J Biol Chem, 100348.

Larsen, L.E., Stoekenbroek, R.M., Kastelein, J.J.P., and Holleboom, A.G. (2019). Moving Targets: Recent Advances in Lipid-Lowering Therapies. Arterioscler Thromb Vasc Biol *39*, 349-359.

Law, A., and Scott, J. (1990). A cross-species comparison of the apolipoprotein B domain that binds to the LDL receptor. J Lipid Res *31*, 1109-1120.

Lecureux, L.W., and Wattenberg, B.W. (1994). The regulated degradation of a 3-hydroxy-3-methylglutaryl-coenzyme A reductase reporter construct occurs in the endoplasmic reticulum. J Cell Sci *107 (Pt 9)*, 2635-2642.

Leiper, J.M., Bayliss, J.D., Pease, R.J., Brett, D.J., Scott, J., and Shoulders, C.C. (1994). Microsomal triglyceride transfer protein, the abetalipoproteinemia gene product, mediates the secretion of apolipoprotein B-containing lipoproteins from heterologous cells. J Biol Chem *269*, 21951-21954.

Leon, S., and Subramani, S. (2007). A conserved cysteine residue of Pichia pastoris Pex20p is essential for its recycling from the peroxisome to the cytosol. J Biol Chem *282*, 7424-7430.

Leung, G.K., Veniant, M.M., Kim, S.K., Zlot, C.H., Raabe, M., Bjorkegren, J., Neese, R.A., Hellerstein, M.K., and Young, S.G. (2000). A deficiency of microsomal triglyceride transfer protein reduces apolipoprotein B secretion. J Biol Chem *275*, 7515-7520.

Li, W., Bengtson, M.H., Ulbrich, A., Matsuda, A., Reddy, V.A., Orth, A., Chanda, S.K., Batalov, S., and Joazeiro, C.A. (2008). Genome-wide and functional annotation of human E3 ubiquitin ligases identifies MULAN, a mitochondrial E3 that regulates the organelle's dynamics and signaling. PLoS One *3*, e1487.

Liang, J.S., Kim, T., Fang, S., Yamaguchi, J., Weissman, A.M., Fisher, E.A., and Ginsberg, H.N. (2003). Overexpression of the tumor autocrine motility factor receptor Gp78, a ubiquitin protein ligase, results in increased ubiquitinylation and decreased secretion of apolipoprotein B100 in HepG2 cells. J Biol Chem *278*, 23984-23988.

Liang, S., Wu, X., Fisher, E.A., and Ginsberg, H.N. (2000). The amino-terminal domain of apolipoprotein B does not undergo retrograde translocation from the endoplasmic reticulum to the cytosol. Proteasomal degradation of nascent apolipoprotein B begins at the carboxyl terminus of the protein, while apolipoprotein B is still in its original translocon. J Biol Chem *275*, 32003-32010.

Liao, W., Hui, T.Y., Young, S.G., and Davis, R.A. (2003). Blocking microsomal triglyceride transfer protein interferes with apoB secretion without causing retention or stress in the ER. J Lipid Res *44*, 978-985.

Liao, W., Yeung, S.C., and Chan, L. (1998). Proteasome-mediated degradation of apolipoprotein B targets both nascent peptides cotranslationally before translocation and full-length apolipoprotein B after translocation into the endoplasmic reticulum. J Biol Chem *273*, 27225-27230.

Libby, P., Buring, J.E., Badimon, L., Hansson, G.K., Deanfield, J., Bittencourt, M.S., Tokgozoglu, L., and Lewis, E.F. (2019). Atherosclerosis. Nat Rev Dis Primers *5*, 56.

Libby, P., and Everett, B.M. (2019). Novel Antiatherosclerotic Therapies. Arterioscler Thromb Vasc Biol *39*, 538-545.

Lilley, B.N., and Ploegh, H.L. (2005). Multiprotein complexes that link dislocation, ubiquitination, and extraction of misfolded proteins from the endoplasmic reticulum membrane. Proc Natl Acad Sci U S A *102*, 14296-14301.

Linton, M.F., Farese, R.V., Jr., and Young, S.G. (1993). Familial hypobetalipoproteinemia. J Lipid Res *34*, 521-541.

Linton, M.R.F., Yancey, P.G., Davies, S.S., Jerome, W.G., Linton, E.F., Song, W.L., Doran, A.C., and Vickers, K.C. (2000). The Role of Lipids and Lipoproteins in Atherosclerosis. In Endotext, K.R. Feingold, B. Anawalt, A. Boyce, G. Chrousos, W.W. de Herder, K. Dhatariya, K. Dungan, A. Grossman, J.M. Hershman, J. Hofland, *et al.*, eds. (South Dartmouth (MA)).

Liou, S.T., Cheng, M.Y., and Wang, C. (2007). SGT2 and MDY2 interact with molecular chaperone YDJ1 in Saccharomyces cerevisiae. Cell Stress Chaperones *12*, 59-70.

Lu, H., Zhou, Q., He, J., Jiang, Z., Peng, C., Tong, R., and Shi, J. (2020). Recent advances in the development of protein-protein interactions modulators: mechanisms and clinical trials. Signal Transduct Target Ther *5*, 213.

Lu, J.P., Wang, Y., Sliter, D.A., Pearce, M.M., and Wojcikiewicz, R.J. (2011). RNF170 protein, an endoplasmic reticulum membrane ubiquitin ligase, mediates inositol 1,4,5-trisphosphate receptor ubiquitination and degradation. J Biol Chem *286*, 24426-24433.

Lu, Z., and Cyr, D.M. (1998). The conserved carboxyl terminus and zinc finger-like domain of the co-chaperone Ydj1 assist Hsp70 in protein folding. J Biol Chem *273*, 5970-5978.

Mann, C.J., Anderson, T.A., Read, J., Chester, S.A., Harrison, G.B., Kochl, S., Ritchie, P.J., Bradbury, P., Hussain, F.S., Amey, J., *et al.* (1999). The structure of vitellogenin provides a molecular model for the assembly and secretion of atherogenic lipoproteins. J Mol Biol *285*, 391-408.

Mattoo, R.U.H., Sharma, S.K., Priya, S., Finka, A., and Goloubinoff, P. (2013). Hsp110 is a bona fide chaperone using ATP to unfold stable misfolded polypeptides and reciprocally collaborate with Hsp70 to solubilize protein aggregates. J Biol Chem *288*, 21399-21411.

Mattson, G., Conklin, E., Desai, S., Nielander, G., Savage, M.D., and Morgensen, S. (1993). A practical approach to crosslinking. Mol Biol Rep *17*, 167-183.

Mayer, M.P., and Bukau, B. (2005). Hsp70 chaperones: cellular functions and molecular mechanism. Cell Mol Life Sci *62*, 670-684.

McClellan, A.J., Scott, M.D., and Frydman, J. (2005). Folding and quality control of the VHL tumor suppressor proceed through distinct chaperone pathways. Cell *121*, 739-748.

McConnell, J.R., and McAlpine, S.R. (2013). Heat shock proteins 27, 40, and 70 as combinational and dual therapeutic cancer targets. Bioorg Med Chem Lett *23*, 1923-1928.

McCracken, A.A., and Brodsky, J.L. (1996). Assembly of ER-associated protein degradation in vitro: dependence on cytosol, calnexin, and ATP. J Cell Biol *132*, 291-298.

McDowell, G.S., and Philpott, A. (2013). Non-canonical ubiquitylation: mechanisms and consequences. Int J Biochem Cell Biol *45*, 1833-1842.

McGowan, M.P., Tardif, J.C., Ceska, R., Burgess, L.J., Soran, H., Gouni-Berthold, I., Wagener, G., and Chasan-Taber, S. (2012). Randomized, placebo-controlled trial of mipomersen in patients with severe hypercholesterolemia receiving maximally tolerated lipid-lowering therapy. PLoS One *7*, e49006.

McIsaac, R.S., Silverman, S.J., McClean, M.N., Gibney, P.A., Macinskas, J., Hickman, M.J., Petti, A.A., and Botstein, D. (2011). Fast-acting and nearly gratuitous induction of gene expression and protein depletion in Saccharomyces cerevisiae. Mol Biol Cell *22*, 4447-4459.

McLeod, R.S., Zhao, Y., Selby, S.L., Westerlund, J., and Yao, Z. (1994). Carboxyl-terminal truncation impairs lipid recruitment by apolipoprotein B100 but does not affect secretion of the truncated apolipoprotein B-containing lipoproteins. J Biol Chem *269*, 2852-2862.

Meacham, G.C., Lu, Z., King, S., Sorscher, E., Tousson, A., and Cyr, D.M. (1999). The Hdj-2/Hsc70 chaperone pair facilitates early steps in CFTR biogenesis. EMBO J *18*, 1492-1505.

Meex, S.J., Andreo, U., Sparks, J.D., and Fisher, E.A. (2011). Huh-7 or HepG2 cells: which is the better model for studying human apolipoprotein-B100 assembly and secretion? J Lipid Res *52*, 152-158.

Melnyk, A., Rieger, H., and Zimmermann, R. (2015). Co-chaperones of the mammalian endoplasmic reticulum. Subcell Biochem *78*, 179-200.

Menzies, S.A., Volkmar, N., van den Boomen, D.J., Timms, R.T., Dickson, A.S., Nathan, J.A., and Lehner, P.J. (2018). The sterol-responsive RNF145 E3 ubiquitin ligase mediates the degradation of HMG-CoA reductase together with gp78 and Hrd1. Elife *7*.

Merki, E., Graham, M.J., Mullick, A.E., Miller, E.R., Crooke, R.M., Pitas, R.E., Witztum, J.L., and Tsimikas, S. (2008). Antisense oligonucleotide directed to human apolipoprotein B-100 reduces lipoprotein(a) levels and oxidized phospholipids on human apolipoprotein B-100 particles in lipoprotein(a) transgenic mice. Circulation *118*, 743-753.

Meusser, B., Hirsch, C., Jarosch, E., and Sommer, T. (2005). ERAD: the long road to destruction. Nat Cell Biol *7*, 766-772.

Michels, A.A., Kanon, B., Bensaude, O., and Kampinga, H.H. (1999). Heat shock protein (Hsp) 40 mutants inhibit Hsp70 in mammalian cells. J Biol Chem *274*, 36757-36763.

Milne, R., Theolis, R., Jr., Maurice, R., Pease, R.J., Weech, P.K., Rassart, E., Fruchart, J.C., Scott, J., and Marcel, Y.L. (1989). The use of monoclonal antibodies to localize the low density lipoprotein receptor-binding domain of apolipoprotein B. J Biol Chem *264*, 19754-19760.

Misaghi, S., Pacold, M.E., Blom, D., Ploegh, H.L., and Korbel, G.A. (2004). Using a small molecule inhibitor of peptide: N-glycanase to probe its role in glycoprotein turnover. Chem Biol *11*, 1677-1687.

Mitchell, D.M., Zhou, M., Pariyarath, R., Wang, H., Aitchison, J.D., Ginsberg, H.N., and Fisher, E.A. (1998). Apoprotein B100 has a prolonged interaction with the translocon during which its lipidation and translocation change from dependence on the microsomal triglyceride transfer protein to independence. Proc Natl Acad Sci U S A *95*, 14733-14738.

Morgan, H.D., Dean, W., Coker, H.A., Reik, W., and Petersen-Mahrt, S.K. (2004). Activation-induced cytidine deaminase deaminates 5-methylcytosine in DNA and is expressed in pluripotent tissues: implications for epigenetic reprogramming. J Biol Chem *279*, 52353-52360.

Morimoto, R.I. (2008). Proteotoxic stress and inducible chaperone networks in neurodegenerative disease and aging. Genes Dev *22*, 1427-1438.

Morito, D., Hirao, K., Oda, Y., Hosokawa, N., Tokunaga, F., Cyr, D.M., Tanaka, K., Iwai, K., and Nagata, K. (2008). Gp78 cooperates with RMA1 in endoplasmic reticulum-associated degradation of CFTRDeltaF508. Mol Biol Cell *19*, 1328-1336.

Morrow, M.W., and Brodsky, J.L. (2001). Yeast ribosomes bind to highly purified reconstituted Sec61p complex and to mammalian p180. Traffic *2*, 705-716.

Musialik, J., Boguszewska-Chachulska, A., Pojda-Wilczek, D., Gorzkowska, A., Szymanczak, R., Kania, M., Kujawa-Szewieczek, A., Wojcieszyn, M., Hartleb, M., and Wiecek, A. (2020). A Rare Mutation in The APOB Gene Associated with Neurological Manifestations in Familial Hypobetalipoproteinemia. Int J Mol Sci *21*.

Nakatsukasa, K., Huyer, G., Michaelis, S., and Brodsky, J.L. (2008). Dissecting the ER-associated degradation of a misfolded polytopic membrane protein. Cell *132*, 101-112.

Nandakumar, R., Matveyenko, A., Thomas, T., Pavlyha, M., Ngai, C., Holleran, S., Ramakrishnan, R., Ginsberg, H.N., Karmally, W., Marcovina, S.M., *et al.* (2018). Effects of mipomersen, an apolipoprotein B100 antisense, on lipoprotein (a) metabolism in healthy subjects. J Lipid Res *59*, 2397-2402.

Narasimhan, S.D. (2017). Beyond Statins: New Therapeutic Frontiers for Cardiovascular Disease. Cell *169*, 971-973.

Need, A.C., Shashi, V., Hitomi, Y., Schoch, K., Shianna, K.V., McDonald, M.T., Meisler, M.H., and Goldstein, D.B. (2012). Clinical application of exome sequencing in undiagnosed genetic conditions. J Med Genet *49*, 353-361.

Needham, P.G., and Brodsky, J.L. (2013). How early studies on secreted and membrane protein quality control gave rise to the ER associated degradation (ERAD) pathway: the early history of ERAD. Biochim Biophys Acta *1833*, 2447-2457.

Needham, P.G., Guerriero, C.J., and Brodsky, J.L. (2019). Chaperoning Endoplasmic Reticulum-Associated Degradation (ERAD) and Protein Conformational Diseases. Cold Spring Harb Perspect Biol *11*.

Ngosuwan, J., Wang, N.M., Fung, K.L., and Chirico, W.J. (2003). Roles of cytosolic Hsp70 and Hsp40 molecular chaperones in post-translational translocation of presecretory proteins into the endoplasmic reticulum. J Biol Chem *278*, 7034-7042.

Nillegoda, N.B., Kirstein, J., Szlachcic, A., Berynskyy, M., Stank, A., Stengel, F., Arnsburg, K., Gao, X., Scior, A., Aebersold, R., *et al.* (2015). Crucial HSP70 co-chaperone complex unlocks metazoan protein disaggregation. Nature *524*, 247-251.

Nillegoda, N.B., Stank, A., Malinverni, D., Alberts, N., Szlachcic, A., Barducci, A., De Los Rios, P., Wade, R.C., and Bukau, B. (2017). Evolution of an intricate J-protein network driving protein disaggregation in eukaryotes. Elife *6*.

Nillegoda, N.B., Wentink, A.S., and Bukau, B. (2018). Protein Disaggregation in Multicellular Organisms. Trends Biochem Sci *43*, 285-300.

Nishikawa, S., Brodsky, J.L., and Nakatsukasa, K. (2005). Roles of molecular chaperones in endoplasmic reticulum (ER) quality control and ER-associated degradation (ERAD). J Biochem *137*, 551-555.

Okiyoneda, T., Apaja, P.M., and Lukacs, G.L. (2011). Protein quality control at the plasma membrane. Curr Opin Cell Biol *23*, 483-491.

Olofsson, S.O., Bjursell, G., Bostrom, K., Carlsson, P., Elovson, J., Protter, A.A., Reuben, M.A., and Bondjers, G. (1987). Apolipoprotein B: structure, biosynthesis and role in the lipoprotein assembly process. Atherosclerosis *68*, 1-17.

Olofsson, S.O., and Boren, J. (2012). Apolipoprotein B secretory regulation by degradation. Arterioscler Thromb Vasc Biol *32*, 1334-1338.

Osaki, Y., Saito, A., Kanemoto, S., Kaneko, M., Matsuhisa, K., Asada, R., Masaki, T., Orii, K., Fukao, T., Tomatsu, S., *et al.* (2018). Shutdown of ER-associated degradation pathway rescues functions of mutant iduronate 2-sulfatase linked to mucopolysaccharidosis type II. Cell Death Dis *9*, 808.

Oyadomari, S., Yun, C., Fisher, E.A., Kreglinger, N., Kreibich, G., Oyadomari, M., Harding, H.P., Goodman, A.G., Harant, H., Garrison, J.L., *et al.* (2006). Cotranslocational degradation protects the stressed endoplasmic reticulum from protein overload. Cell *126*, 727-739.

Pan, M., Cederbaum, A.I., Zhang, Y.L., Ginsberg, H.N., Williams, K.J., and Fisher, E.A. (2004). Lipid peroxidation and oxidant stress regulate hepatic apolipoprotein B degradation and VLDL production. J Clin Invest *113*, 1277-1287.

Pan, M., Maitin, V., Parathath, S., Andreo, U., Lin, S.X., St Germain, C., Yao, Z., Maxfield, F.R., Williams, K.J., and Fisher, E.A. (2008). Presecretory oxidation, aggregation, and autophagic destruction of apoprotein-B: a pathway for late-stage quality control. Proc Natl Acad Sci U S A *105*, 5862-5867.

Paquet, M.E., Cohen-Doyle, M., Shore, G.C., and Williams, D.B. (2004). Bap29/31 influences the intracellular traffic of MHC class I molecules. J Immunol *172*, 7548-7555.

Parini, P., Jiang, Z.Y., Einarsson, C., Eggertsen, G., Zhang, S.D., Rudel, L.L., Han, T.Q., and Eriksson, M. (2009). ACAT2 and human hepatic cholesterol metabolism: identification of important gender-related differences in normolipidemic, non-obese Chinese patients. Atherosclerosis *207*, 266-271.

Pariyarath, R., Wang, H., Aitchison, J.D., Ginsberg, H.N., Welch, W.J., Johnson, A.E., and Fisher, E.A. (2001). Co-translational interactions of apoprotein B with the ribosome and translocon during lipoprotein assembly or targeting to the proteasome. J Biol Chem *276*, 541-550.

Park, H.K., Yoon, N.G., Lee, J.E., Hu, S., Yoon, S., Kim, S.Y., Hong, J.H., Nam, D., Chae, Y.C., Park, J.B., *et al.* (2020). Unleashing the full potential of Hsp90 inhibitors as cancer therapeutics through simultaneous inactivation of Hsp90, Grp94, and TRAP1. Exp Mol Med *52*, 79-91.

Park, S.H., Bolender, N., Eisele, F., Kostova, Z., Takeuchi, J., Coffino, P., and Wolf, D.H. (2007). The cytoplasmic Hsp70 chaperone machinery subjects misfolded and endoplasmic reticulum import-incompetent proteins to degradation via the ubiquitin-proteasome system. Mol Biol Cell *18*, 153-165.

Park, S.H., Kukushkin, Y., Gupta, R., Chen, T., Konagai, A., Hipp, M.S., Hayer-Hartl, M., and Hartl, F.U. (2013). PolyQ proteins interfere with nuclear degradation of cytosolic proteins by sequestering the Sis1p chaperone. Cell *154*, 134-145.

Park, S.Y., Choi, H.K., Seo, J.S., Yoo, J.Y., Jeong, J.W., Choi, Y., Choi, K.C., and Yoon, H.G. (2015). DNAJB1 negatively regulates MIG6 to promote epidermal growth factor receptor signaling. Biochim Biophys Acta *1853*, 2722-2730.

Parrales, A., Ranjan, A., Iyer, S.V., Padhye, S., Weir, S.J., Roy, A., and Iwakuma, T. (2016). DNAJA1 controls the fate of misfolded mutant p53 through the mevalonate pathway. Nat Cell Biol *18*, 1233-1243.

Parsell, D.A., Kowal, A.S., Singer, M.A., and Lindquist, S. (1994). Protein disaggregation mediated by heat-shock protein Hsp104. Nature *372*, 475-478.

Patel, S.B., and Grundy, S.M. (1996). Interactions between microsomal triglyceride transfer protein and apolipoprotein B within the endoplasmic reticulum in a heterologous expression system. J Biol Chem *271*, 18686-18694.

Pearce, M.M., Wang, Y., Kelley, G.G., and Wojcikiewicz, R.J. (2007). SPFH2 mediates the endoplasmic reticulum-associated degradation of inositol 1,4,5-trisphosphate receptors and other substrates in mammalian cells. J Biol Chem *282*, 20104-20115.

Peterson, B.G., Glaser, M.L., Rapoport, T.A., and Baldridge, R.D. (2019). Cycles of autoubiquitination and deubiquitination regulate the ERAD ubiquitin ligase Hrd1. Elife *8*.

Phung, T.L., Roncone, A., Jensen, K.L., Sparks, C.E., and Sparks, J.D. (1997). Phosphoinositide 3-kinase activity is necessary for insulin-dependent inhibition of apolipoprotein B secretion by rat hepatocytes and localizes to the endoplasmic reticulum. J Biol Chem *272*, 30693-30702.

Pons, V., Rolland, C., Nauze, M., Danjoux, M., Gaibelet, G., Durandy, A., Sassolas, A., Levy, E., Terce, F., Collet, X., *et al.* (2011). A severe form of abetalipoproteinemia caused by new splicing mutations of microsomal triglyceride transfer protein (MTTP). Hum Mutat *32*, 751-759.

Powell, L.M., Wallis, S.C., Pease, R.J., Edwards, Y.H., Knott, T.J., and Scott, J. (1987). A novel form of tissue-specific RNA processing produces apolipoprotein-B48 in intestine. Cell *50*, 831-840.

Preissler, S., and Deuerling, E. (2012). Ribosome-associated chaperones as key players in proteostasis. Trends Biochem Sci *37*, 274-283.

Preston, G.M., and Brodsky, J.L. (2017). The evolving role of ubiquitin modification in endoplasmic reticulum-associated degradation. Biochem J *474*, 445-469.

Preston, G.M., Guerriero, C.J., Metzger, M.B., Michaelis, S., and Brodsky, J.L. (2018). Substrate Insolubility Dictates Hsp104-Dependent Endoplasmic-Reticulum-Associated Degradation. Mol Cell *70*, 242-253 e246.

Qian, Y.Q., Patel, D., Hartl, F.U., and McColl, D.J. (1996). Nuclear magnetic resonance solution structure of the human Hsp40 (HDJ-1) J-domain. J Mol Biol *260*, 224-235.

Quistgaard, E.M. (2021). BAP31: Physiological functions and roles in disease. Biochimie *186*, 105-129.

Raabe, M., Veniant, M.M., Sullivan, M.A., Zlot, C.H., Bjorkegren, J., Nielsen, L.B., Wong, J.S., Hamilton, R.L., and Young, S.G. (1999). Analysis of the role of microsomal triglyceride transfer protein in the liver of tissue-specific knockout mice. J Clin Invest *103*, 1287-1298.

Raal, F.J., Santos, R.D., Blom, D.J., Marais, A.D., Charng, M.J., Cromwell, W.C., Lachmann, R.H., Gaudet, D., Tan, J.L., Chasan-Taber, S., *et al.* (2010). Mipomersen, an apolipoprotein B synthesis inhibitor, for lowering of LDL cholesterol concentrations in patients with homozygous familial hypercholesterolaemia: a randomised, double-blind, placebo-controlled trial. Lancet *375*, 998-1006.

Rad, M.R., Kirchrath, L., and Hollenberg, C.P. (1994). A putative P-type Cu(2+)-transporting ATPase gene on chromosome II of Saccharomyces cerevisiae. Yeast *10*, 1217-1225.

Rahim, A., Nafi-valencia, E., Siddiqi, S., Basha, R., Runyon, C.C., and Siddiqi, S.A. (2012). Proteomic analysis of the very low density lipoprotein (VLDL) transport vesicles. J Proteomics *75*, 2225-2235.

Rampelt, H., Kirstein-Miles, J., Nillegoda, N.B., Chi, K., Scholz, S.R., Morimoto, R.I., and Bukau, B. (2012). Metazoan Hsp70 machines use Hsp110 to power protein disaggregation. EMBO J *31*, 4221-4235.

Rauch, J.N., and Gestwicki, J.E. (2014). Binding of human nucleotide exchange factors to heat shock protein 70 (Hsp70) generates functionally distinct complexes in vitro. J Biol Chem *289*, 1402-1414.

Ravid, T., Doolman, R., Avner, R., Harats, D., and Roitelman, J. (2000). The ubiquitin-proteasome pathway mediates the regulated degradation of mammalian 3-hydroxy-3-methylglutaryl-coenzyme A reductase. J Biol Chem *275*, 35840-35847.

Ravid, T., Kreft, S.G., and Hochstrasser, M. (2006). Membrane and soluble substrates of the Doa10 ubiquitin ligase are degraded by distinct pathways. EMBO J *25*, 533-543.

Rebeaud, M.E., Mallik, S., Goloubinoff, P., and Tawfik, D.S. (2021). On the evolution of chaperones and cochaperones and the expansion of proteomes across the Tree of Life. Proc Natl Acad Sci U S A *118*.

Reiner, Z. (2014). Resistance and intolerance to statins. Nutr Metab Cardiovasc Dis *24*, 1057-1066.

Reiner, Z., De Bacquer, D., Kotseva, K., Prugger, C., De Backer, G., Wood, D., and Group, E.I.S. (2013). Treatment potential for dyslipidaemia management in patients with coronary heart disease across Europe: findings from the EUROASPIRE III survey. Atherosclerosis *231*, 300-307.

Reiner, Z., and Tedeschi-Reiner, E. (2013). Prevalence and types of persistent dyslipidemia in patients treated with statins. Croat Med J *54*, 339-345.

Reyes-Soffer, G., Moon, B., Hernandez-Ono, A., Dionizovik-Dimanovski, M., Jimenez, J., Obunike, J., Thomas, T., Ngai, C., Fontanez, N., Donovan, D.S., *et al.* (2016). Complex effects of inhibiting hepatic apolipoprotein B100 synthesis in humans. Sci Transl Med *8*, 323ra312.

Roberts, S.A., Lawrence, M.S., Klimczak, L.J., Grimm, S.A., Fargo, D., Stojanov, P., Kiezun, A., Kryukov, G.V., Carter, S.L., Saksena, G., *et al.* (2013). An APOBEC cytidine deaminase mutagenesis pattern is widespread in human cancers. Nat Genet *45*, 970-976.

Robson, A., and Collinson, I. (2006). The structure of the Sec complex and the problem of protein translocation. EMBO Rep *7*, 1099-1103.

Rosenberg, B.R., Hamilton, C.E., Mwangi, M.M., Dewell, S., and Papavasiliou, F.N. (2011). Transcriptome-wide sequencing reveals numerous APOBEC1 mRNA-editing targets in transcript 3' UTRs. Nat Struct Mol Biol *18*, 230-236.

Rosenzweig, R., Nillegoda, N.B., Mayer, M.P., and Bukau, B. (2019). The Hsp70 chaperone network. Nat Rev Mol Cell Biol *20*, 665-680.

Rubenstein, E.M., Kreft, S.G., Greenblatt, W., Swanson, R., and Hochstrasser, M. (2012). Aberrant substrate engagement of the ER translocon triggers degradation by the Hrd1 ubiquitin ligase. J Cell Biol *197*, 761-773.

Rudel, L.L., Lee, R.G., and Cockman, T.L. (2001). Acyl coenzyme A: cholesterol acyltransferase types 1 and 2: structure and function in atherosclerosis. Curr Opin Lipidol *12*, 121-127.

Rutkowski, D.T., Kang, S.W., Goodman, A.G., Garrison, J.L., Taunton, J., Katze, M.G., Kaufman, R.J., and Hegde, R.S. (2007). The role of p58IPK in protecting the stressed endoplasmic reticulum. Mol Biol Cell *18*, 3681-3691.

Rutledge, A.C., Qiu, W., Zhang, R., Kohen-Avramoglu, R., Nemat-Gorgani, N., and Adeli, K. (2009). Mechanisms targeting apolipoprotein B100 to proteasomal degradation: evidence that degradation is initiated by BiP binding at the N terminus and the formation of a p97 complex at the C terminus. Arterioscler Thromb Vasc Biol *29*, 579-585.

Rutledge, A.C., Qiu, W., Zhang, R., Urade, R., and Adeli, K. (2013). Role of cysteine-protease CGHC motifs of ER-60, a protein disulfide isomerase, in hepatic apolipoprotein B100 degradation. Arch Biochem Biophys *537*, 104-112.

Sabatine, M.S., Giugliano, R.P., Keech, A.C., Honarpour, N., Wiviott, S.D., Murphy, S.A., Kuder, J.F., Wang, H., Liu, T., Wasserman, S.M., *et al.* (2017). Evolocumab and Clinical Outcomes in Patients with Cardiovascular Disease. N Engl J Med *376*, 1713-1722.

Sahi, C., Lee, T., Inada, M., Pleiss, J.A., and Craig, E.A. (2010). Cwc23, an essential J protein critical for pre-mRNA splicing with a dispensable J domain. Mol Cell Biol *30*, 33-42.

Saibil, H. (2013). Chaperone machines for protein folding, unfolding and disaggregation. Nat Rev Mol Cell Biol *14*, 630-642.

Sakata, N., Stoops, J.D., and Dixon, J.L. (1999). Cytosolic components are required for proteasomal degradation of newly synthesized apolipoprotein B in permeabilized HepG2 cells. J Biol Chem *274*, 17068-17074.

Sane, A.T., Seidman, E., Peretti, N., Kleme, M.L., Delvin, E., Deslandres, C., Garofalo, C., Spahis, S., and Levy, E. (2017). Understanding Chylomicron Retention Disease Through Sar1b Gtpase Gene Disruption: Insight From Cell Culture. Arterioscler Thromb Vasc Biol *37*, 2243-2251.

Schamel, W.W., Kuppig, S., Becker, B., Gimborn, K., Hauri, H.P., and Reth, M. (2003). A high-molecular-weight complex of membrane proteins BAP29/BAP31 is involved in the retention of membrane-bound IgD in the endoplasmic reticulum. Proc Natl Acad Sci U S A *100*, 9861-9866.

Schilke, B.A., Ciesielski, S.J., Ziegelhoffer, T., Kamiya, E., Tonelli, M., Lee, W., Cornilescu, G., Hines, J.K., Markley, J.L., and Craig, E.A. (2017). Broadening the functionality of a J-protein/Hsp70 molecular chaperone system. PLoS Genet *13*, e1007084.

Schmidt, B.Z., Watts, R.J., Aridor, M., and Frizzell, R.A. (2009). Cysteine string protein promotes proteasomal degradation of the cystic fibrosis transmembrane conductance regulator (CFTR) by increasing its interaction with the C terminus of Hsp70-interacting protein and promoting CFTR ubiquitylation. J Biol Chem *284*, 4168-4178.

Schonfeld, G., Lin, X., and Yue, P. (2005). Familial hypobetalipoproteinemia: genetics and metabolism. Cell Mol Life Sci *62*, 1372-1378.

Schuldiner, M., Metz, J., Schmid, V., Denic, V., Rakwalska, M., Schmitt, H.D., Schwappach, B., and Weissman, J.S. (2008). The GET complex mediates insertion of tail-anchored proteins into the ER membrane. Cell *134*, 634-645.

Schulz, R., and Schluter, K.D. (2017). PCSK9 targets important for lipid metabolism. Clin Res Cardiol Suppl *12*, 2-11.

Scott, J., Wallis, S.C., Davies, M.S., Wynne, J.K., Powell, L.M., and Driscoll, D.M. (1989). RNA editing: a novel mechanism for regulating lipid transport from the intestine. Gut *30 Spec No*, 35-43.

Segrest, J.P., Jones, M.K., and Dashti, N. (1999). N-terminal domain of apolipoprotein B has structural homology to lipovitellin and microsomal triglyceride transfer protein: a "lipid pocket" model for self-assembly of apob-containing lipoprotein particles. J Lipid Res *40*, 1401-1416.

Segrest, J.P., Jones, M.K., De Loof, H., Brouillette, C.G., Venkatachalapathi, Y.V., and Anantharamaiah, G.M. (1992). The amphipathic helix in the exchangeable apolipoproteins: a review of secondary structure and function. J Lipid Res *33*, 141-166.

Segrest, J.P., Jones, M.K., De Loof, H., and Dashti, N. (2001). Structure of apolipoprotein B-100 in low density lipoproteins. J Lipid Res *42*, 1346-1367.

Segrest, J.P., Jones, M.K., Mishra, V.K., Anantharamaiah, G.M., and Garber, D.W. (1994). apoB-100 has a pentapartite structure composed of three amphipathic alpha-helical domains alternating with two amphipathic beta-strand domains. Detection by the computer program LOCATE. Arterioscler Thromb *14*, 1674-1685.

Sever, N., Song, B.L., Yabe, D., Goldstein, J.L., Brown, M.S., and DeBose-Boyd, R.A. (2003). Insig-dependent ubiquitination and degradation of mammalian 3-hydroxy-3-methylglutaryl-CoA reductase stimulated by sterols and geranylgeraniol. J Biol Chem *278*, 52479-52490.

Sharifi, M., Futema, M., Nair, D., and Humphries, S.E. (2017). Genetic Architecture of Familial Hypercholesterolaemia. Curr Cardiol Rep *19*, 44.

Shen, Y., and Hendershot, L.M. (2005). ERdj3, a stress-inducible endoplasmic reticulum DnaJ homologue, serves as a cofactor for BiP's interactions with unfolded substrates. Mol Biol Cell *16*, 40-50.

Shevtsov, M., Multhoff, G., Mikhaylova, E., Shibata, A., Guzhova, I., and Margulis, B. (2019). Combination of Anti-Cancer Drugs with Molecular Chaperone Inhibitors. Int J Mol Sci *20*.

Shimano, H. (2009). SREBPs: physiology and pathophysiology of the SREBP family. FEBS J *276*, 616-621.

Shiraishi, E., Inouhe, M., Joho, M., and Tohoyama, H. (2000). The cadmium-resistant gene, CAD2, which is a mutated putative copper-transporter gene (PCA1), controls the intracellular cadmium-level in the yeast S. cerevisiae. Curr Genet *37*, 79-86.

Siddiqi, S.A., Gorelick, F.S., Mahan, J.T., and Mansbach, C.M., 2nd (2003). COPII proteins are required for Golgi fusion but not for endoplasmic reticulum budding of the pre-chylomicron transport vesicle. J Cell Sci *116*, 415-427.

Sikka, P., Kapoor, S., Bindra, V.K., Sharma, M., Vishwakarma, P., and Saxena, K.K. (2011). Statin intolerance: now a solved problem. J Postgrad Med *57*, 321-328.

Simon, D., Aden, D.P., and Knowles, B.B. (1982). Chromosomes of human hepatoma cell lines. Int J Cancer *30*, 27-33.

Smith, N., Adle, D.J., Zhao, M., Qin, X., Kim, H., and Lee, J. (2016). Endoplasmic Reticulum-associated Degradation of Pca1p, a Polytopic Protein, via Interaction with the Proteasome at the Membrane. J Biol Chem *291*, 15082-15092.

Song, B.L., Sever, N., and DeBose-Boyd, R.A. (2005). Gp78, a membrane-anchored ubiquitin ligase, associates with Insig-1 and couples sterol-regulated ubiquitination to degradation of HMG CoA reductase. Mol Cell *19*, 829-840.

Soti, C., Nagy, E., Giricz, Z., Vigh, L., Csermely, P., and Ferdinandy, P. (2005). Heat shock proteins as emerging therapeutic targets. Br J Pharmacol *146*, 769-780.

Sparks, J.D., O'Dell, C., Chamberlain, J.M., and Sparks, C.E. (2013). Insulin-dependent apolipoprotein B degradation is mediated by autophagy and involves class I and class III phosphatidylinositide 3-kinases. Biochem Biophys Res Commun *435*, 616-620.

Sparks, J.D., and Sparks, C.E. (1990). Insulin modulation of hepatic synthesis and secretion of apolipoprotein B by rat hepatocytes. J Biol Chem *265*, 8854-8862.

Stark, J.L., Mehla, K., Chaika, N., Acton, T.B., Xiao, R., Singh, P.K., Montelione, G.T., and Powers, R. (2014). Structure and function of human DnaJ homologue subfamily a member 1 (DNAJA1) and its relationship to pancreatic cancer. Biochemistry *53*, 1360-1372.

Stefanadis, C., Antoniou, C.K., Tsiachris, D., and Pietri, P. (2017). Coronary Atherosclerotic Vulnerable Plaque: Current Perspectives. J Am Heart Assoc *6*.

Stevenson, J., Huang, E.Y., and Olzmann, J.A. (2016). Endoplasmic Reticulum-Associated Degradation and Lipid Homeostasis. Annu Rev Nutr *36*, 511-542.

Strickland, E., Qu, B.H., Millen, L., and Thomas, P.J. (1997). The molecular chaperone Hsc70 assists the in vitro folding of the N-terminal nucleotide-binding domain of the cystic fibrosis transmembrane conductance regulator. J Biol Chem *272*, 25421-25424.

Sun, X.M., Eden, E.R., Tosi, I., Neuwirth, C.K., Wile, D., Naoumova, R.P., and Soutar, A.K. (2005). Evidence for effect of mutant PCSK9 on apolipoprotein B secretion as the cause of unusually severe dominant hypercholesterolaemia. Hum Mol Genet *14*, 1161-1169.

Sun, Z., and Brodsky, J.L. (2018). The degradation pathway of a model misfolded protein is determined by aggregation propensity. Mol Biol Cell *29*, 1422-1434.

Surendran, P., Drenos, F., Young, R., Warren, H., Cook, J.P., Manning, A.K., Grarup, N., Sim, X., Barnes, D.R., Witkowska, K., *et al.* (2016). Trans-ancestry meta-analyses identify rare and common variants associated with blood pressure and hypertension. Nat Genet *48*, 1151-1161.

Suzuki, T., Huang, C., and Fujihira, H. (2016). The cytoplasmic peptide:N-glycanase (NGLY1) - Structure, expression and cellular functions. Gene *577*, 1-7.

Suzuki, T., Kitajima, K., Emori, Y., Inoue, Y., and Inoue, S. (1997). Site-specific de-N-glycosylation of diglycosylated ovalbumin in hen oviduct by endogenous peptide: N-glycanase as a quality control system for newly synthesized proteins. Proc Natl Acad Sci U S A *94*, 6244-6249.

Talmud, P.J., Converse, C., Krul, E., Huq, L., McIlwaine, G.G., Series, J.J., Boyd, P., Schonfeld, G., Dunning, A., and Humphries, S. (1992). A novel truncated apolipoprotein B (apo B55) in a patient with familial hypobetalipoproteinemia and atypical retinitis pigmentosa. Clin Genet *42*, 62-70.

Tatu, U., and Helenius, A. (1999). Interaction of newly synthesized apolipoprotein B with calnexin and calreticulin requires glucose trimming in the endoplasmic reticulum. Biosci Rep *19*, 189-196.

Terada, K., and Mori, M. (2000). Human DnaJ homologs dj2 and dj3, and bag-1 are positive cochaperones of hsc70. J Biol Chem *275*, 24728-24734.

Thomas, E.R., Atanur, S.S., Norsworthy, P.J., Encheva, V., Snijders, A.P., Game, L., Vandrovcova, J., Siddiq, A., Seed, M., Soutar, A.K., *et al.* (2013). Identification and biochemical analysis of a novel APOB mutation that causes autosomal dominant hypercholesterolemia. Mol Genet Genomic Med *1*, 155-161.

Tsai, J., Qiu, W., Kohen-Avramoglu, R., and Adeli, K. (2007). MEK-ERK inhibition corrects the defect in VLDL assembly in HepG2 cells: potential role of ERK in VLDL-ApoB100 particle assembly. Arterioscler Thromb Vasc Biol *27*, 211-218.

Tsai, Y.C., Leichner, G.S., Pearce, M.M., Wilson, G.L., Wojcikiewicz, R.J., Roitelman, J., and Weissman, A.M. (2012). Differential regulation of HMG-CoA reductase and Insig-1 by enzymes of the ubiquitin-proteasome system. Mol Biol Cell *23*, 4484-4494.

van de Weijer, M.L., Luteijn, R.D., and Wiertz, E.J. (2015). Viral immune evasion: Lessons in MHC class I antigen presentation. Semin Immunol *27*, 125-137.

van den Boomen, D.J.H., Volkmar, N., and Lehner, P.J. (2020). Ubiquitin-mediated regulation of sterol homeostasis. Curr Opin Cell Biol *65*, 103-111.

Veatch, J.R., McMurray, M.A., Nelson, Z.W., and Gottschling, D.E. (2009). Mitochondrial dysfunction leads to nuclear genome instability via an iron-sulfur cluster defect. Cell *137*, 1247-1258.

Vembar, S.S., and Brodsky, J.L. (2008). One step at a time: endoplasmic reticulum-associated degradation. Nat Rev Mol Cell Biol *9*, 944-957.

Vembar, S.S., Jonikas, M.C., Hendershot, L.M., Weissman, J.S., and Brodsky, J.L. (2010). J domain co-chaperone specificity defines the role of BiP during protein translocation. J Biol Chem *285*, 22484-22494.

Venter, J.C., Adams, M.D., Myers, E.W., Li, P.W., Mural, R.J., Sutton, G.G., Smith, H.O., Yandell, M., Evans, C.A., Holt, R.A., *et al.* (2001). The sequence of the human genome. Science *291*, 1304-1351.

von der Malsburg, K., Shao, S., and Hegde, R.S. (2015). The ribosome quality control pathway can access nascent polypeptides stalled at the Sec61 translocon. Mol Biol Cell *26*, 2168-2180.

Walsh, M.T., Iqbal, J., Josekutty, J., Soh, J., Di Leo, E., Ozaydin, E., Gunduz, M., Tarugi, P., and Hussain, M.M. (2015). Novel Abetalipoproteinemia Missense Mutation Highlights the Importance of the N-Terminal beta-Barrel in Microsomal Triglyceride Transfer Protein Function. Circ Cardiovasc Genet *8*, 677-687.

Walsh, P., Bursac, D., Law, Y.C., Cyr, D., and Lithgow, T. (2004). The J-protein family: modulating protein assembly, disassembly and translocation. EMBO Rep *5*, 567-571.

Wang, B., Heath-Engel, H., Zhang, D., Nguyen, N., Thomas, D.Y., Hanrahan, J.W., and Shore, G.C. (2008). BAP31 interacts with Sec61 translocons and promotes retrotranslocation of CFTRDeltaF508 via the derlin-1 complex. Cell *133*, 1080-1092.

Wang, Y.J., Bian, Y., Luo, J., Lu, M., Xiong, Y., Guo, S.Y., Yong, H., Lin, X., Li, Q., Chang, C.C.Y., *et al.* (2017). Corrigendum: Cholesterol and fatty acids regulate cysteine ubiquitylation of ACAT2 through competitive oxidation. Nat Cell Biol *19*, 1441.

Wangeline, M.A., Vashistha, N., and Hampton, R.Y. (2017). Proteostatic Tactics in the Strategy of Sterol Regulation. Annu Rev Cell Dev Biol *33*, 467-489.

Ward, N.C., Watts, G.F., and Eckel, R.H. (2019). Response by Ward et al to Letter Regarding Article, "Statin Toxicity: Mechanistic Insights and Clinical Implications". Circ Res *124*, e121-e122.

Webster, J.M., Tiwari, S., Weissman, A.M., and Wojcikiewicz, R.J. (2003). Inositol 1,4,5-trisphosphate receptor ubiquitination is mediated by mammalian Ubc7, a component of the endoplasmic reticulum-associated degradation pathway, and is inhibited by chelation of intracellular Zn2+. J Biol Chem *278*, 38238-38246.

Weisgraber, K.H., Innerarity, T.L., Rall, S.C., Jr., and Mahley, R.W. (1985). Apolipoprotein E: receptor binding properties. Adv Exp Med Biol *183*, 159-171.

Welty, F.K. (2020). Hypobetalipoproteinemia and abetalipoproteinemia: liver disease and cardiovascular disease. Curr Opin Lipidol *31*, 49-55.

Welty, F.K., Ordovas, J., Schaefer, E.J., Wilson, P.W., and Young, S.G. (1995a). Identification and molecular analysis of two apoB gene mutations causing low plasma cholesterol levels. Circulation *92*, 2036-2040.

Welty, F.K., Seman, L., and Yen, F.T. (1995b). Purification of the apolipoprotein B-67-containing low density lipoprotein particle and its affinity for the low density lipoprotein receptor. J Lipid Res *36*, 2622-2629.

Wentink, A., Nussbaum-Krammer, C., and Bukau, B. (2019). Modulation of Amyloid States by Molecular Chaperones. Cold Spring Harb Perspect Biol *11*.

Werner, E.D., Brodsky, J.L., and McCracken, A.A. (1996). Proteasome-dependent endoplasmic reticulum-associated protein degradation: an unconventional route to a familiar fate. Proc Natl Acad Sci U S A *93*, 13797-13801.

Wetterau, J.R., Aggerbeck, L.P., Bouma, M.E., Eisenberg, C., Munck, A., Hermier, M., Schmitz, J., Gay, G., Rader, D.J., and Gregg, R.E. (1992). Absence of microsomal triglyceride transfer protein in individuals with abetalipoproteinemia. Science *258*, 999-1001.

Wetterau, J.R., Combs, K.A., Spinner, S.N., and Joiner, B.J. (1990). Protein disulfide isomerase is a component of the microsomal triglyceride transfer protein complex. J Biol Chem *265*, 9800-9807.

White, A.L., Graham, D.L., LeGros, J., Pease, R.J., and Scott, J. (1992). Oleate-mediated stimulation of apolipoprotein B secretion from rat hepatoma cells. A function of the ability of apolipoprotein B to direct lipoprotein assembly and escape presecretory degradation. J Biol Chem *267*, 15657-15664.

Whitfield, A.J., Marais, A.D., Robertson, K., Barrett, P.H., van Bockxmeer, F.M., and Burnett, J.R. (2003). Four novel mutations in APOB causing heterozygous and homozygous familial hypobetalipoproteinemia. Hum Mutat *22*, 178.

Wiegman, A., Gidding, S.S., Watts, G.F., Chapman, M.J., Ginsberg, H.N., Cuchel, M., Ose, L., Averna, M., Boileau, C., Boren, J., *et al.* (2015). Familial hypercholesterolaemia in children and adolescents: gaining decades of life by optimizing detection and treatment. Eur Heart J *36*, 2425-2437.

Williams, J.M., Inoue, T., Banks, L., and Tsai, B. (2013). The ERdj5-Sel1L complex facilitates cholera toxin retrotranslocation. Mol Biol Cell *24*, 785-795.

Wojcikiewicz, R.J., Ernst, S.A., and Yule, D.I. (1999). Secretagogues cause ubiquitination and down-regulation of inositol 1, 4,5-trisphosphate receptors in rat pancreatic acinar cells. Gastroenterology *116*, 1194-1201.

Wojcikiewicz, R.J., Furuichi, T., Nakade, S., Mikoshiba, K., and Nahorski, S.R. (1994). Muscarinic receptor activation down-regulates the type I inositol 1,4,5-trisphosphate receptor by accelerating its degradation. J Biol Chem *269*, 7963-7969.

Wojcikiewicz, R.J., and Nahorski, S.R. (1991). Chronic muscarinic stimulation of SH-SY5Y neuroblastoma cells suppresses inositol 1,4,5-trisphosphate action. Parallel inhibition of inositol 1,4,5-trisphosphate-induced Ca2+ mobilization and inositol 1,4,5-trisphosphate binding. J Biol Chem *266*, 22234-22241.

Wojcikiewicz, R.J., Pearce, M.M., Sliter, D.A., and Wang, Y. (2009). When worlds collide: IP(3) receptors and the ERAD pathway. Cell Calcium *46*, 147-153.

Wong, E., and Goldberg, T. (2014). Mipomersen (kynamro): a novel antisense oligonucleotide inhibitor for the management of homozygous familial hypercholesterolemia. P T *39*, 119-122.

Wu, X., Zhou, M., Huang, L.S., Wetterau, J., and Ginsberg, H.N. (1996). Demonstration of a physical interaction between microsomal triglyceride transfer protein and apolipoprotein B during the assembly of ApoB-containing lipoproteins. J Biol Chem *271*, 10277-10281.

Xiao, J., Kim, L.S., and Graham, T.R. (2006). Dissection of Swa2p/auxilin domain requirements for cochaperoning Hsp70 clathrin-uncoating activity in vivo. Mol Biol Cell *17*, 3281-3290.

Xu, D., Tong, X., Sun, L., Li, H., Jones, R.D., Liao, J., and Yang, G.Y. (2019). Inhibition of mutant Kras and p53-driven pancreatic carcinogenesis by atorvastatin: Mainly via targeting of the farnesylated DNAJA1 in chaperoning mutant p53. Mol Carcinog *58*, 2052-2064.

Yamaguchi, J., Conlon, D.M., Liang, J.J., Fisher, E.A., and Ginsberg, H.N. (2006). Translocation efficiency of apolipoprotein B is determined by the presence of beta-sheet domains, not pause transfer sequences. J Biol Chem *281*, 27063-27071.

Yamamoto, Y.H., Kimura, T., Momohara, S., Takeuchi, M., Tani, T., Kimata, Y., Kadokura, H., and Kohno, K. (2010). A novel ER J-protein DNAJB12 accelerates ER-associated degradation of membrane proteins including CFTR. Cell Struct Funct *35*, 107-116.

Yamanaka, S., Poksay, K.S., Arnold, K.S., and Innerarity, T.L. (1997). A novel translational repressor mRNA is edited extensively in livers containing tumors caused by the transgene expression of the apoB mRNA-editing enzyme. Genes Dev *11*, 321-333.

Yan, W., Gale, M.J., Jr., Tan, S.L., and Katze, M.G. (2002). Inactivation of the PKR protein kinase and stimulation of mRNA translation by the cellular co-chaperone P58(IPK) does not require J domain function. Biochemistry *41*, 4938-4945.

Yang, C.Y., Gu, Z.W., Weng, S.A., Kim, T.W., Chen, S.H., Pownall, H.J., Sharp, P.M., Liu, S.W., Li, W.H., Gotto, A.M., Jr., *et al.* (1989a). Structure of apolipoprotein B-100 of human low density lipoproteins. Arteriosclerosis *9*, 96-108.

Yang, C.Y., Kim, T.W., Pao, Q., Chan, L., Knapp, R.D., Gotto, A.M., Jr., and Pownall, H.J. (1989b). Structure and conformational analysis of lipid-associating peptides of apolipoprotein B-100 produced by trypsinolysis. J Protein Chem *8*, 689-699.

Yeung, S.J., Chen, S.H., and Chan, L. (1996). Ubiquitin-proteasome pathway mediates intracellular degradation of apolipoprotein B. Biochemistry *35*, 13843-13848.

Yokota, S., Kitahara, M., and Nagata, K. (2000). Benzylidene lactam compound, KNK437, a novel inhibitor of acquisition of thermotolerance and heat shock protein induction in human colon carcinoma cells. Cancer Res *60*, 2942-2948.

Youker, R.T., Walsh, P., Beilharz, T., Lithgow, T., and Brodsky, J.L. (2004). Distinct roles for the Hsp40 and Hsp90 molecular chaperones during cystic fibrosis transmembrane conductance regulator degradation in yeast. Mol Biol Cell *15*, 4787-4797.

Young, S.G., Hubl, S.T., Smith, R.S., Snyder, S.M., and Terdiman, J.F. (1990). Familial hypobetalipoproteinemia caused by a mutation in the apolipoprotein B gene that results in a truncated species of apolipoprotein B (B-31). A unique mutation that helps to define the portion of the apolipoprotein B molecule required for the formation of buoyant, triglyceride-rich lipoproteins. J Clin Invest *85*, 933-942.

Younger, J.M., Chen, L., Ren, H.Y., Rosser, M.F., Turnbull, E.L., Fan, C.Y., Patterson, C., and Cyr, D.M. (2006). Sequential quality-control checkpoints triage misfolded cystic fibrosis transmembrane conductance regulator. Cell *126*, 571-582.

Yu, H., Kaung, G., Kobayashi, S., and Kopito, R.R. (1997). Cytosolic degradation of T-cell receptor alpha chains by the proteasome. J Biol Chem *272*, 20800-20804.

Yu, H.Y., Ziegelhoffer, T., and Craig, E.A. (2015a). Functionality of Class A and Class B J-protein co-chaperones with Hsp70. FEBS Lett *589*, 2825-2830.

Yu, H.Y., Ziegelhoffer, T., Osipiuk, J., Ciesielski, S.J., Baranowski, M., Zhou, M., Joachimiak, A., and Craig, E.A. (2015b). Roles of intramolecular and intermolecular interactions in functional regulation of the Hsp70 J-protein co-chaperone Sis1. J Mol Biol *427*, 1632-1643.

Zarouchlioti, C., Parfitt, D.A., Li, W., Gittings, L.M., and Cheetham, M.E. (2018). DNAJ Proteins in neurodegeneration: essential and protective factors. Philos Trans R Soc Lond B Biol Sci *373*.

Zelcer, N., Sharpe, L.J., Loregger, A., Kristiana, I., Cook, E.C., Phan, L., Stevenson, J., and Brown, A.J. (2014). The E3 ubiquitin ligase MARCH6 degrades squalene monooxygenase and affects 3-hydroxy-3-methyl-glutaryl coenzyme A reductase and the cholesterol synthesis pathway. Mol Cell Biol *34*, 1262-1270.

Zhang, H., Peters, K.W., Sun, F., Marino, C.R., Lang, J., Burgoyne, R.D., and Frizzell, R.A. (2002). Cysteine string protein interacts with and modulates the maturation of the cystic fibrosis transmembrane conductance regulator. J Biol Chem *277*, 28948-28958.

Zhang, H., Schmidt, B.Z., Sun, F., Condliffe, S.B., Butterworth, M.B., Youker, R.T., Brodsky, J.L., Aridor, M., and Frizzell, R.A. (2006). Cysteine string protein monitors late steps in cystic fibrosis transmembrane conductance regulator biogenesis. J Biol Chem *281*, 11312-11321.

Zhang, T., Xu, Y., Liu, Y., and Ye, Y. (2015a). gp78 functions downstream of Hrd1 to promote degradation of misfolded proteins of the endoplasmic reticulum. Mol Biol Cell *26*, 4438-4450.

Zhang, X.L., Zhu, Q.Q., Zhu, L., Chen, J.Z., Chen, Q.H., Li, G.N., Xie, J., Kang, L.N., and Xu, B. (2015b). Safety and efficacy of anti-PCSK9 antibodies: a meta-analysis of 25 randomized, controlled trials. BMC Med *13*, 123.

Zhang, Y., Nijbroek, G., Sullivan, M.L., McCracken, A.A., Watkins, S.C., Michaelis, S., and Brodsky, J.L. (2001). Hsp70 molecular chaperone facilitates endoplasmic reticulum-associated protein degradation of cystic fibrosis transmembrane conductance regulator in yeast. Mol Biol Cell *12*, 1303-1314.

Zhou, M., Fisher, E.A., and Ginsberg, H.N. (1998). Regulated Co-translational ubiquitination of apolipoprotein B100. A new paradigm for proteasomal degradation of a secretory protein. J Biol Chem *273*, 24649-24653.

Zhou, M., Wu, X., Huang, L.S., and Ginsberg, H.N. (1995). Apoprotein B100, an inefficiently translocated secretory protein, is bound to the cytosolic chaperone, heat shock protein 70. J Biol Chem *270*, 25220-25224.

Zimmermann, T.S., Lee, A.C., Akinc, A., Bramlage, B., Bumcrot, D., Fedoruk, M.N., Harborth, J., Heyes, J.A., Jeffs, L.B., John, M., *et al.* (2006). RNAi-mediated gene silencing in non-human primates. Nature *441*, 111-114.